REACTION DYNAMICS IN SUPERCRITICAL MEDIA

Thesis submitted for the degree of

Doctor of Philosophy

at the University of Leicester

by

Nicola Emma Durling MChem (Leicester)

Department of Chemistry

University of Leicester

October 2003

UMI Number: U180413

Dissertation Publishing

REACTION DYNAMICS IN SUPERCRITICAL MEDIA

NICOLA EMMA DURLING

UNIVERSITY OF LEICESTER

2003

ABSTRACT

An *in situ* dielectric method is used to measure aromatic solubilities as a function of pressure and to follow the progress of an Esterification, Aldol and Friedel-Crafts reactions in supercritical (sc) difluoromethane (HFC 32). This is achieved by measuring the changes in the sc solution capacitance as the composition of the sc system changes.

The solubility of *p*-hydroxybenzoic, *p*-toluic, *p*-aminobenzoic and *p*-chlorobenzoic acids and also *p*-chlorophenol and *p*-aminophenol is determined in sc HFC 32 at 363 K using the dielectric method, and presented as a function of pressure. The compounds are shown to be more soluble than in the commonly employed sc solvent, CO_2, under comparative conditions. The enhancement factor is used as a way of expressing solubility to remove the effect of vapour pressure and the observed trend in solubility is found to be highly dependent on the polarity of the substituents present on the aromatic ring.

The use of the *in situ* dielectric method for monitoring a reaction in a sc fluid is proposed. The Esterification, Aldol and Friedel-Crafts reactions in sc HFC 32 were used to test the applicability of this technique. These are the first reported reactions to be carried out in sc HFC 32. The rate/equilibrium constants for these reactions are determined and found to decrease with increasing pressure. It is proposed that the observed high reaction rates at low pressure are due to local composition enhancements.

Determination of solvent-solute interactions is key to the understanding of solvent properties in liquids and sc fluids. The Kamlet-Taft parameters were determined for HFC 32 and 1,1,1,2-tetrafluoroethane (HFC 134a) as a function of temperature and pressure in the range 313 to 403 K and 50 to 220 bar using three solvatochromic dyes. It is shown that both solvents exhibit considerable hydrogen bond donor and acceptor properties and these parameters also obey the three region density model often invoked when describing the polarisability/dipolarity parameter in sc fluids.

ACKNOWLEDGEMENTS

'It's all in the chemistry.'

S Club 7

CONTENTS

CHAPTER 1

INTRODUCTION

1.1 Introduction

There are serious environmental concerns facing the manufacturers of industrial scale organic solvents, so there is an increased need to develop environmentally conscious, economical reaction media. Supercritical (sc) fluids may be an answer. However, for the development of synthetic processes based on sc solvents, a detailed knowledge of the effect of the solvent on reaction dynamics is required. It is well known that the solvent in a chemical process can also affect both the mechanism and kinetics of a reaction.[1] In a chemical reaction the solvent should ideally be:

(i)   Highly chemically stable

(ii)   Easy to handle

(iii)   Of optimum viscosity to allow the required mass transport

(iv)   Inexpensive

(v)   Non toxic and environmentally acceptable

In this work, complex solvent effects and the effect of physical conditions on the kinetics and mechanism of chemical reactions are investigated. All of these properties will change markedly in a sc fluid and this tunability of the solvent suggests an unprecedented ability to select the product distribution obtained from a chemical reaction. In particular, the solvent properties of sc difluoromethane (HFC 32) and 1, 1, 1, 2-tetrafluoroethane (HFC 134a) will be assessed.

1.2 Supercritical Fluids

Scientists and engineers have been aware of the enhanced solvent characteristics of sc fluid solvents for more than one hundred years.[2] However, it is only within the last two decades that sc fluids have been the focus of a number of research and development programs and much media hype.

A sc fluid is formed if the temperature and pressure of a single substance simultaneously exceed that of the critical point[3] but below the pressure required to condense it into a solid. Figure 1.1 shows a typical phase diagram, where P_c and T_c are the critical pressure and temperature respectively. Figure 1.2 shows the phase transitions to a sc fluid pictorially.

At high temperatures and pressures the molecules of a sc phase will have high kinetic energy and therefore it acts like a gas. At the same time, the density of a sc fluid is intermediate between a gas and a liquid, so solvent molecules have large

interactions with solutes. Hence sc fluids have solvent properties similar to those for liquids and transport properties similar to those for gases. Typical values for a selection of physical properties of a sc fluid are compared to those of a gas and a liquid in Table1.1.[4]
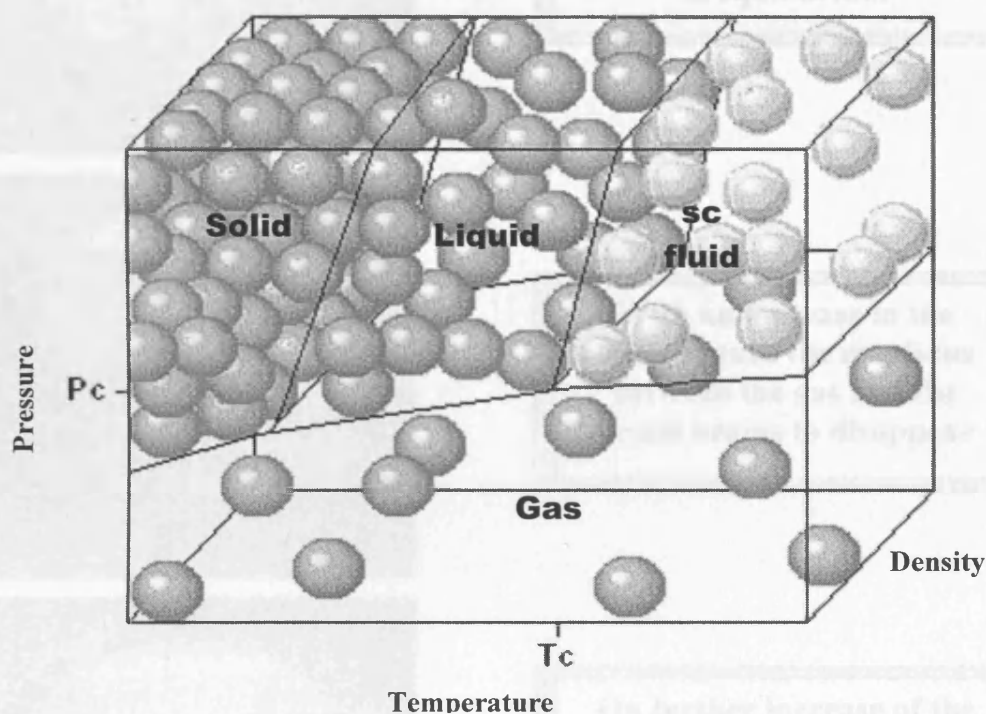
Figure 1.1 Phase diagram of a typical substance

Over recent years sc fluids have been of great interest because it has been recognised that fluid density is a highly tuneable function of pressure. Density-dependent properties such as viscosity and dielectric constant can therefore be changed by up to an order of magnitude at temperatures close to that of the critical point simply by altering the pressure.

Physical Property	Gas	Supercritical Fluid	Liquid
Density (g cm^{-3})	10^{-3}	0.1-1	1
Viscosity (g cm^{-1} s^{-1})	10^{-4}	10^{-3} - 10^{-4}	10^{-2}
Diffusivity (cm^2 s^{-1})	10^{-1}	10^{-3} - 10^{-4}	$< 10^{-5}$

Table 1.1 Comparison of some physical properties of a gas, sc fluid and a liquid
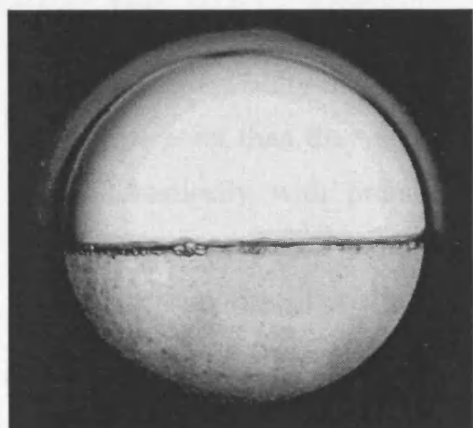
The liquid and gaseous phase of a supercritical fluid in equilibrium
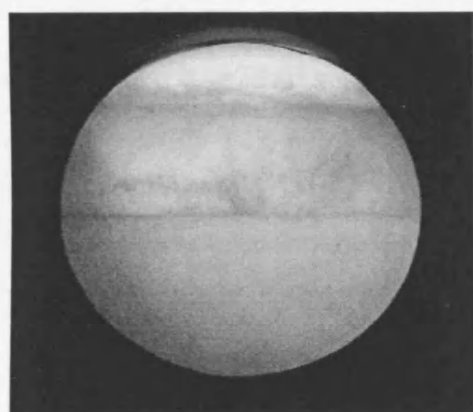
With an increase in the temperature the meniscus between the gas and the liquid begins to disappear
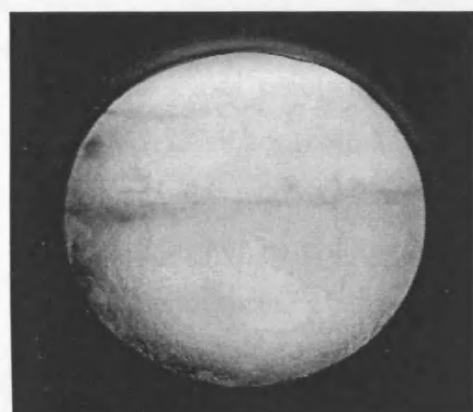
On further increase of the temperature the meniscus is even less apparent as the densities of the gas and liquid are similar

The critical temperature and pressure have been reached and one homogeneous supercritical phase is observed

Figure 1.2 The stages of forming a sc fluid[5]

Not all properties of sc fluids are intermediate between those of gases and liquids; compressibility and heat capacity, for example, are significantly higher near the critical point than they are in liquids or gases. Properties of a compound may change drastically with pressure close to the critical point but most show no discontinuity.

The majority of studies involving sc fluids have focused on carbon dioxide (CO_2), ethene, ethane and water as solvents. The first three fluids all have critical temperatures below 308.15 K. As a general trend it is seen that the greater the polarity of a substance the higher its critical temperature.[6] The polarity of water would make it an ideal solvent but unfortunately it has critical values (T_c = 647.35 K, p_c = 220.5 bar)[7] that make it impractical for widespread use in industrial applications. Carbon dioxide (T_c = 304.55 K, p_c = 72.3 bar)[8] is by far the most widely used sc fluid because it is non-toxic, non-flammable and readily available in high purity with a very accessible critical temperature. Carbon dioxide also exhibits low miscibility with water and is a moderately good solvent for many low-to-medium molecular weight organics. Reported solubilities for non-polar solids and liquids in sc CO_2 range between 0.1 to 10 mol %.[9]

The major problem encountered with sc CO_2 and other commonly used sc fluids, such as ethane, is that they are non-polar, which precludes the dissolution of a number of polar solutes. This can be overcome to an extent by the introduction of polar modifiers or an appropriate surfactant but these have their own disadvantages associated with them. Halogenated aliphatic compounds have also been investigated as alternative sc solvents because they are more polar than CO_2 and still have accessible critical constants.[10,11] More recently still it has been suggested that hydrofluorocarbons are a promising class of sc solvents because they are relatively polar yet still exhibit moderately low critical constants.[12]

1.3 Hydrofluorocarbons

Hydrofluorocarbons (HFCs) have replaced a number of chlorofluorocarbons (CFCs) in the refrigeration and propellants industries[13,14] and without justification HFCs have been associated with the same environmental problems as CFCs. The environmental impact of these HFCs was the focus of intensive research in 1989 by the Alternative Fluorocarbons Environmental Acceptability Study (AFEAS). This research program concluded that HFCs contain no chlorine and do not contribute to

ozone depletion because hydroxyl radicals break them down in the lower atmosphere to simple inorganic species that are readily present in the atmosphere.[15,16] It is found however, that a few HFCs may form trifluoroacetyl halides that will dissolve in water to give trifluoroacetate (TFA) salts.[16,17] These salts will then be present in rain and seawater at very low concentrations but micro-organisms naturally present in soils and sediments can degrade them.

Another environmental concern facing the Earth is the greenhouse effect. Hydrofluorocarbons do not accumulate in the atmosphere to the same extent as CFCs so their contribution to the greenhouse effect is greatly reduced. Atmospheric decay rates of HFCs do vary but the lifetimes are much less than those of CO_2. For a relatively short lived gas like HFC 134a, the concentration and hence contribution to global warming drops rapidly to zero after emission but the contribution due to emission of a long lived gas like CO_2 persists for more than 500 years as shown in Figure 1.3.[16]
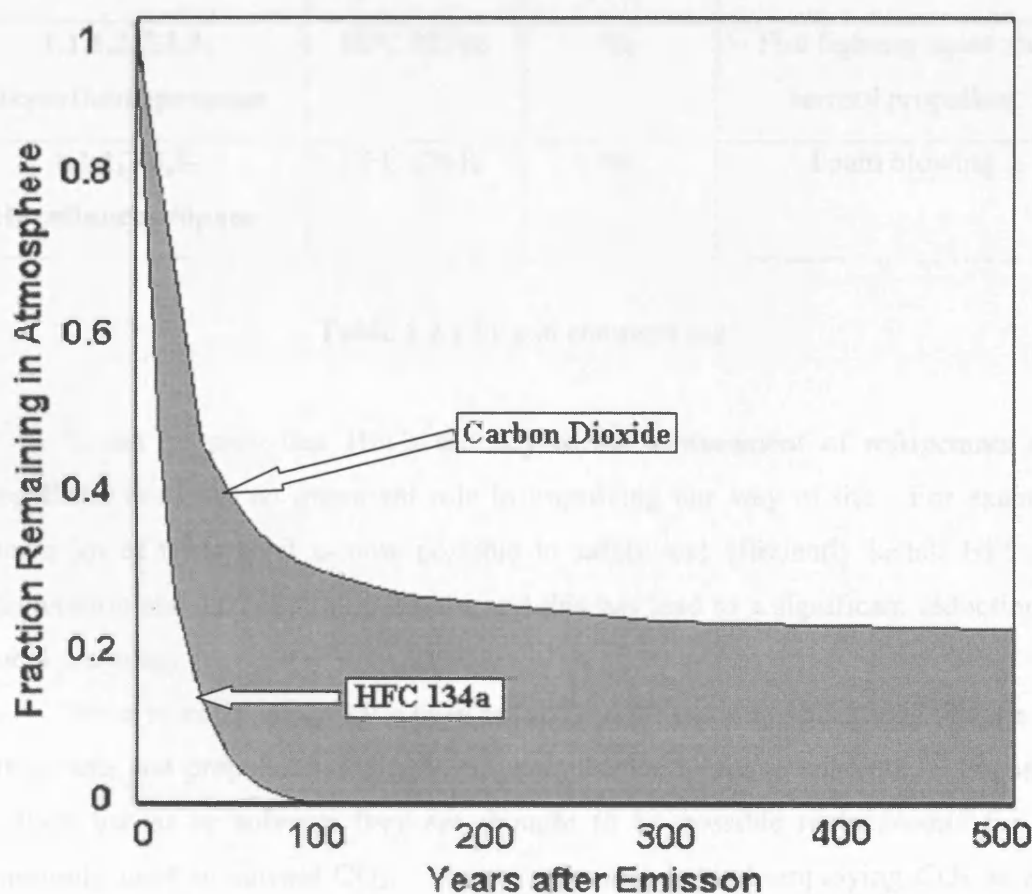
Figure 1.3 The decay of HFC 134a compared to CO_2[16]

6

After much work within the gases industry HFCs were found to have the most useful properties to be replacements for CFCs and lead candidates were identified and developed to try to meet the needs of the refrigeration, foam blowing, medical and specialist aerosol industries. These are summarised in Table 1.2.[18] In these applications specific properties of the HFCs such as benign toxicity, solvency, density, boiling point and flammability are exploited.

Name	Abbreviation	Flammable	Application
1,1,1,2-Tetrafluoroethane	HFC 134a	No	Refrigeration, aerosol, foam blowing and medical
1,1-Difluoroethane	HFC 152a	Yes	General aerosol
Difluoromethane	HFC 32	Yes	Refrigeration blends
1,1,1-Trifluoroethane	HFC 143a	Yes	Refrigeration blends
Pentafluoroethane	HFC 125	No	Refrigeration blends
1,1,1,2,3,3,3-Heptafluoropropane	HFC 227ea	No	Fire fighting agent and aerosol propellant
1,1,1,3,3,3-Hexafluoropropane	HFC 236fa	No	Foam blowing

Table 1.2 HFCs in common use

It can be seen that HFCs are key to the replacement of refrigerants and propellants and play an important role in improving our way of life. For example after a lot of research it is now possible to safely and efficiently install HFCs in refrigeration and air conditioning units and this has lead to a significant reduction in global warming.

More recently HFCs have been researched for use on applications outside the refrigerants and propellants industry, in particular their uses as solvents.[19] Focusing on their use as sc solvents they are thought to be possible replacements for the commonly used sc solvent CO_2. The main reasons behind employing CO_2 as a sc solvent are thought to be environmental and economic factors. However, the major problem that is encountered with the use of sc CO_2 for extraction and reaction

purposes is the low solubility of polar solutes due to its low dielectric constant. The "green" aspect of using sc CO_2 as a solvent can then be negated if large volumes or high pressures are required to solubilise the solutes because of the large energy contribution associated with such processes. To circumvent these problems, polar modifying agents have been added to CO_2 to increase the solvent polarity. These modifying fluids add to the cost of the process and may also be left as residues, which may be problematic if the product is to be used for human consumption.[20-22]

Recently, it has been highlighted that some HFC fluids such as HFC 32 and HFC 134a are relatively polar solvents in the sc state[23-25] and this allows them to be used as efficient extraction and reaction solvents either on there own or in conjunction with CO_2. These solvents are also readily available and non-toxic. Three well-researched HFCs are shown in Table 1.3 where it can be seen that they all have critical temperatures below 375 K[26,27] and gaseous dipole moments greater than 1.5 D.[13,14]

Hydrofluorocarbon	T_c (K)	p_c (bar)	ρ_c (kg m^{-3})	μ (D)
1,1,1,2-Tetrafluoroethane (HFC 134a)	374.21	40.59	511.90	2.06
Difluoromethane (HFC 32)	351.26	57.82	424.00	1.99
Pentafluoroethane (HFC 125)	339.33	36.29	571.30	1.56

Table 1.3 The critical constants and dipole moments of HFC 134a, HFC 32 and HFC 125

Journal and patent literature contain numerous possible applications outside the refrigeration and propellants industry where HFCs can be advantageous. Some of these applications include dry-cleaning, the treatment of sludge to remove contaminants, [28] natural product extraction[19] and HPLC mobile phases.[29-31]

1.4 Industrial and Academic Applications of Supercritical Fluids

The unique solvent properties of sc fluids offer a series of technical advantages that has resulted in their exploitation in chromatography (section 1.4.1),[32,33] electrochemical applications (section 1.4.2),[12,34-38] extraction and separation processes (section 1.4.3)[39,40] and chemical reactions (section 1.4.4).[41]

1.4.1 Chromatography

In the 1960s it was recognised that sc mobile phases could be employed in chromatographic analysis.[42] Supercritical fluid chromatography (SFC) uses sc gases as a mobile phase[42,43] to transport a mixture of substances over the stationary phase. The solvent power of the mobile phase is determined by its density and so, for a sc fluid, can easily be modified by pressure. Furthermore, separation of the eluted compounds is easily achieved by pressure release. Due to the enhanced mass transport properties in sc fluids, high molecular mass compounds can be dissolved and efficiently separated at relatively low temperatures.[43,44] Supercritical fluid chromatography is therefore an important analytical technique that can provide a fundamental knowledge of solubility and partitioning behaviour of a wide range of molecular mass compounds which is essential in designing chemical processes.

Hupe et al.[45] have reviewed the theory and fundamentals behind SFC in detail. The most commonly employed mobile phase in SFC is sc CO_2[44,46-48] but, as this is a relatively non-polar fluid, modifiers are often added to change the solvent strength of the mobile phase.[49-51] Using a more polar sc fluid can increase the solvent strength of a mobile phase and recent work by Vayisoglu-Giray et al.[31] and Ineos Fluor[19] have taken advantage of this by employing HFC 134a in its liquid and sc state. It would appear that for many separations HFC 134a offers better separation than sc CO_2 and if the process is to be scaled-up, HFC 134a is potentially easier and less expensive than that employing sc CO_2 due to the lower pressures required.[19]

Supercritical fluid chromatography is a useful analytical technique and as awareness in the field has increased so has the research. Early studies included the separation of oligomers,[52] polystyrene,[53] and high molecular weight compounds.[54] Analysis of aromatics in diesel fuel[55] and plant materials[56] have also been studied by this technique. A recent review by Chester and Pinkston[57] describes some of the most recent applications that have employed SFC. These include food related separations, work with natural products and applications in forensic science.[58,59]

1.4.2 Electrochemical Applications

If electrochemical investigations are to be carried out in a solvent-electrolyte system the medium must display suitably high conductivity and electrochemical stability over the potential range of interest. Therefore, to understand voltammetry in sc fluids it is useful to take conductivity measurements for a range of fluid conditions.

Most work into electrical conductivity of sc media has focused on aqueous solutions[60-63] and by contrast, the electrical conductivity of electrolytes in non-aqueous solutions has received relatively little attention.[12,64-66] The conductivity of the medium is important for electrosynthesis but the viscosity of the medium also has to be considered as this affects the rate of mass transport of an electroactive species to and from the electrode surface. Supercritical fluids have a low viscosity (Table 1.1), which leads to enhanced rates of mass transport and therefore their possible applicability as solvents for electrosynthesis.

Bard and co-workers have performed the most extensive investigations into electrochemistry in sc media[34,35,67-69] employing a number of polar sc solvents such as acetonitrile (T_c = 547.85 K, p_c = 48.3 bar), ammonia (T_c = 406 K, p_c = 112.5 bar) and water (T_c = 645.35 K, p_c = 221 bar).

Olsen and Tallman have recently demonstrated that polar halogenated solvents can be used for electrochemical investigations in both the liquid and sc states.[12,70] Their work showed that chlorodifluoromethane (T_c = 406.15 K, p_c = 49.7 bar) and trifluoromethane (T_c = 298.25 K, p_c = 47.5 bar) could be made conducting via the dissolution of tetrabutylammonium tetrafluoroborate (TBABF$_4$).[12] However, because the dielectric constant is still quite low (ε = 2.31) problems with solubility, ion association and electrolyte adsorption on the electrode surface are still encountered. From their results they proposed that hydrofluorocarbon solvents would be extremely promising candidates for use in sc electrochemistry.

Abbott and co-workers have carried out electrochemical investigations using hydrofluorocarbon solvents,[37,65,66] in particular liquid and sc HFC 134a and HFC 32. In their work they illustrated that these solvents are ideal for electrochemical investigations in the sc state and that the redox potential of the commonly used standard solute ferrocene in electrochemical investigations is largely unaffected by changes in pressure. Results also suggested that ionic atmosphere effects are insignificant in sc fluids at lower pressures due to low ionic strengths and high ionic mobilities.

1.4.3 Extraction and Separation Processes

The solubility of compounds in sc fluids has been the most extensively investigated area of sc fluid research. The solubility is the concentration or mole

fraction of a substrate in the sc phase when it is in equilibrium with the pure substrate, at a particular temperature and pressure. Solubility data give an insight into how well a sc fluid performs as a solvent for a particular solute, which is of key importance in process design. The solubility of a compound is mainly influenced by its chemical functionality, nature of the sc fluid solvent, and the operating conditions. Although the solubility and extractability of a compound in a sc fluid are governed by different molecular interactions (solute-solvent interactions versus solute-matrix or solute-solute interactions), knowledge of the solubility of a compound in a sc fluid gives an indication of the extractability of that compound in that sc solvent.

Solubility data provide important information on the efficacy of separation between the solute and the sc fluid and therefore the employment of this in supercritical fluid extraction (SFE), where solvent properties can be tuned to maximise the solubility of the extract.[39,40] An ideal extraction method should be rapid, simple and inexpensive to perform. It should yield quantitative recovery of the target analytes without loss or degradation and the sample obtained should be immediately ready for analysis without additional concentration or fractionation steps. No additional laboratory wastes should be generated. Liquid solvent extractions fail to meet a number of these goals but SFE has emerged as a promising tool to overcome these difficulties.

The SFE literature shows that approximately 98 % of developed applications have employed CO_2 as the extractant. Supercritical CO_2 has significant advantages as it has accessible critical parameters, low toxicity and chemical inertness. However, the main difficulty in using sc CO_2 arises when polar analytes are to be extracted. To overcome this drawback of CO_2 two strategies are employed. The first is to make the CO_2 more polar by adding small amounts of a more polar fluid e.g. methanol and the second possibility is to use an extractant fluid which is more polar.[71]

The development of sc fluids for use in extraction processes started in the 1960s primarily in Europe then later in the United States. European researchers emphasised extraction from botanical substrates, for example, spices,[72,73] herbs,[74] coffee[39,40,75] and tea,[39,40,76] using predominately sc CO_2. By the 1980s there were several large-scale SFE processes in operation in Germany, the United Kingdom and the United States. The largest of these processes is the decaffeination of coffee and tea.[40] For the decaffeination of coffee the wet green coffee beans are extracted and for tea the already fermented tea is treated. The extraction of hops is the second

largest application because nearly all producers of hop extracts have now changed from the methylene chloride process to the sc fluid process.[39] The number of commercial SFE plants as of 2000 is shown in Table 1.4.[77]

After two decades of extraction process development that has been dedicated, mainly, to natural products many new applications are under investigation or at commercial scale[39,40,77] as shown in Table 1.4. Other examples include the treatment of soil and waste[78-80] and at present industrial sectors rely on CFCs to clean metals, plastics, composites, ceramics, optical materials and a wide variety of other matrixes from organic components but SFE has been studied and identified as a possible alternative.[71,77]

Sector	Number of Plants	America	Asia/Australia	Europe
Coffee & Tea	5	1	0	4
Hops	7	4	1	2
Nicotine	3	1	1	1
Chemistry	5	3	1	1
Environmental	5	2	3	0
Spices	12	1	5	6
Fats & Oils	8	0	3	5
Medicinal Plants	7	0	1	6
Flavours	7	0	3	4
Total	59	12	18	29

Table 1.4 Commercial plants for SFE[77]

In synthetic chemistry, SFE is an attractive alternative to conventional methods for the purification of reaction products, such as vitamins, pharmaceuticals and many other high-value products.[81] However, its technical use is mainly restricted to applications in the food industry for extraction from natural products[82] and in some cases for the fractionation of the products.[83] For example, in paprika extraction[84] the first step involves separation of oleoresins and in the second step aroma and essential

oil. This also occurs in rosemary extraction where the antioxidants are separated from the aroma and essential oil.[85,86]

Supercritical fluid extraction is a growing area and too many applications have been studied to mention here. The main potential areas of interest at present in SFE are in the purification of polymers, which takes advantage of the different solubilities of polymers depending on the chain length, and the removal of flame-retardants from plastic materials, especially electronic parts. Supercritical fluids have also found use in the textiles industry. They can be used for cleaning, which at present uses halogenated solvents and also for the dyeing of textiles where the dyestuff is dissolved in the sc fluid and this mixture penetrates the whole fibre. By controlled pressure release the dyestuff remains in and on the fibres.[87]

1.4.4 Chemical Reactions

Another area of interest for sc fluids is their use in the field of reaction solvents where the range of applications is rapidly widening.[41] Excluding the fact that nature has been doing chemistry in sc H_2O in the Earth's crust for a very long time, the first reactions observed in sc fluids were reported in the nineteenth century. It was Baron Cagniard de La Tour who noted in 1822, that near critical water seemed particularly reactive.[88] His pioneering work initiated studies of sc fluid reactions during the next few decades in H_2O at temperatures above T_c, as reviewed in great detail by Morey.[89]

There are numerous advantages associated with the use of sc fluids in chemical synthesis, all of which are based on the unique combination of properties of either the materials themselves or the sc state. A very important incentive for the use of sc fluids in synthetic chemistry comes from the increasing demand for environmentally and toxicologically benign processes for the production of high value chemicals. Many reactions that occur in sc fluids can occur in liquid solvents but there are considerable examples where the use of a sc fluid can cause the rate of reaction to increase.[41,90,91] Supercritical fluids have a number of unique properties that may bring about an increase in the rate but it is not always easy to identify the dominant contributor. In general, the unique combination of gas-like diffusivity and viscosity, the liquid-like density and the pressure-dependent solvating power and/or polarity is the fascinating basis for chemical research using sc fluid solvents in synthesis. These factors account for the unusual reactivity in this media and it should

be noted that different types of reaction might benefit particularly from a specific property.

Since 1945 the sc fluid literature has become extensive with a sharp increase in publications over the last 5 to 10 years. The literature covers a wide range of reactions including inorganic, organometallic, organic, photochemical, polymerisation and catalytic.[41,92] Even though a wide range of reactions have been studied the solvent commonly utilised in these reactions is sc CO_2.

A unique sc fluid property is that it has no surface tension and can diffuse rapidly to occupy the entire volume of a system. This means that if any other gases are introduced to the system they too will diffuse to fill the entire volume and therefore the sc fluid and the gases will be totally miscible. Processes such as hydrogenation,[41,92-96] hydroformylation[41,92,97,98] and oxidation[41,92,99] can take advantage of the complete miscibility of permanent gases H_2, CO, and O_2 respectively in a sc fluid. Rathke et al. who reported the hydroformylation of propylene using sc CO_2[98] observed this advantage. In 1994 Noyori and co-workers reported a hydrogenation reaction also employing sc CO_2.[94] Both groups were looking for a method of avoiding the previously encountered problem of gas-liquid mixing. Noyori carried out the hydrogenation of CO_2 to formic acid using homogeneous ruthenium (II) phosphine catalysts[94] and from this work they found this reaction to be very rapid. When compared to the same reaction in conventional solvents it was found that the reaction proceeded 18 times faster in sc CO_2. Since this initial work a number of research groups have looked into the advantages of carrying out reactions that involve a gaseous reagent. From this research it has been shown that increased gas miscibility and the fact that the reaction parameters can be controlled independently give optimum reaction selectivity, increased reaction rate and very high conversion.[41,92,100-102]

A number of studies have been devoted to determining the influence of either bulk or local density variations on stoichiometric reactions.[103-105] A classical example is the Diels-Alder reaction, where the endo/exo and ortho/para selectivity appears to be controlled to some extent by variation of the bulk density.[106-111] Several groups have investigated these density effects on rates and selectivities where a number of conflicting results and conclusions have been drawn.[41,92,103-111]

Paulaitis and Alexander carried out the first Diels-Alder reaction in a sc fluid. They studied the effect of sc CO_2 pressure on the reaction rate of maleic anhydride

and isoprene.[106] This reaction was chosen as the mechanism was thought to be the same irrespective of the solvent medium. The conclusions drawn from their studies showed that the reaction rate increased slightly with increasing pressure.

Kim and Johnston took the Diels-Alder reaction a step further and looked at the product selectivity as a function of sc fluid density.[107] They studied the reaction of cyclopentadiene and methyl acrylate because two isomeric products are formed (endo and exo). Results showed that the endo selectivity increases with pressure (density) at constant temperature but at constant pressure the selectivity decreases with temperature. Their selectivity observations were explained in terms of the difference in dipole moment of the endo and exo products with the endo being more polar.

These Diels-Alder reactions were some of the earliest reported synthetic organic reactions in sc media. Since these pioneering studies, numerous other organic reactions have been carried out in sc CO_2 as reviewed recently by Rayner et al.[92] There are too many reactions to discuss in this section and for a more thorough treatise the readers are directed to other literatures.[41,92] Industrial uses of sc fluids as reaction media are also becoming more prolific and include for example the synthesis of ammonia, low density polyethylene and the oxidative destruction of chemical wastes using sc H_2O.[41]

The majority of organic reactions have been carried out in sc CO_2 and even though its numbers are dramatically lower, sc H_2O is the second most common sc solvent. The use of sc solvents for reactions that bridge the gap between non-polar CO_2 and polar H_2O are very limited. This is surprising since these medium polarity solvents may overcome some of the problems encountered with reagent solubility in sc CO_2 and the conditions used will be nowhere near as harsh as those using sc H_2O. Some examples can be found in the literature where more polar solvents than CO_2 have been employed and the advantages of these solvents are apparent.

The photodimerisation of isophorone in sc fluoroform (CHF_3) and CO_2 is reported by Johnston et al. as a function of pressure.[112] This reaction produces three isomeric products, one being polar and two being relatively non-polar. Their investigation looked at the selectivity of the products formed and compared the results of the two fluids. In the more polar sc CHF_3, where its dielectric constant changes with pressure the product ratio was found to be dependent on pressure. However, in

sc CO_2 the product ratio was independent of pressure and the product ratio was found to be lower (0.1:1 compared to 1:1 in sc CHF_3).

Fox and co-workers demonstrated that the rate of the Michael addition of piperidine to methyl propiolate in sc CHF_3 and non-polar sc ethane depends on fluid density.[113] They saw a difference in the observed rate constants between the two solvents that was attributed to the reaction's dependence on the solvent dielectric constant. The reaction proceeds through a highly polar transition state, which would be consistent with better stabilisation by the more polar solvent sc CHF_3.

Other reactions have been carried out in medium polarity sc media and examples include the polymerisation of methyl methacrylate in sc HFC 32,[114] catalytic cyclopropanation in sc CHF_3[115] and an aldol reaction in sc CHF_3.[116] In these reactions the pressure dependency of the dielectric constant was found to influence reaction rates, mechanisms and selectivities.

1.5 References

(1)   Laider K. *Chemical Kinetics*, 3 ed.; Harper Collins Publishers: New York, **1987**.

(2)   Hannay J, B.; Hogart J. *Proc. R. Soc. London* **1879**, *29*, 324.

(3)   Stanley H, E. *Phase Transitions and Critical Phenomena*; Clarendon press: Oxford, **1987**.

(4)   van Wase U.; Swaid I.; Schneider G, M. *Angew. Chem. Int. Ed. Engl.* **1980**, *19*, 575.

(5)   http://www.chem.leeds.ac.uk/People/CMR/.

(6)   Savage P, F.; Goplan S.; Mizan T, I.; Martino C, J.; Brook E, E. *AIChE J.* **1995**, *41*, 1723.

(7)   Reid R, C.; Prausnitz J, M.; Poling B, E. *The Properties of Gases and Liquids*, 4 ed.; McGraw-Hill: New York, **1987**.

(8)   Vermilyea D, A.; Indig M, E. *J. Electrochem. Soc.* **1972**, *119*, 39.

(9)   Bartle K, D.; Clifford A, A.; Jafar S, A.; Shilstone G, F. *J. Phys. Chem. Ref. Data* **1991**, *20*, 713.

(10)   Yonker C, R.; Futakami M.; Kobayashi T.; Yamasaki K. *J. Phys. Chem.* **1986**, *90*, 3022.

(11)   Kajimoto O.; Futakami M.; Kobayashi T.; Yamasaki K. *J. Phys. Chem.* **1988**, *92*, 1347.

(12)   Olsen S, A.; Tallman D, E. *Anal. Chem.* **1996**, *68*, 2054.

(13)   Meyer C, W.; Morrison G. *J. Phys. Chem.* **1991**, *95*, 3860.

(14)   Meyer C, W.; Morrison G. *J. Chem. Eng. Data* **1991**, *36*, 409.

(15)   Ravishankara A, R. *Science* **1994**, *263*, 71.

(16)   http://www.afeas.org.

(17)   Frank H; Christoph E, H.; Holm-Hansen O; Bullister J, L. *Environ. Sci. Technol.* **2002**, *36*, 12.

(18)   Noakes T. *J. Fluor. Chem.* **2002**, *118*, 35.

(19)   Corr S. *J. Fluor. Chem.* **2002**, *118*, 55.

(20)   Anitescu G.; Tavlarides L, L. *J. Supercrit. Fluids* **1997**, *11*, 37.

(21)   Anitescu G.; Tavlarides L, L. *J. Supercrit. Fluids* **1999**, *14*, 197.

(22)   Foster N, R.; Singh H.; Yun J, S, L.; Tomasko D, L.; MacNaughton S, J. *Ind. Eng. Chem. Res.* **1993**, *32*, 2849.

(23)   Abbott A, P.; Eardley C, A. *J. Phys. Chem. B* **1998**, *102*, 8574.

(24)   Abbott A, P.; Eardley C, A.; Tooth R, J. *J. Chem. Eng. Data* **1999**, *44*, 112.

(25)   Abbott A, P.; Eardley C, A. *J. Phys. Chem. B* **1999**, *103*, 2504.

(26)   Tillner-Roth R.; Baehr H, D. *J. Phys. Chem. Ref. Data* **1994**, *23*, 657.

(27)   Tillner-Roth R.; Yokozeki A. *J. Phys. Chem. Ref. Data* **1997**, *26*, 1273.

(28)   Wilde P. WO 9824517 **1998**.

(29)   Handley A, J.; Clarke R, D.; Powell R, L. US 5824225 **1998**.

(30)   Cantrell G, O.; Blackwell J, A. *J. Chromatogr. A* **1997**, *782*, 237.

(31)   Vayisoglu-Giray E, S.; Johnson B, R.; Frere B, G, A, M.; Bartle K, D.; Clifford A, A. *Fuel* **1998**, *77*, 1533.

(32)   Yonker C, R.; Wright B, W.; Udseth H, R.; Smith R, D. *Ber. Bunsen-Ges. Phys. Chem.* **1984**, *88*, 908.

(33)   Wright B, W.; Smith, R. D. *Chromatographia* **1984**, *18*, 542.

(34)   Crooks R, M.; Fan F, F.; Bard A, J. *J. Am. Chem. Soc.* **1984**, *106*, 6581.

(35)   Crooks R, M.; Bard A, J. *J. Electroanal. Chem.* **1988**, *243*, 117.

(36)   Philips M, E.; Deakin M, R.; Novotny M, V.; Wightman R, M. *J. Phys. Chem.* **1987**, *91*, 3934.

(37)   Abbott A, P.; Eardley C, A.; Harper J, C.; Hope E, G. *J. Electroanal. Chem.* **1998**, *457*, 1.

(38)   Abbott A, P.; Harper J, C. *Phys. Chem. Chem. Phys.* **1999**, *1*, 839.

(39)   Taylor L, T. *Supercritical Fluid Extraction*; J. Wiley & Sons: New York, **1996**.

(40)   McHugh M.; Krakonis V, J. *Supercritical Fluid Extraction*, 2 ed.; Butterworth-Heinemann: Boston, **1994**.

(41)   Jessop P, G.; Leitner W. *Chemical Synthesis using Supercritical Fluids*; Wiley-VCH: Weinheim, **1999**.

(42)   Klesper E.; Corwin A, H.; Turner D, A. *J. Org. Chem.* **1962**, *27*, 700.

(43)   Conaway J, E.; Graham J, A.; Rogers L, B. *J. Chromatogr. Sci* **1978**, *16*, 102.

(44)   Smith R, M. *Supercritical Fluid Chromatography*; Royal Society of Chemistry: London, **1988**.

(45)   Hupe K, P.; McNair H, M.; Kok W, T.; Bruin G, J.; Poppe H.; Poole C.; Chester T, L.; Wimalasena R, L.; Wilson G, S. *LC-GC* **1992**, *10*, 211.

(46)   Grob K. *J. High. Res. Chromatogr.* **1983**, *6*, 178.

(47)   Wheeler J, R.; McNally M, E. *J. Chromatogr.* **1987**, *410*, 343.

(48) Wu N.; Chen Z.; Medina J, C.; Bradshaw J, S.; Lee M, L. *J. Microcolumn Sep.* **2000**, *12*, 454.

(49) Pyo D. *Microchem. J.* **2001**, *68*, 183.

(50) Gritti F.; Felix G.; Archard M-F.; Hardouin F. *Chromatographia* **2001**, *53*, 201.

(51) Brenner B, A. *Anal. Chem.* **1998**, *70*, 4594.

(52) Schmitz F, P.; Klesper E. *Polymer Bulletin* **1981**, *14*, 679.

(53) Schmitz F, P. *Polymer Comm.* **1983**, *24*, 142.

(54) Jackson W, P.; Markides K, E.; Lee M, L. *J. High Resolut. Chromatogr., Chromatogr. Comm.* **1986**, *9*, 213.

(55) Brooks M, W.; Uden P, C. *J. Chromatogr.* **1993**, *637*, 179.

(56) Namiesnik J.; Gorecki T. *JPC-J. Planar Chromat-Mod. TLC* **2000**, *13*, 404.

(57) Chester T, L.; Pinkston J, D. *Anal. Chem.* **2002**, *74*, 2801.

(58) Radcliffe C.; Maguire K.; Lockwood B. *J. Biochem. Biophys. Methods* **2000**, *43*, 261.

(59) McAvoy Y.; Dost K.; Jones D, C.; Cole M, D.; George M, W.; Davidson G. *Forensic Science International* **1999**, *99*, 123.

(60) Franck E, U. *Z. Phys. Chem., N. F.* **1956**, *8*, 92.

(61) Quist A, S.; Marshall W, L. *J. Phys. Chem.* **1965**, *69*, 2984.

(62) Yeatts L, B.; Dunn L, A.; Marshall W, L. *J. Phys. Chem.* **1971**, *75*, 1099.

(63) Marshall W, L. *J. Chem. Eng. Data* **1987**, *32*, 221.

(64) Abbott A, P.; Harper J, C. *J. Chem. Soc., Faraday Trans.* **1996**, *92*, 3895.

(65) Abbott A, P.; Eardley C, A. *J. Phys. Chem. B* **2000**, *104*, 9351.

(66) Abbott A, P.; Durling N, E. *Phys. Chem. Chem. Phys.* **2001**, *3*, 579.

(67) McDonald A, C.; Fan F, F.; Bard A, J. *J. Phys. Chem.* **1986**, *90*, 796.

(68) Cabrera C, R.; Bard A, J. *J. Electroanal. Chem.* **1989**, *273*, 147.

(69) Bard A, J.; Faulkner L, R. *Electrochemical Methods*; Wiley: New York, **1980**.

(70) Olsen S, A.; Tallman D, E. *Anal. Chem.* **1994**, *66*, 503.

(71) Gamse T.; Marr R. *Preceedings of the 2nd European School on Industrial Applications of Supercritical State Fluid Technology* **2001**, *Barcelona*, April 2.

(72) Illes V.; Daood H, G.; Biacs P, A.; Gnayfeed M, H.; Meszaros B. *J. Chromatogr. Sci* **1999**, *37*, 345.

(73) Lack E.; Seidlitz H. *Process Technol. Proc.* **1996**, *12*, 253.

(74)   Ma X.; Yu X.; Zheng Z.; Mao J. *Chromatographia* **1991**, *32*, 40.

(75)   Dean J, R.; Liu B.; Ludkin E. *Methods Biotecnol.* **2000**, *13*, 17.

(76)   Chang C, J.; Chiu K-L.; Chen Y-L. *Food Chem.* **1999**, *68*, 109.

(77)   Gamse T. *High Pressure Chemical Engineering Summer School* **2002**, *Graz/Maribor*, June 27th.

(78)   Misch B.; Firus A.; Brunner G. *J. Supercrit. Fluids* **2000**, *17*, 227.

(79)   Sahle-Demessie E. *Environ. Technol.* **2000**, *21*, 447.

(80)   Laitnen A.; Michaux A.; Aaltanen O. *Environ. Technol.* **1994**, *15*, 715.

(81)   Chester T, L.; Pinkston J, D.; Raynie D, E. *Anal. Chem.* **1998**, *70*, 301.

(82)   Steytler D. *Sep. Processes Food Biotechnol. Ind.* **1996**, 17.

(83)   Zosel K. *Angew. Chem. Int. Ed. Engl.* **1978**, *17*, 702.

(84)   Vesper H.; Nitz S. *Adv. Food Sci.* **1997**, *17*, 172.

(85)   Senorans F, J.; Ibanez E.; Cavero S.; Tabera J.; Reglero G. *J. Chromatogr. A* **2000**, *870*, 491.

(86)   Tena M, T.; Valcorcel M.; Hidalgo P, J.; Ubera J, L. *Anal. Chem* **1997**, *69*, 521.

(87)   Montero G, A.; Smith C, B.; Hendrix W, A.; Butcher D, L. *Ind. Eng. Chem. Res.* **2000**, *39*, 4806.

(88)   Cagniard de la Tour C. *Ann. Chim. Phys.* **1822**, *21*, 178.

(89)   Morey G, W.; Niggli P, J. *J. Am. Chem. Soc* **1913**, *35*, 1086.

(90)   King J, W.; Holliday R, L.; List G, R.; Sisyder J, M. *J. Amer. Oil Chem. Soc.* **2001**, *78*, 107.

(91)   Lin B,; Akgerman A. *Ind. Eng. Chem. Res.* **2001**, *40*, 1113.

(92)   Oakes S, R.; Clifford A, A.; Raynor C, M. *J. Chem. Soc. Perkin Trans.* **2001**, *1*, 917.

(93)   Jessop P, G.; Hsiao Y.; Ikariya T.; Noyori R. *J. Am. Chem. Soc.* **1996**, *118*, 344.

(94)   Jessop P, G.; Ikariya T.; Noyori R. *Nature* **1994**, *368*, 231.

(95)   Tsang C, Y.; Streett W, B. *Chem. Eng. Sci.* **1981**, *36*, 993.

(96)   Xiao .J; Nefkens S, C, A.; Jessop P, G.; Ikariya T.; Noyori R. *Tetrahedron Lett.* **1996**, *37*, 2813.

(97)   Koch D.; Leitner W. *J. Am. Chem. Soc* **1998**, *120*, 13398.

(98)   Rathke J, W.; Klingler R, J.; Krause T, R. *Organometallics* **1991**, *10*, 1350.

(99)   Nelson W, M.; Puri I, K. *Ind. Eng. Chem. Res.* **1997**, *36*, 3446.

(100) Jessop P, G.; Hsiao Y.; Ikariya T.; Noyori R. *J. Am. Chem. Soc.* **1994**, *116*, 8851.

(101) Hitzler M, G.; Smail F, R.; Ross S, K.; Poliakoff M. *Org. Proc. Res. Dev.* **1998**, *2*, 137.

(102) Hitzler M, G.; Poliakoff M. *J. Chem. Soc., Chem. Comm.* **1997**, 1667.

(103) Thompson R, L.; Glaser R.; Bush D.; Liotta C, L.; Eckert C, A. *Ind. Eng. Chem. Res.* **1999**, *38*, 4220.

(104) Reaves J, T.; Roberts C, B. *J. Chem. Soc., Chem. Eng. Comm.* **1999**, *171*, 117.

(105) Dillow A, K.; Brown J, S.; Liotta C, L.; Eckert C, A. *J. Phys. Chem. A* **1998**, *102*, 7609.

(106) Paulaitis M, E.; Alexander G, C. *Pure Appl. Chem.* **1987**, *59*, 61.

(107) Kim S.; Johnston K, P. *J. Chem. Soc., Chem. Eng. Comm.* **1988**, *63*, 49.

(108) Ikushima Y.; Saita N.; Arai M.; Blanch H, W. *J. Phys. Chem.* **1995**, *99*, 8941.

(109) Isaacs N, S.; Keating N. *J. Chem. Soc., Chem. Comm.* **1992**, 876.

(110) Weinstein R, D.; Renslo A, R.; Vanheiser R, L.; Harns J, G.; Terter J, W. *J. Phys. Chem.* **1996**, *100*, 12337.

(111) Korzenski M, B.; Kalis J, W. *Tetrahedron Lett.* **1997**, *38*, 5611.

(112) Hrnjez B, J.; Mehta A, J.; Fox M, A.; Johnston K, P. *J. Am. Chem. Soc.* **1989**, *111*, 2662.

(113) Rhodes T, A.; O'Shea K.; Bennett G.; Johnston K, P.; Fox M, A. *J. Phys. Chem.* **1995**, *99*, 9903.

(114) Abbott A, P.; Durling N, E.; Hope E, G.; Lange S.; Vakusic S. *in press* **2003**.

(115) Wynne D, C.; Jessop P, G. *Angew. Chem. Int. Ed. Engl.* **1999**, *38*, 1143.

(116) Mikami K.; Matsukawa S.; Kayaki Y.; Ikariya T. *Tetrahedron Lett.* **2000**, *41*, 1931.

CHAPTER 2

EXPERIMENTAL

2.1 Materials

2.1.1 Solvents

The solvents used in this work are shown in Table 2.1 and all solvents were used as received.

Solvent	Abbreviation	Source	Purity
Difluoromethane	HFC 32	Ineos Fluor	>99%
1,1,1,2-Tetrafluoroethane	HFC 134a	Ineos Fluor	>99%
Carbon Dioxide	CO_2	BOC Limited	>99%
Dichloroethane	DCE	BDH Chemicals	98 %
Cyclohexane	CH	Fisher	98 %

Table 2.1 Solvents used in this work

2.1.2 Solutes

The solutes employed in the solubility studies and their purity, molecular weight (MW) and melting points (m.p.) are shown in Table 2.2. Each solute was used as received.

2.1.3 Extraction Capsules

Paracetamol and aspirin capsules used in the extraction studies were supplied by GlaxoSmithKline and used as received. A placebo of the non-active ingredients was also supplied and used as received.

2.1.4 Solvatochromic Probes

The solvatochromic dyes *N,N*-dimethyl-4-nitroaniline (Lancaster, 99 %) and 4-nitroaniline (Aldrich, 99 %) were used as received. The data for Nile Red (Aldrich, 99 %) was taken from the literature.[1,2] Dye concentrations ranged from 10^{-5} to 10^{-6} mol dm^{-3}, such that solute-solute interactions could be ignored.

Solutes	Company	Purity %	MW	m.p. °C
Naphthalene	Fisons	98	128.17	80-82
Anthracene	BDH Chemicals Ltd	97	178.23	216-218
o-**hydroxybenzoic acid**	Fisons	97	138.13	158-160
m-**hydroxybenzoic acid**	BDH Chemicals Ltd	98	138.13	201-203
p-**hydroxybenzoic acid**	BDH Chemicals Ltd	98	138.13	215-217
p-**toluic acid**	Aldrich	98	136.15	180-182
p-**aminobenzoic acid**	BDH Chemicals Ltd	98	137.14	187-189
p-**chlorobenzoic acid**	Aldrich	99	156.57	239-241
o-**chlorobenzoic acid**	Aldrich	98	156.57	138-140
p-**aminophenol**	BDH Chemicals Ltd	98	109.13	188-190
p-**chlorophenol**	BDH Chemicals Ltd	98	128.56	43-45
p-**acetamidophenol**	Aldrich	98	151.17	169-172
Acetyl salicylic acid	BDH Chemicals Ltd	98	180.16	138-140

Table 2.2 Properties of the solutes employed in the solubility studies

2.2 Instrumentation

2.2.1 High Pressure Apparatus

A schematic of the high-pressure apparatus is shown in Figure 2.1. The reaction vessel was constructed from 316 stainless steel and was rated to 1.5 kbar. The internal volume of the cell, lined with a layer of Teflon (1 mm thick), was 24.7 cm^3. An o-ring covered in Teflon was used to provide a high-pressure seal between the head and base of the cell and the electrical feedthroughs (RS Components Ltd.) employed were sealed with swagelok fittings. Prior to each experiment the cell was purged with the appropriate gas. The pressure was then applied using a model 10-500 pump (Hydraulic Engineering Corp.; Los Angeles, CA) driven by compressed air and retained at a given value (± 2 bar) using a UCC type PGE 1001.600 manometer. The temperature of the cell was measured using an iron/constantan thermocouple, the tip of which was in contact with the solvent close to the centre of the cell. This was held at a given value (± 0.5 K) using a CAL 9900 controlled heater.
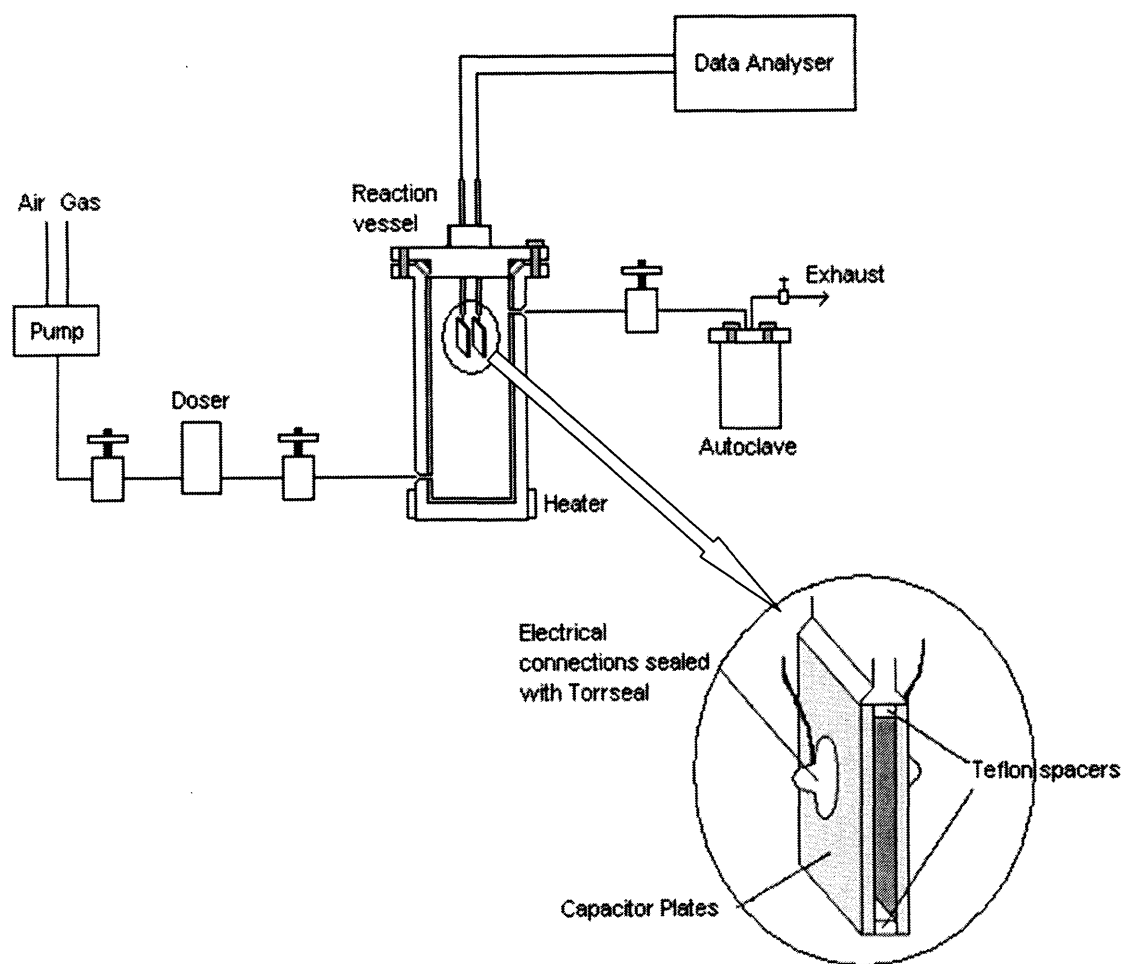
Figure 2.1 High Pressure Apparatus

2.2.2 Capacitance Cell

The cell consists of two rectangular stainless steel plates, (attached to the electrical feedthroughs) with an area of 6.6 cm^2, held 1 mm apart by Teflon spacers as shown in the enlargement in Figure 2.1. The dielectric constant, ε, was measured in this capacitance cell with capacitance C_0 such that the measured capacitance was given by

$$C = \varepsilon C_0 \tag{2.1}$$

Cell capacitances were measured at 65 kHz with a 20 mV ac voltage amplitude using a 1254 frequency response analyser and a 1286 potentiostat (both Solartron Instruments) controlled by ZPLOT software. The acquired data were analysed using ZVIEW software. The cell geometrical capacitance was 14.6 pF. The uncertainty of each capacitance measurement was 50 fF. The capacitor was tested with several pure solvents of known dielectric constant including acetonitrile, dichloromethane, acetone and toluene where the dielectric constant was found to vary by no more than 1 % from literature values. The dielectric constant was calculated from the average cell capacitance obtained from five experimental runs.

2.2.3 Optical Cell

A Shimadzu Model UV-1601 Spectrophotometer was used to measure the solvatochromic shift of 4-nitroaniline and N,N-dimethyl-4-nitroaniline in the visible absorbance region. The optical high-pressure cell is shown in Figure 2.2. This cell was constructed from brass and 316 stainless steel with 1 cm thick sapphire windows. The gas seals were made from Teflon. The cell path length was 1 cm and the cell volume was 1 cm^3. Light was fed into and out of the high-pressure cell by fibre-optic cables (Hellma, Müllheim, FRG) fitted with a 662 QX prism adapter.

2.3 Experimental Measurements

2.3.1 Solubility Measurements

The cell shown in Figure 2.3 was used to carry out solubility measurements. Excess solute was loaded into the reaction vessel and placed between the two metal sieves. The capacitance was measured as described in section 2.2.2 as a function of pressure at constant temperature. The solubility of solid solutes in a sc fluid is found by converting capacitance values to dielectric constant values. This change in
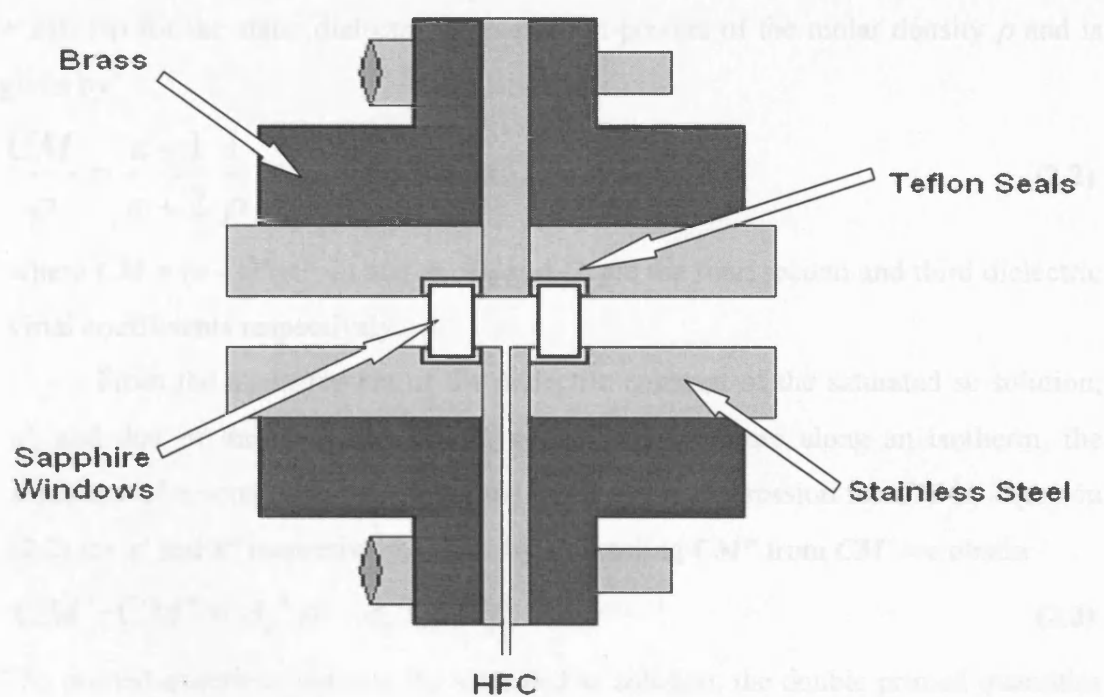
Figure 2.2 The high-pressure optical cell
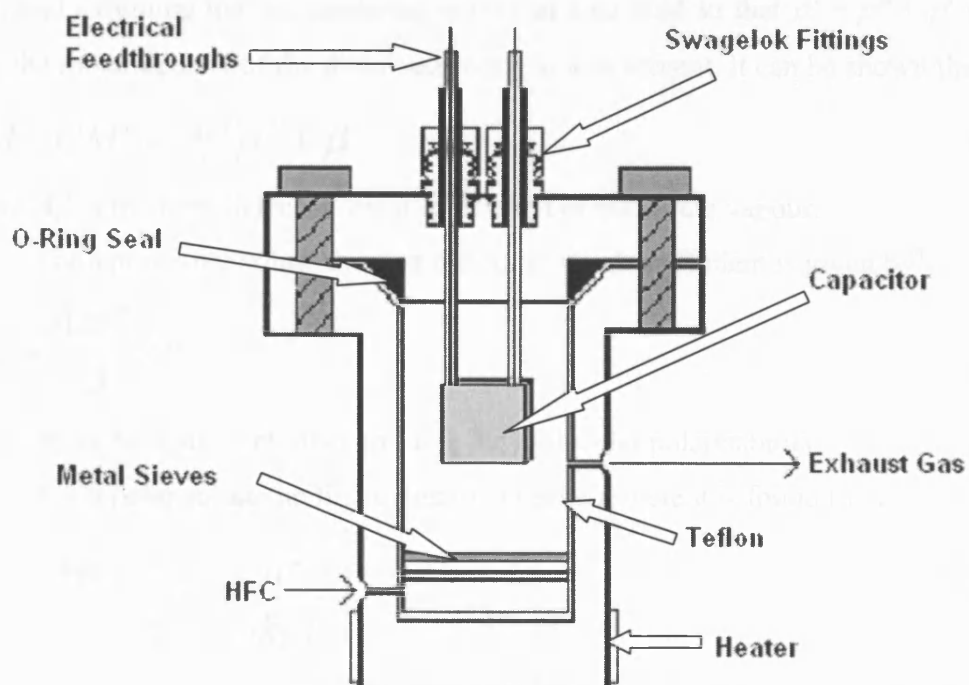
Figure 2.3 The capacitance reaction vessel

dielectric constant with density is defined by the Clausius-Mossotti function $((\varepsilon - 1)/(\varepsilon + 2))$. $1/\rho$ for the static dielectric constant ε in powers of the molar density ρ and is given by[3]

$$\frac{CM}{\rho} = \frac{\varepsilon - 1}{\varepsilon + 2}\frac{1}{\rho} = A_e + B_e\rho + C_e\rho^2 + \ldots\ldots \qquad (2.2)$$

where $CM = (\varepsilon - 1)/(\varepsilon + 2)$ and A_e, B_e and C_e are the first, second and third dielectric virial coefficients respectively.

From the measurement of the dielectric constant of the saturated sc solution, ε', and that of the pure solvent, ε'', at the same pressure along an isotherm, the solubility of a solute can be determined by using the expression for CM in Equation (2.2) for ε' and ε'' respectively. Thus, by subtracting CM'' from CM' we obtain

$$CM' - CM'' = A_e'\rho' - A_e''\rho'' + \beta \qquad (2.3)$$

The primed quantities indicate the saturated sc solution, the double primed quantities belong to the sc solvent and β represents the difference between the second and higher order terms in ρ' and ρ''.

From the definition of the first dielectric virial coefficient,[4] use of Equation (2.3) and assuming that no clustering occurs in a sc fluid so that $\rho' = \rho'' + \rho^s$ where ρ^s is the molar density of the dissolved solute in a sc solvent, it can be shown that[3]

$$CM' - CM'' = A_e{}^s\rho^s + \beta \qquad (2.4)$$

where $A_e{}^s$ is the first dielectric virial coefficient of the solute vapour.

For a non-polar solute the first dielectric virial coefficient is given by[4]

$$A_e{}^s = \frac{4\pi Na}{3}\alpha \qquad (2.5)$$

where N_a is Avogadros number and α is the molecular polarisability.

For a polar solute the first dielectric virial coefficient is found to be[5]

$$A_e{}^s = \frac{4\pi Na}{3}\left(\alpha + \frac{\mu^2}{3k_BT}\right) \qquad (2.6)$$

where μ is the permanent dipole moment, k_B is the Boltzman constant and T is the temperature in Kelvin.

Equation (2.4) then gives the working relation for the solubility determination, which is

$$\rho^s = \frac{CM' - CM''}{A_e^{\ s}} - \frac{\beta}{A_e^{\ s}}$$

(2.7)

where $(\beta/A_e^{\ s})$ is the correction to the solubility ρ^s arising from the difference (**CM'**-**CM''**) and relative to the difference of the higher order terms ρ' and ρ''.

2.3.2 Extraction Technique

The capsule to be extracted from was placed in the bottom of the reaction vessel shown in Figure 2.1 and trapped by a metal sieve. Extraction was left to occur for a given length of time at the desired temperature and pressure. Trapping of the extract takes place by rapid depressurisation into the autoclave shown in Figure 2.1. The extract was then analysed by GC-MS (Perkin Elmer)

2.3.3 Solvatochromic Measurements

The optical cell shown in Figure 2.2 was used to measure the solvatochromic shift of two indicator dyes at various temperatures and pressures. A small amount of the desired dye was loaded into the cell and subsequently heated and pressurised to the desired conditions. The system was left to equilibrate for 15 minutes then absorbance spectra were taken as described in section 2.2.3. The wavelength of absorbance maximum was calculated from the average of five spectra.

2.3.4 Reaction Kinetics Measurements

The apparatus shown in Figure 2.1 was used to measure the capacitance of a number of the reactions described in section 2.4. The technique for carrying out these reactions is described in section 2.4. Whilst the reaction system was left to react for the desired time, capacitance readings were taken at specific intervals by the technique described in section 2.2.2. The changes in capacitance and hence the dielectric constant of the reaction with time could then be calculated. On analysis of the reactants and products as described in section 2.4 the change in concentration of the reactants/products with time can be deduced and reaction kinetics obtained.

2.4 Reactions

2.4.1 Friedel-Crafts Alkylation

The apparatus shown in Figure 2.1 was used to carry out the Friedel-Crafts alkylation of anisole (Aldrich, 99 %) and toluene (Fisher, 98 %) using 2-methyl-2-propanol (*tert*-butylchloride) (Aldrich, 99.5 %) or 2-chloro-2-methylpropane (BDH, 99 %) with *p*-toluenesulphonic acid monohydrate (Lancaster, 98 %) as the acid catalyst. The reactants were placed into the doser and the acid catalyst in the reaction vessel. This was then heated to the desired temperature and subsequently pressurised pushing the reactants from the doser into the reaction vessel. The system was left to react for the desired time and where applicable capacitance measurements were taken (section 2.3.4). The products were trapped by depressurisation into a larger volume autoclave, which also stopped the reaction and the products were analysed by GC-MS (Perkin Elmer).

2.4.2 Esterification

The esterification of benzoic acid (Scientific & Chemical Supplies Ltd, 98 %) with 1-butanol (Fisher, 98 %) using *p*-toluenesulphonic acid as the catalyst was carried out. The apparatus and technique is described in section 2.4.1.

2.4.3 Aldol Condensation

The acid catalysed aldol condensation of cyclohexanone (Aldrich, 98 %) was carried out using the technique described in section 2.4.1 once again employing *p*-toluenesulphonic acid as the catalyst.

2.5 References

(1)   Abbott A, P.; Eardley C, A. *J. Phys. Chem. B* **1998**, *102*, 8574.

(2)   Abbott A, P.; Eardley C, A. *J. Phys. Chem. B* **1999**, *103*, 2504.

(3)   Hourri A.; St-Arnaud J, M.; Bose T, K. *Rev. Sci. Instru.* **1998**, *69*, 2732.

(4)   Hourri A.; St-Arnaud J, M.; Bose T, K. *J. Chem. Phys.* **1997**, *106*, 1780.

(5)   Barao T.; Nieto de Castro C, A.; Mardolcar U, V.; Okambawa R.; St-Arnaud J, M. *J. Chem. Eng. Data* **1995**, *40*, 1242.

CHAPTER

3

SOLUBILITY RELATIONS AND MODELLING IN SUPERCRITICAL DIFLUOROMETHANE

3.1 Introduction

The knowledge of the solubility of a substance in a supercritical (sc) fluid is essential for the feasibility study or the design efficiency of any sc fluid extraction process or chemical reaction. A suitable experimental technique for the measurement of the solubility of organic compounds in sc fluids needs to be fast, simple and precise. The most common methods employed to date for measuring solubilities are gravimetric, chromatographic and spectroscopic techniques but each of these methods has limitations.

This work looks to assess the validity of a recently proposed dielectric method for the measurement of solubilities in sc fluids. Previous research employing dielectrometry has shown it to be a quick, simple and precise *in situ* method for the measurement of solubilities.[1] The scope of the dielectrometry technique is also assessed in this work by measuring the solubilities of a wide range of polar and non-polar solutes in sc CO_2 and in the more polar fluid HFC 32.

This work reports the first measured solubilities of organic solutes in sc HFC 32 at 363 K employing the dielectrometry method. Supercritical HFC 32 is used in this work due to its higher dielectric constant compared to that of sc CO_2. The higher polarity of HFC 32 should result in higher solubilities of polar solutes than in CO_2, making HFC 32 an attractive replacement solvent for use in sc fluid applications involving polar compounds such as extraction and as a solvent in chemical reactions.

3.1.1 Solubility in Supercritical Fluids

Solubility is amongst the most important physicochemical properties of solutes dissolved in sc fluids. On one hand knowledge of it is essential to determine if substances can be processed using sc fluids and on the other it gives valuable information about the solute-solvent interactions in solution.[2] Solubility data are typically presented in the form of solubility isotherms, where it is readily apparent that solubility increases rapidly at low pressures around the critical pressure, whereas at higher pressures the increase in solubility is less pronounced. The shape of the solubility isotherm reflects changes in the density with pressure.

The ability of a sc fluid to dissolve solids was first reported more than 100 years ago by Hannay and Hogarth,[3] who studied the solubility of inorganic salts in sc ethanol. Subsequent work by Buckner in 1906[4] showed that the solubility of organic solutes in sc CO_2 was orders of magnitude higher than that predicted by vapour

pressure considerations. Since then, the interest in the quantitative determination of solubility has increased continuously. Several substances have been employed as sc fluids in order to carry out different processes although sc CO_2 is by far the most frequently used. Over the last few decades, the solubilities of solids and liquids in sc fluids have been measured extensively,[2,5-8] with work up to 1989 being reviewed by Bartle *et al.*[9]

Solubility measurements of compounds in sc HFCs are very limited. Stahl and co-workers determined solubilities of different alkaloids in sc N_2O, CO_2 and CHF_3.[10] Their results showed that the solubility of these alkaloids was higher in CHF_3 than the other solvents. Taylor *et al.* measured the solubility of two sulphur containing analytes in sc CO_2, CHF_3 and HFC 134a.[11] Results showed that both analytes had much higher solubilities in HFC 134a than in the other two solvents. Recently, it has been highlighted by Abbott *et al.* that HFC 134a is a relatively polar solvent, even in the sc state, which may enhance the solubility of polar solutes.[12-14] Therefore, the increased solubility in HFC 134a may be a consequence of the higher dielectric constant of the medium. Water solubility has also been measured in sc HFC 134a by the use of near IR spectroscopy.[15]

A significant problem associated with the wide spread use of these HFC fluids in the sc state is the lack of solubility data. To begin to overcome this problem this work measures the first solubilities in sc HFC 32 for a variety of substituted aromatic hydrocarbons at 363 K and a variety of pressures.

3.1.2 Measurement Techniques

The experimental methods most frequently employed to measure the solubility of substances in sc fluids are gravimetric, chromatographic and spectroscopic, of which the gravimetric method developed by Eckert,[16] Paulaitis,[17] Reid[18] and their co-workers in the late 1970s is most widely used. Of these methods spectroscopic techniques give the most meaningful data but they can only be used if the solute has one or more absorption bands in the UV/VIS/IR wavelength ranges, which can be used to determine its concentration. Implementation of these techniques meets certain experimental difficulties, as relatively small changes in pressure frequently vary the solubility by several orders of magnitude, which complicates measurements. At concentrations above 10^{-1} mol dm^{-3} and in the case of turbid or opaque solutions, optical techniques are inapplicable and other less accurate gravimetric methods will

have to be employed. The choice of an adequate experimental method for the determination of solubility in a sc fluid is therefore important.

In the late 1990s it was proposed that dielectrometry could be used to measure the solubility of polar solutes in sc fluids.[1,19,20] Polar solutes cause a change in the dielectric constant, ε, of the medium and the extent of this dielectric constant change with respect to the pure solute (at the same temperature and pressure) can be related to the solute concentration and hence its solubility. This technique has the advantage that it can be used when solubilities are high (> 10^{-3} mol dm^{-3}) or if the solution is turbid. It is also simple to use, inexpensive and permits direct *in situ* measurements of solute solubility in sc fluids.

To date this dielectrometry technique has only been applied in a few cases for solubility measurements in sc CO_2. Fedotov *et al.* initially measured the solubility of numerous polar compounds in sc CO_2 including acetonitrile, acetone and manganese cyclopentadienyltricarbonyl as a function of pressure.[19,20] Then later Hourri and co-workers measured the solubility of naphthalene in sc CO_2 as a function of temperature and pressure to assess the validity of the technique by comparing their results to published data.[1] They found that their results agreed to better than 4 % of those published previously.

As sc CO_2 is a non-polar solvent the use of this technique may be rather limited because the low solubility of polar solutes means that the overall change in the dielectric constant is relatively small. In the current work it is demonstrated that this method is ideal for use with HFC fluids where the dielectric constant change is considerably larger.

3.1.3 Solubility Modelling

As stated earlier, solubility is one of the most important physicochemical properties of solutes dissolved in sc fluids. Knowledge of solubility is essential to determine whether substances can be processed using sc fluids and it gives valuable information about solute-solvent interactions in solution. An important solute property that significantly affects solubility is its vapour pressure. The enhancement factor, E, is often used instead of solubility giving

$$y_2 = E \frac{p_2}{p} \tag{3.1}$$

The enhancement factor represents the solubility increase in the sc solvent over that in the ideal gas mixture, p_2 is the vapour pressure of the pure solid, p is the system pressure and y_2 is the observed solubility.[21]

Numerous solubility measurements for a number of solutes in different sc fluids have been carried out. The fact that solubility is a function of the sc fluid, the solute, the temperature, and the pressure translates into a demand for experimental data. To reduce this demand several procedures have been adopted to describe and correlate solubility (or enhancement factor) of solutes in sc fluids and their changes with temperature and density. Equations of state (EOS) are frequently employed to describe the change of solubilities with the thermodynamic parameters.

Cubic EOS are often used to describe the solubility at different temperatures and pressures but the main limitation of these is the need to describe a combining rule which can be used to express the mixture parameters. The application of simple virial EOS has proved successful at representing the dependence of the solubility of the solutes on the thermodynamic variables.[22,23] It has been proposed that the spread of the electrostatic potential on the solutes surface may be a relevant quantity to predict the solubility of solids in sc fluids.[24] This basic procedure only seems to describe the solubility fundamentally in terms of the changes of the vapour pressure of the pure solute. Recently, a few laboratories have developed more general thermodynamic methods to describe and predict the equilibrium properties of binary solutions.[25,26]

There are several theories to predict the solubility of solutes in sc fluids but still cubic EOS are the most commonly employed. An example is the Redlich-Kwong EOS but densities at high pressure are the weak point of this.[27] The Guigard-Stiver EOS introduced a density-dependent solute solubility parameter, which requires the critical pressure and density of the sc fluid, as well as the solutes melting point, liquid molar volume and enthalpy of fusion.[28] However, if the solute properties are unknown the most widely used technique for correlating sc fluid solubilities is that proposed by Chrastil.[29] On the other hand if the solute properties are known the Peng-Robinson (PR) EOS is the most widely used.[30] The PR EOS is

$$P = \frac{RT}{v-b} - \frac{a(T)}{v(v+b)+b(v-b)}$$

(3.2)

where v is the molar volume, a accounts for intermolecular interactions between the species in the mixture, and b accounts for size differences between the species of the

mixture. The pure component parameters a and b can be expressed in terms of the critical temperature, T_c, and pressure, p_c, of the pure substance. So for the PR equation

$$a = \left(\frac{0.45724R^2T_c^2}{p_c} \right)\alpha \qquad (3.3)$$

and

$$b = \frac{0.07780RT_c}{p_c} \qquad (3.4)$$

The quantity α is taken to be temperature dependent and is determined from pure component vapour pressures. The main problem associated with solid-fluid phase equilibrium calculations using the PR EOS is the lack of known vapour pressures of the relatively non-volatile solids. The α values determined from vapour pressures of saturated liquids are generally not suitable for extrapolation to the sublimation curve, or suitable for the solvent in the sc region.[21]

As binary systems are being used it is necessary to define the relationship between the EOS parameters for the pure component and for the mixtures, that is, the dependence of the mixture parameters on the composition. The conventional mixing rules frequently employed are the quadratic mixing rules, where

$$a(T) = \sum_i \sum_j y_i y_j a_{ij} \qquad (3.5)$$

and

$$b = \sum_i y_i b_i \qquad (3.6)$$

and the combining rule for a_{ij} is given by

$$aij = \sqrt{a_{ii}a_{jj}}\left(1 - k_{ij}\right) \qquad (3.7)$$

where a_{ii} and b_i are the pure component parameters and k_{ij} is an adjustable binary interaction parameter, which in general must be determined from experimental data. The proper choice of mixing rules for the determination of mixing parameters is very important in phase equilibrium calculations, especially if the solutions are highly asymmetric. The quadratic mixing rules are simple but often inadequate for asymmetric, polar components and mixtures, but a number of more complex rules are available in the literature.[31,32]

3.2 Results and Discussion

3.2.1 Solubility of Solids in Supercritical HFC 32

To gain an appreciation of the factors that affect the solubility of a compound, the solubility of a wide range of solutes had to be measured whereby the identities of the solutes are changed systematically. To achieve this, the organic solutes employed in these studies were derived from either a benzoic acid or a phenolic backbone.

For each different solubility study involving a compound with a benzoic acid backbone a different functional group was added to the *para* position. The affect of the functional group on solubility could then be assessed. Solubility measurement involving the phenol backbone followed the same procedure, whereby, for each different study a different functional group was present at the *para* position. The measured solubilities for this wide range of aromatic derivatives could then be compared as a function of the polarity of the functional group. A broad understanding of the factors that affect solubility in HFC 32 should then be achieved.

Firstly, before any new solubility measurements were obtained it was necessary to test the reliability of the dielectrometry technique. Measuring the solubility of known solutes and comparing the results to published data tested this reliability. The solubility of naphthalene was measured in sc CO_2 at 318 K and a variety of pressures. The measured dielectric constant values for pure CO_2 and CO_2-naphthalene at saturation are shown in Figure 3.1. Each reported dielectric constant reading is the average of five replicate readings where results were found to vary by no more than ± 0.03. On addition of naphthalene the dielectric constant of the system can be seen to have increased, which suggests that naphthalene must be soluble in CO_2.

The results in Figure 3.1 were then used to calculate the solubility of naphthalene in this system by the method described in Chapter 2. Figure 3.2 and Table 2 of the appendix show the calculated solubility results for naphthalene at 318 K and a variety of pressures. It can be seen from this figure that there is good agreement between this work using the dielectric method and previously published results using dielectrometry[1] and a gravimetric method,[33] where the results measured in this work are found to be vary by no more than 4 % from the previously published data.

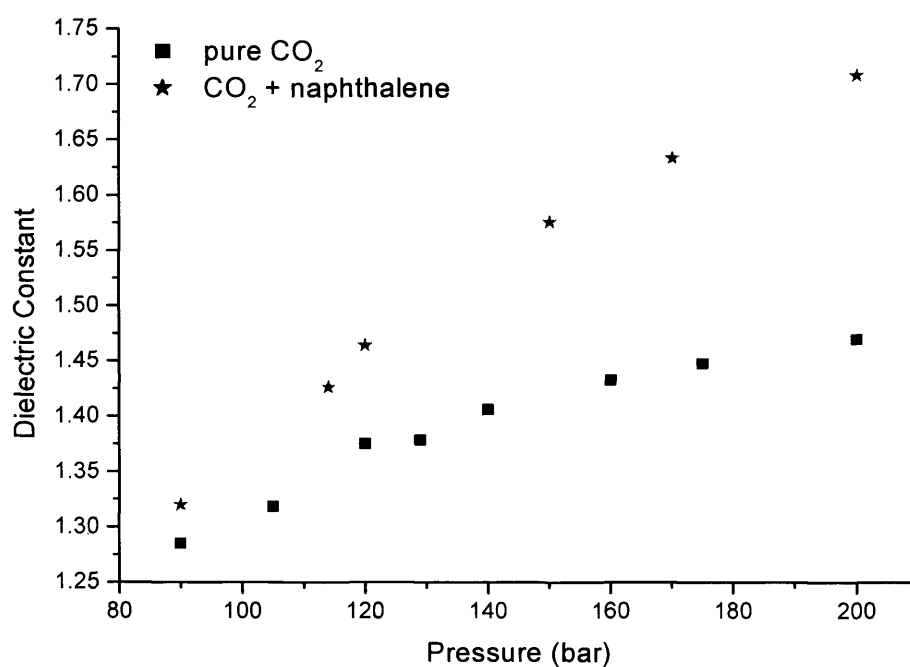**Figure 3.1** Plots of the measured dielectric constant for pure CO_2 and that of CO_2-naphthalene at saturation at 318 K
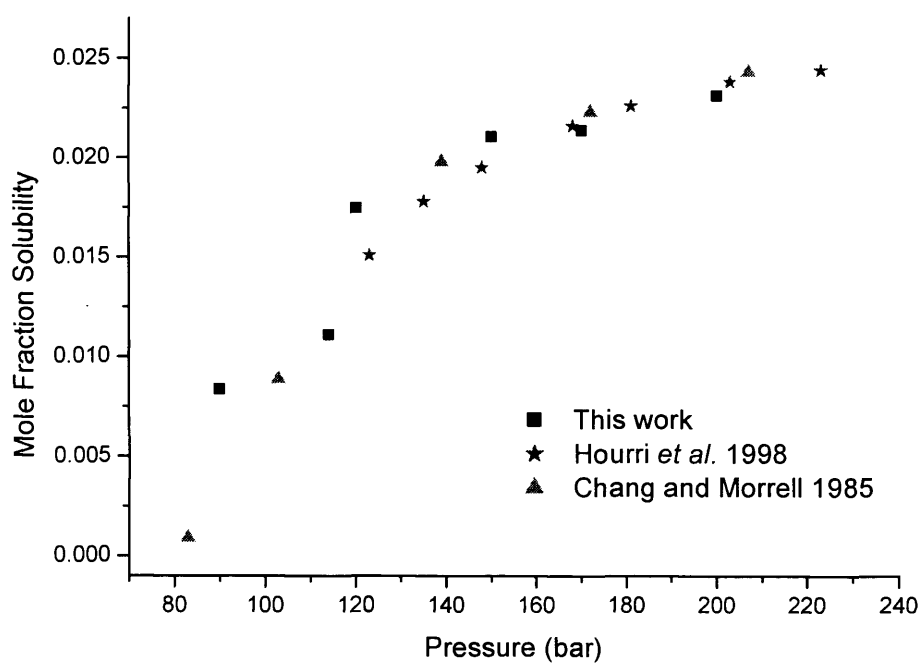
Figure 3.2 Comparison of naphthalene solubility between this work and published data[1,33] in sc CO_2 at 318 K

The reliability of this technique for measuring the solubility of liquid solutes was then tested using water in HFC 134a along three isotherms at a variety of pressures. The results at 383 K were compared to the data published by Jackson *et al.*[15] Their initial work on water solubility in HFC 134a at 383 K has been extended here to measure the water solubility at 343 and 363 K. The measured dielectric constant for the three isotherms for pure HFC 134a and HFC 134a-water at saturation are shown in Figure 3.3. The change in dielectric constant on addition of water is only small indicating that water solubility in this solvent is low, which is what would be expected for highly polar water in a lower polarity solvent.

The experimentally calculated solubilities for water in HFC 134a are shown in Figure 3.4 and Tables 3 to 5 in the appendix. From this plot it can be seen that there is good agreement between this work and published data. Also as the temperature and pressure increase water solubility increases, which is what is expected due to vapour pressure and density considerations.

To calculate solubilities in HFC 32 the dielectric constant of the pure solvent needs to be found over the temperature and pressure range of interest. Figure 3.5 shows the dielectric constant of HFC 32 at 363 K as a function of pressure. The dielectric constant is considerably higher than that for CO_2 at similar temperatures and pressures ($\varepsilon < 2$) and there is a large change in the dielectric constant with increasing pressure, especially around the critical point, where there is a large change in the density. The greater dielectric constant value of HFC 32 indicates that HFC 32 is a more polar solvent than CO_2, which means that the solubility of polar solutes in this medium should be greater.

Tables 6 to 17 of the appendix show the first solubility measurements in sc HFC 32 at 363 K over a range of pressures for the solutes shown in section 2.1.2. Figures 3.6 and 3.7 are compiled from this data, comparing the effect of substituent on *para* substituted benzoic acids and phenols respectively. The values used in Equation (2.7) for the dielectric constant from five replicate measurements are found to vary by no more than $\pm$ 0.005 which results in the mole fraction solubility fluctuating by no more than $\pm$ 2 %. Further uncertainty arises in the mole fraction solubility value from the calculation of the first dielectric virial coefficient. The molecular polarisabilities used in Equation (2.5) to calculate the first dielectric virial

Figure 3.3 Plots of the measured dielectric constant of pure HFC 134a and that of

HFC 134a-water at saturation along three isotherms

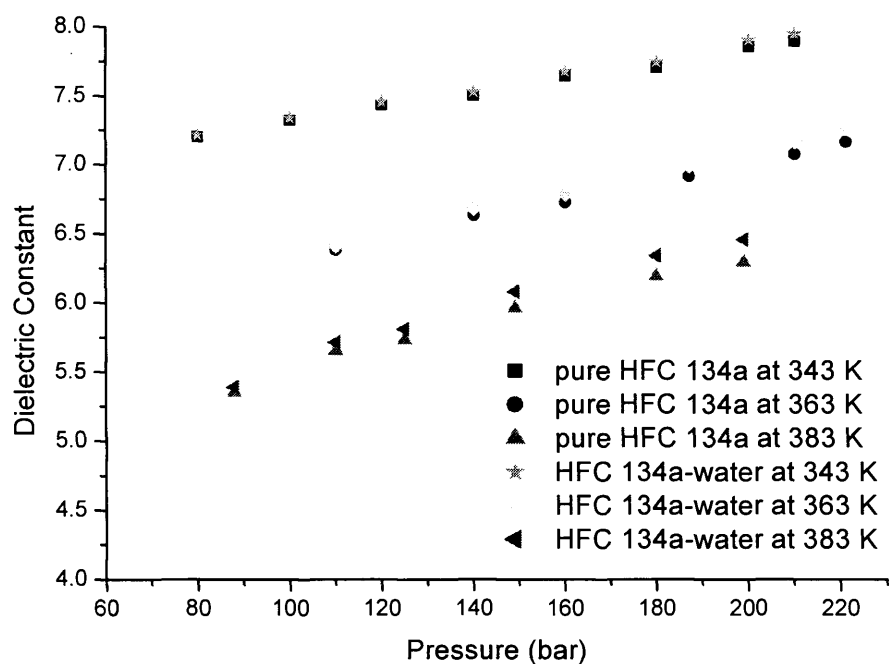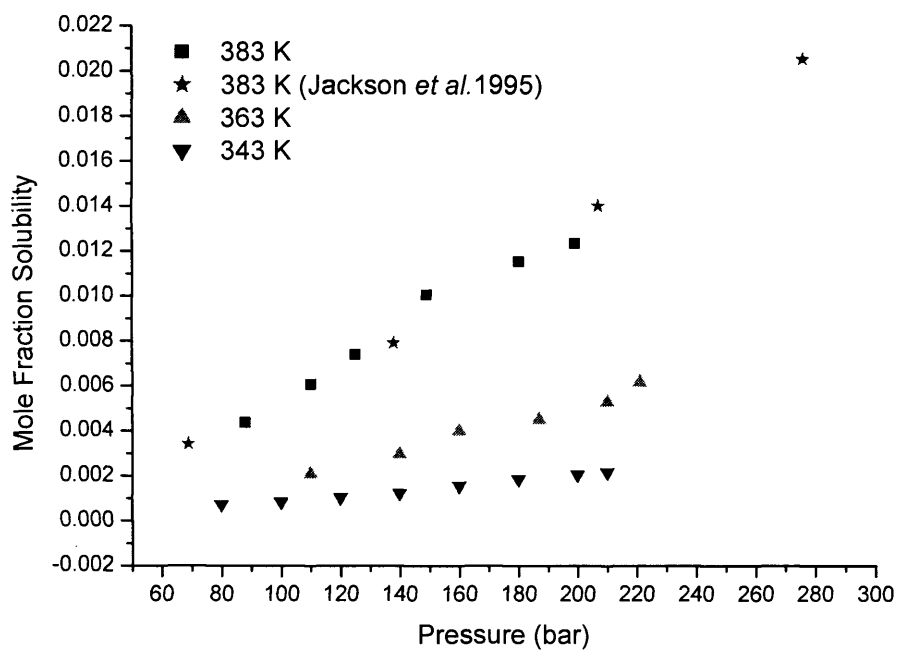**Figure 3.4** Comparison of water solubility between this work and published data[15] in

HFC 134a along three isotherms
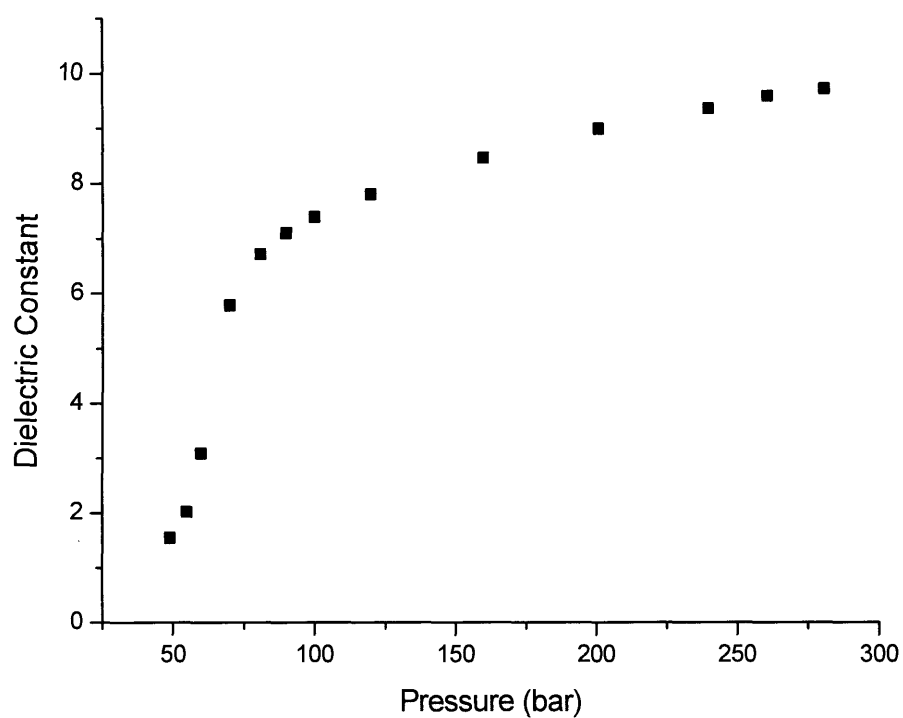
Figure 3.5 The change in dielectric constant of HFC 32 at 363 K with pressure

coefficient were taken from the literature[34] or calculated via an additive method that was introduced by Le Fevre.[35]

The uncertainty in the molecular polarisability value is unknown but if a theoretical maximum uncertainty of 5 % is assumed then the mole fraction solubility is found to fluctuate by no more than ± 0.5 %. For polar solutes the molecular polarisability[34,35] and permanent dipole moment values[36] are needed to calculate the first dielectric virial coefficient from Equation (2.6). In this equation the molecular polarisability is found to be insignificant and the dipole moment value dominates the first dielectric virial coefficient. If a theoretical 5 % uncertainty is taken in both these properties the error in the mole fraction solubility is found to increase to ± 6 %. Actual uncertainties are likely to be less but ± 0.5 % and ± 6 % must be taken as the maximum error limits for the non-polar and polar solutes respectively. The maximum errors will result in a fluctuation of the last mole fraction solubility significant figure shown in the tables in the appendix. The molecular polarisability, dipole moment and first dielectric virial coefficient values for each of the solutes used in this work are shown in Table 1 of the appendix.

In Figures 3.6 and 3.7 the mole fraction solubility is found to increase with increasing pressure for all solutes studied and the solubility is greatly affected by the polarity of the substituent present. For both the benzoic acids and the phenols it can be seen that solubility decreases with the increasing polarity of the substituent. It has been noted previously that the presence of a carboxy group causes a decrease in solubility.[37] This is illustrated here by comparison of Figures 3.6 and 3.7 where it can be observed that the solubility of phenols is approximately two orders of magnitude greater than the corresponding benzoic acids.

For all solutes, the solubility increase with applied pressure, at values above the critical point, shows approximate linearity. For the solutes where solubility measurements have been taken at low pressures it can be seen that the solubility decreases as the pressure approaches the critical value. This observation is consistent with previously published solubility results[9] and is thought to be due to the decrease in dielectric constant in this region, which corresponds to the region of high fluid compressibility.[14]

Figure 3.8 is compiled from the results given in Tables 6 to 8 of the appendix for the solubilities of *ortho-*, *meta-* and *para-*hydroxybenzoic acid (HBA). The solubility results for the HBAs measured by Krukonis *et al.*[38] in sc CO_2 at similar
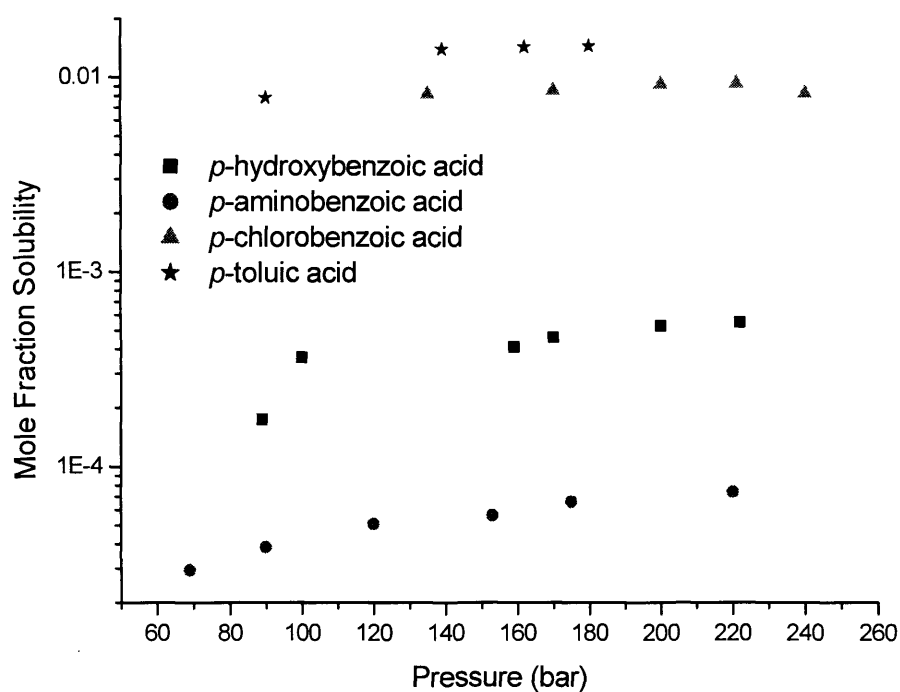
Figure 3.6 Effect of substituent on benzoic acid solubility in sc HFC 32 at 363K
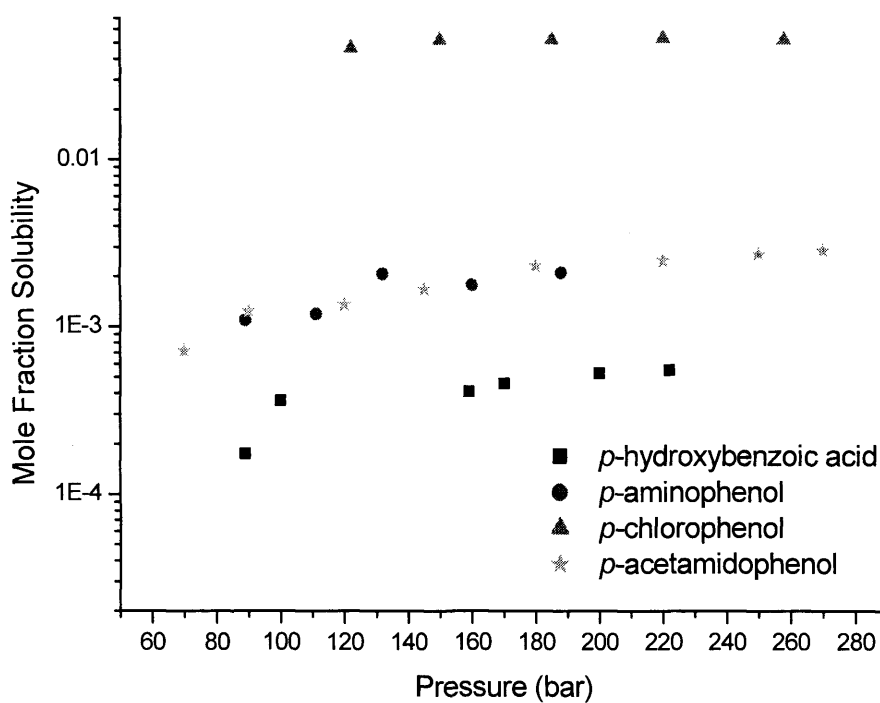
Figure 3.7 Effect of substituent on phenol solubility in sc HFC 32 at 363K
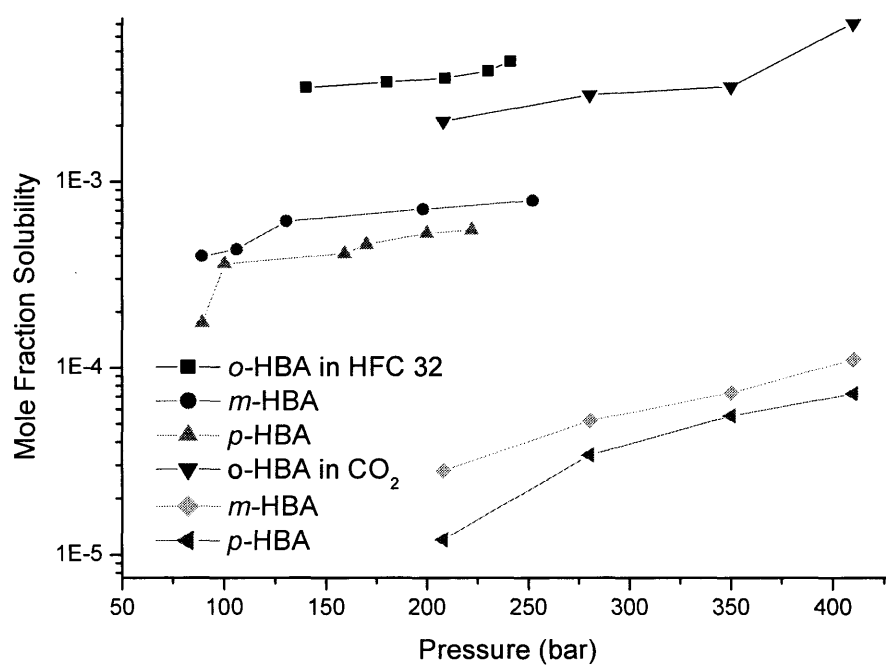
Figure 3.8 Comparison of the solubility of HBAs in sc HFC 32 at 363 K and sc CO_2 at 373 K

temperatures and pressures are also shown. The solubility of each corresponding solute is found to be greater in sc HFC 32. The increase in solubility in this media is what would be expected for a polar solute in this more polar solvent. For these systems a dipole/dipole interaction between the polar solute and HFC 32 exits which would tend to enhance solubility, whereas there exists a dipole/quadrupole interaction with the polar solutes and with the solvent in the CO_2 system.

3.2.2 Modelling Solubility in Supercritical HFC 32

In terms of understanding the effects of the sc solvent on the solubility of a range of solutes, it is generally more profitable to examine the solubility enhancement caused by the solute rather than the absolute solute solubility. The solubility enhancement is simply the ratio of the measured solute concentration in the sc solvent to the concentration of pure solute as a result of its own vapour pressure at the temperature of interest (section 3.1.3). The solubility enhancement for a number of the solutes where the vapour pressure is known is shown in Figure 3.9. From this plot it can be seen that enhancement increases with pressure for all the solutes shown and if it is compared to Figures 3.6 and 3.7, which show pressure versus observed solubility, it can be seen that the order of solute solubility has now been reversed, so as the polarity or number of free polar groups on the solute increases so does the concentration enhancement.

Anthracene, the least polar solute of those studied, shows the lowest solubility enhancement whereas solutes of greater polarity and greater numbers of polar substituent groups appear to increase the degree of enhancement. It is interesting to compare the results for *o*-HBA with the isomeric *p*-HBA. Despite the higher dipole moment and higher absolute solubility in sc HFC 32 *o*-HBA shows a lower solubility enhancement than that for the *p*-HBA and only slightly greater than that for anthracene. This behaviour may be explained on the basis of a degree of intramolecular hydrogen-bonding in *o*-HBA as shown in Figure 3.10. It is possible that the formation of a hydrogen-bond could act to limit the availability or strength of solvation sites for interaction with HFC 32. This hydrogen-bonding *ortho*-interaction is not available for the *para* isomer and is reflected in the lower melting point of the *o*-HBA in comparison to either the *meta*- and *para*- isomer.
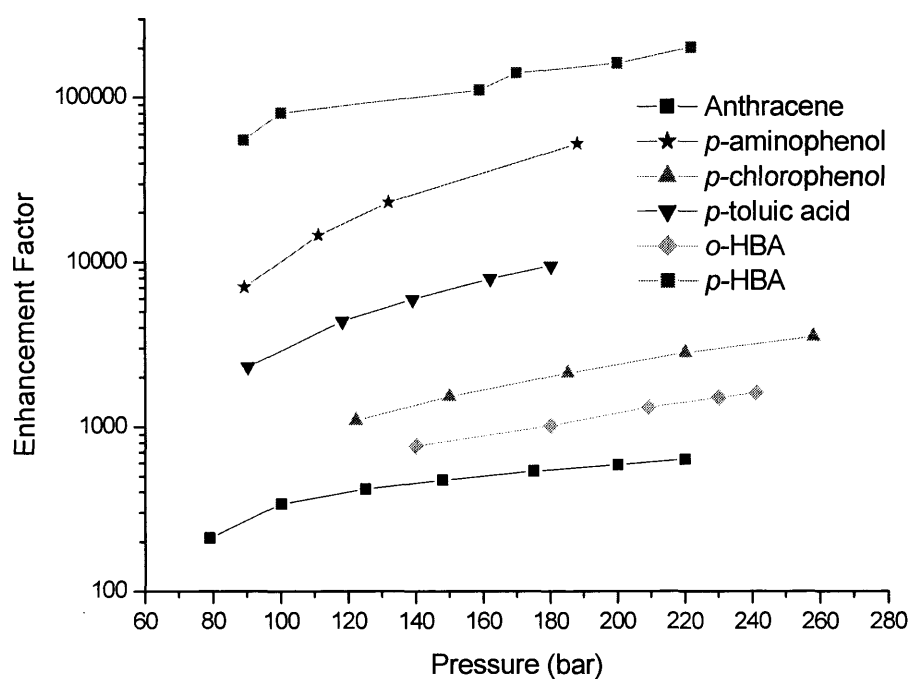
Figure 3.9 Relationship between concentration enhancement and pressure for some of the solutes studied in HFC 32 at 363K
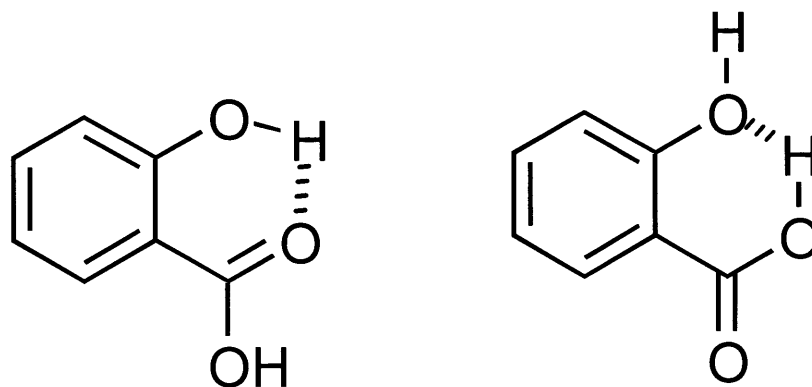
Figure 3.10 Intramolecular hydrogen-bonding for o-HBA

It has been shown previously by Kurnik *et al.* that the solubility of solid solutes in sc CO_2 can be correlated using the PR EOS.[18] The PR EOS used by Kurnik *et al.* is used in this work to correlate the solubility of a number of the solutes in HFC 32 from a knowledge of some of their physical and chemical properties. Details of the pure solute data used in the PR equation are summarised in Table 1 of the appendix. Figures 3.11 – 3.14 show the actual and theoretical solubility estimation curves from the PR EOS for anthracene, o-HBA, p-chlorophenol and p-toluic acid in HFC 32 at 363 K respectively. Due to the lack of known properties for the other solutes in section 3.2.1 these have not yet been modelled. From these plots it can be seen that over the pressure range studied the theoretical results (line) are a reasonable fit to the experimental data (black squares), indicating that the PR EOS can be used for the prediction of sc solubilities employing HFC 32 as the solvent.

In this work it has been shown that the dielectrometry technique can quickly, simply and precisely measure solubilities in HFC 32. It does not appear to be limited by the solution appearance or concentration, which is a limitation in spectroscopic measurements. For the first time solubility measurements have been obtained in HFC 32. Much higher solubilities are obtained compared to sc CO_2 due to its higher dielectric constant. To achieve the same solubilities in CO_2 high pressure would be required or polar modifiers would have to be added. The solvation ability of HFC 32 indicates that it would be a useful solvent in sc extractions and chemical reactions that involve polar extracts or reagents.
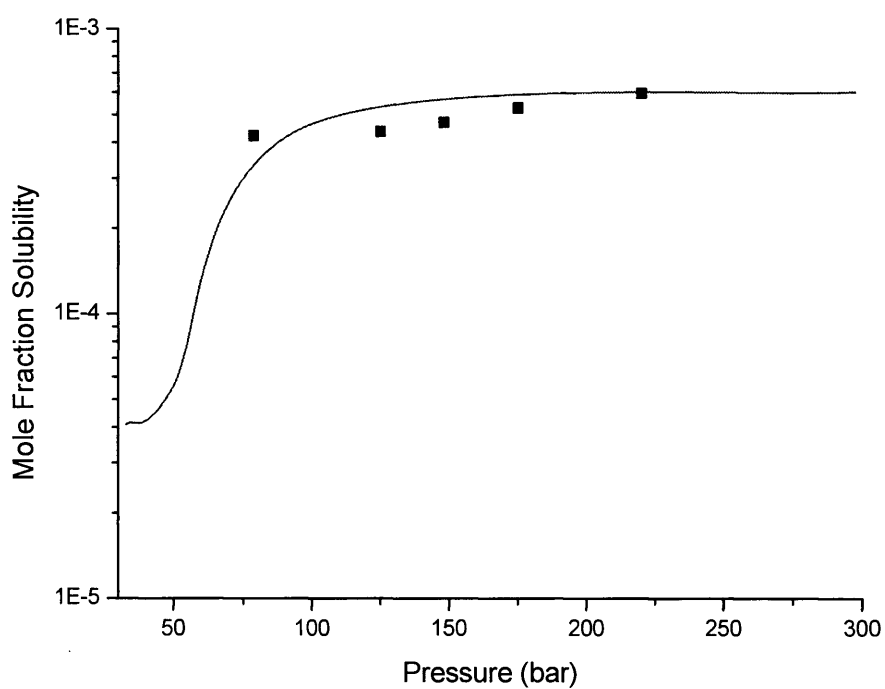
Figure 3.11 Comparison of experimental and theoretical data for anthracene in HFC 32 at 363 K
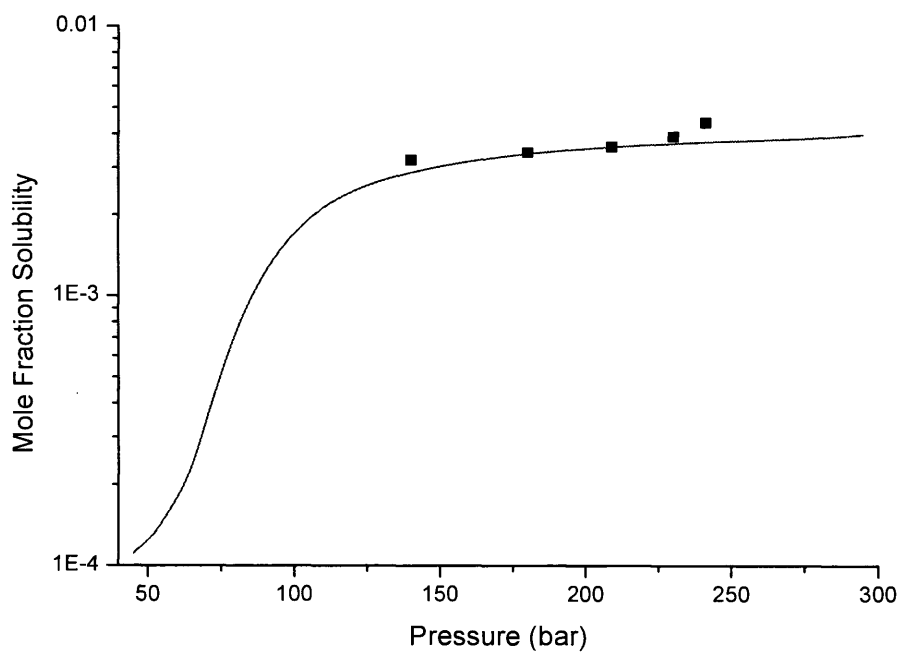
Figure 3.12 Comparison of experimental and theoretical data for o-HBA in HFC 32 at 363 K
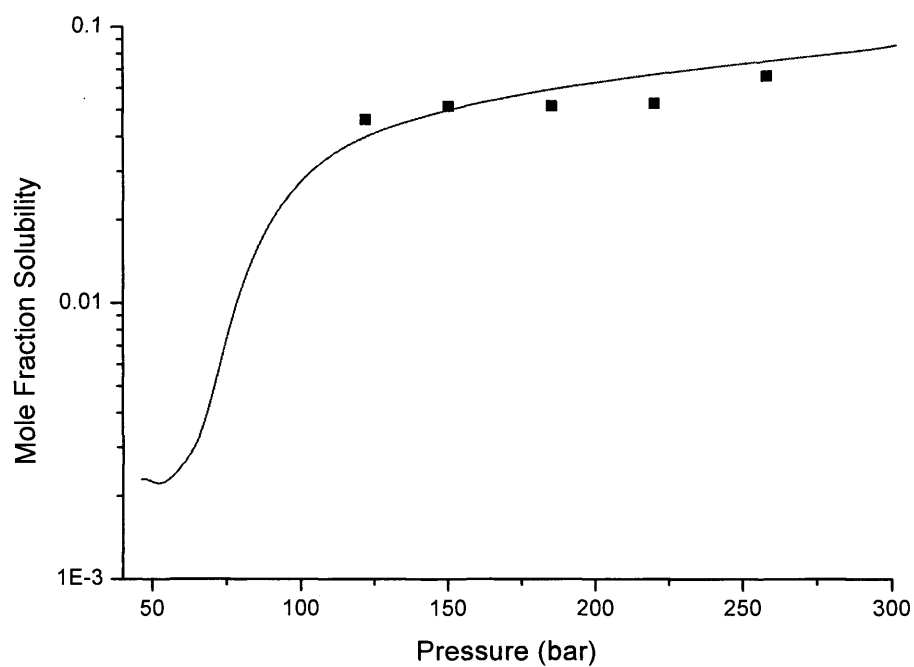
Figure 3.13 Comparison of experimental and theoretical data for p-chlorophenol in HFC 32 at 363 K
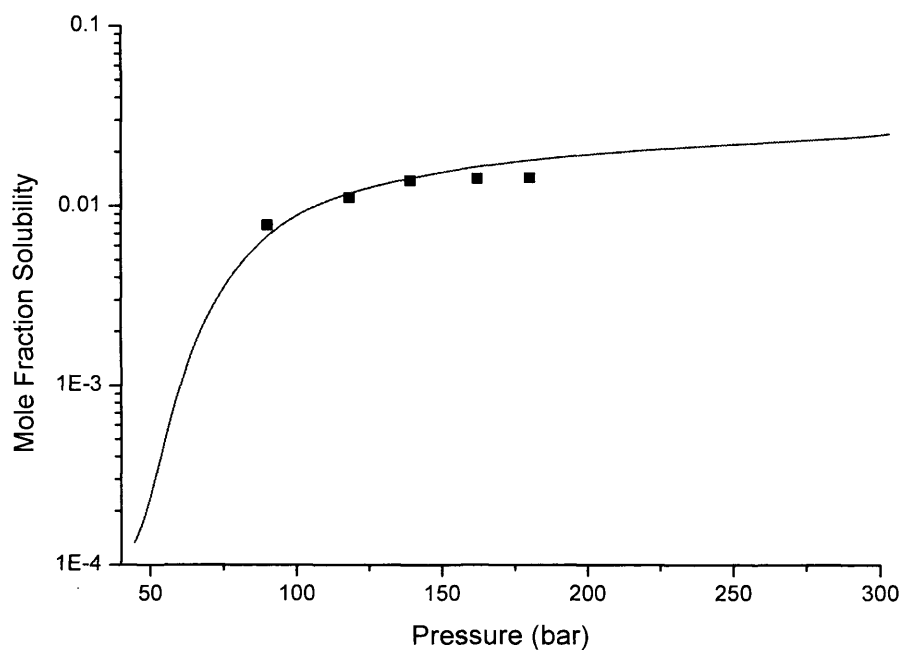
Figure 3.14 Comparison of experimental and theoretical data for p-toluic acid in HFC 32 at 363 K

3.2.3 Extraction using Supercritical HFC 32

The knowledge of the solubility of solutes in sc fluids is crucial if extraction is to be carried out. High solubilities are not necessary but some finite solubility is required to cause extraction. This work looks to assess the use of sc HFC 32 as an extraction fluid to overcome some of the problems faced by GlaxoSmithKline® with the extraction of the active ingredients from paracetamol and aspirin capsules. The main issue at present is that the capsule material is resistant to attack by a number of liquid organic solvents employed by GlaxoSmithKline®, therefore, impeding extraction. The advantage of using HFC 32 for this extraction may arise from its high solubilising power and ability to plasticise and expand the pill coating. The pill coating may then rupture and release the active ingredients for extraction and analysis.

By placing a capsule in the high-pressure optical cell it was observed that swelling of the coating occurs after about 30 minutes, depending on pressure. The swelling continued for a further 30 minutes until the coating was ruptured releasing the ingredients. A test extraction on the placebo of the tablets was carried out to assess whether the sc fluid was extracting the non-active ingredients as well as the active ones. It was found that none of the ingredients in the placebo were soluble in the sc solvent, which makes for a cleaner analysis.

Knowledge of the actual solubilities of the active ingredients, paracetamol and aspirin, under the extraction conditions is necessary. The solubility of paracetamol and aspirin has been measured in HFC 32 at 363 K as a function of pressure and results are shown in Tables 16 and 17 of the appendix. Figure 3.15 displays the mole fraction solubility results for these two solutes. As expected the mole fraction solubility increases with increasing pressure with a rapid increase around the critical pressure. It can also be seen that the mole fraction solubility of aspirin is approximately an order of magnitude greater than that for paracetamol.

Extraction results from the paracetamol and aspirin capsules using HFC 32 at 363 K are shown in Tables 18 to 20 of the appendix. Experiments using CO_2 under similar conditions are also shown for comparison. After extraction, analysis showed that HFC 32, under the conditions studied, selectively extracted the paracetamol or the aspirin from the corresponding capsule. When CO_2 was employed it was found that a small amount of caffeine was extracted from both capsules.
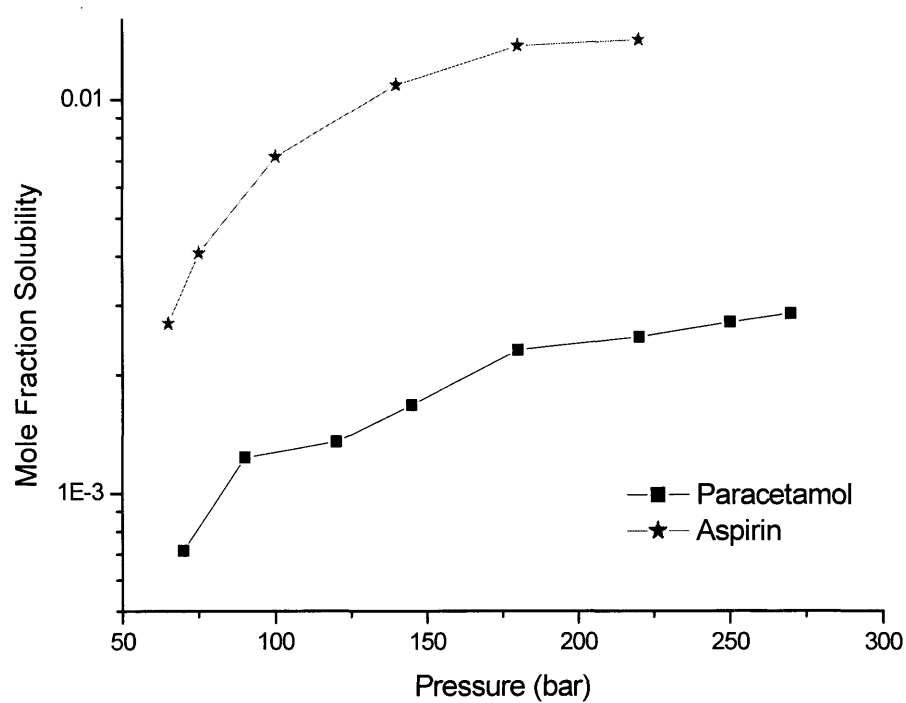
Figure 3.15 Comparison of the mole fraction solubility of paracetamol and aspirin in HFC 32 at 363 K

Figure 3.16 compares the extraction of paracetamol and aspirin as a function of time using HFC 32 at 363 K and 200 ± 20 bar. The amount of aspirin extracted over all time lengths is greater than that for paracetamol, which is expected from the actual solubility of each of these solutes in HFC 32. For both analytes an initial rapid rise in the amount of extract is observed which tails off as the time is increased further. Over the time length studied in this work it appears that extraction is still not complete and the analyte is still being extracted, albeit slowly.

If the amount of analyte extracted is compared to the its actual solubility under the same conditions (paracetamol solubility at 220 bar is 0.040342 mol L^{-1} and the amount extracted at 220 bar after 4 hours is 0.004391 mol L^{-1}; aspirin solubility at 180 bar is 0.212019 mol L^{-1} and the amount extracted at 190 bar after 2 hours is 0.016716 mol L^{-1}) it can be seen that the amount extracted is about an order of magnitude lower. This result indicates that it is not just the solubility of an analyte that governs the extraction process but this also depends on other factors such as the analyte-matrix interaction, analyte location within the matrix and the porosity of the matrix.[39] When considering these other factors the initial rise in Figure 3.16 can be thought of including any effects arising from solubility limitations i.e. the removal of analyte from the outer matrix surfaces where diffusion and extraction will be rapid. The levelling out of the curve is indicative of extraction from deeper within the matrix, which is most time consuming.

Figure 3.16 also shows a few experimental points using sc CO_2 as the extraction solvent at 363 K and 200 ± 10 bar. The amount extracted for both analytes in CO_2 is considerably less than the corresponding analyte in HFC 32. This is due partly to the fact that CO_2 is less polar than HFC 32 so its ability to placticise and expand the capsule coating is reduced. Using the optical cell to inspect the swelling of the capsule it was noted that it took approximately twice as long for the pill coating to rupture compared to HFC 32 at similar temperatures and pressures. Secondly, the non-polar nature of CO_2 will result in a lower actual solubility of these relatively polar active ingredients compared to HFC 32. The lower polarity of CO_2 may also have an influence on matrix effects.

Aspirin extraction after two hours as a function of pressure was also measured in HFC 32 at 363 K. Results are shown in Table 20 of the appendix and in Figure 3.17. It can be seen that extraction increases with pressure, which is to be expected as
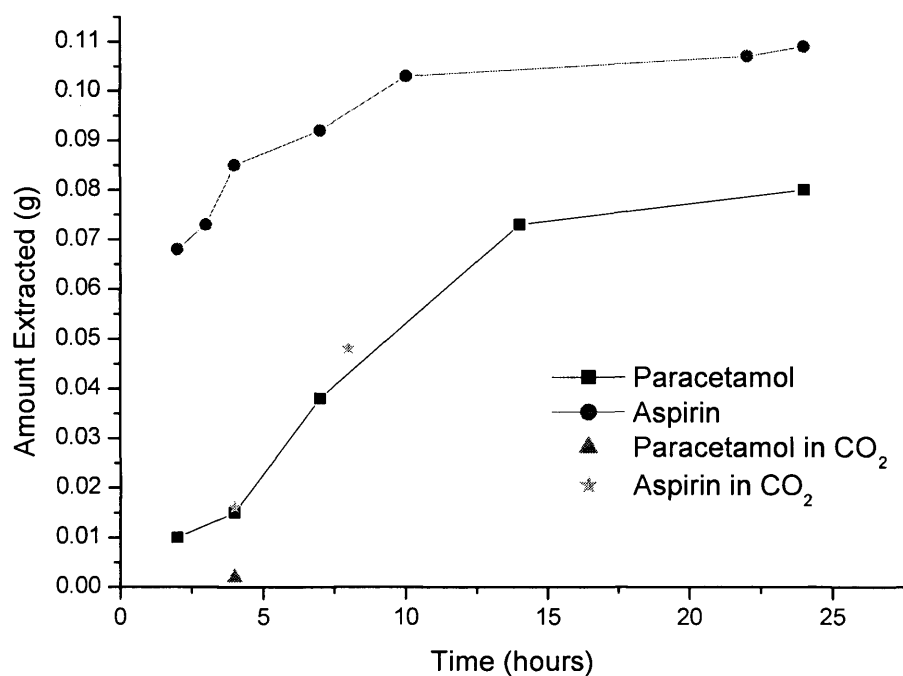
Figure 3.16 Comparison of the amount of paracetamol and aspirin extracted from their capsules as a function of time using HFC 32 at 363 K at 200 ± 20 bar
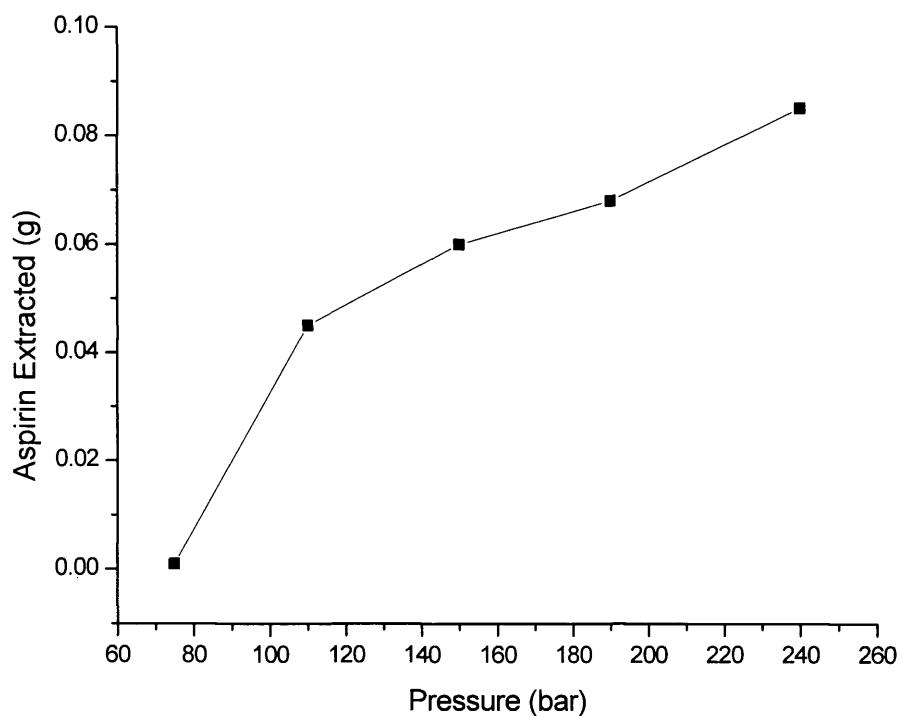
Figure 3.17 Aspirin extraction as a function of pressure in HFC 32 at 363 K

Figure 3.15 shows that an increase in pressure causes an increase in the actual solubility. From visual inspection of the capsule coating as a function of pressure it was also observed that increasing the pressure reduces the time it takes for the pill coating to rupture. An increase in the pressure may also affect the arrangement of the matrix and aid the extraction process by causing the matrix to break down.

If the amount of aspirin extracted in Figure 3.17 is compared to the actual solubility under similar conditions (Figure 3.15) it can be seen that there is approximately an order of magnitude difference. As mentioned earlier this is thought to be due to the time over which the measurements were taken and matrix effects.

This work has shown that HFC 32 can be used as a solvent to carry out sc fluid extraction. The increased polarity of HFC 32 compared to CO_2 makes it an ideal solvent when looking to carry out extractions involving more polar analytes or in systems where the outer coating is hard to penetrate. This preliminary work has demonstrated to GlaxoSmithKline® that SFE can be used to analyse the active ingredients in their pills without initial degradation of the coating. Supercritical fluid extraction may therefore be a faster, cleaner and more viable method for analysis of these systems. It was not the intention of this work to do an exhaustive study to find optimal extraction conditions for these analytes. However, a basic knowledge of the dependency of extraction on the experimental variables has been assessed and from these results it has been found that extraction depends on pressure, time, solvent, actual solubility and matrix effects.

3.3 Conclusions

The first solubility measurements of a number of *p*-benzoic acids and *p*-phenols in HFC 32 at 363 K over a range of pressures are reported in this work. Under the conditions studied the solubility of all solutes was found to increase with increasing pressure. The identity of the functional group at the *para* position of the benzoic acid and phenol backbone was found to have a large affect on the measured solubilities. It was found that the greater the polarity of the solute the lower the solubility. However, when vapour pressure considerations were taken into account and the change in concentration enhancement was measured instead of actual solubility, it was revealed that the enhancement increased as the polarity or number of free polar groups in the solute increased. Opposite trends were observed between the two measurements indicating that the vapour pressure of a solute has a large affect upon solubility. The Peng-Robinson equation-of-state was used to model the solubility data for the solutes where vapour pressure data was available. A good fit was obtained for all solutes over the temperature and pressure range studied showing that the PR EOS can be used to predict solubilities in HFC 32.

It has been shown in this work that the previously proposed dielectrometry method for measuring solubilities is applicable to measuring solubilities in sc HFC 32. The limitations associated with the use of other commonly employed solubility measurement techniques are not observed. It is a quick, simple and precise *in situ* technique that can be applied in different sc solvents to measure the solubility of both polar and non-polar liquid and solid solutes.

The solubility studies have shown that HFC 32 is a relatively polar solvent and should be a useful fluid for sc fluid extraction or chemical reactions, especially if polar compounds are involved, as these have limited solubility in the commonly employed solvent CO_2. Extraction from aspirin and paracetamol capsules was carried out to verify this point by employing HFC 32 as the extraction medium and comparing the results obtained to those for CO_2. HFC 32 was shown to be a suitable medium for carrying out extractions where the rate of extraction depended upon the actual solubility of the extract, time and pressure.

3.4 References

(1)   Hourri A.; St-Arnaud J, M.; Bose T, K. *Rev. Sci. Instru.* **1998**, *69*, 2732.

(2)   Jessop P, G.; Leitner W .*Chemical Synthesis using Supercritical Fluids*; Wiley-VCH: Weinheim, **1999**.

(3)   Hannay J, B.; Hogarth J. *Proc. R. Soc. London* **1879**, *29*, 324.

(4)   Buckner E, H. *Z. Phys. C.* **1906**, *54*, 665.

(5)   Anitescu G.; Tavlarides L, L. *J. Supercrit. Fluids* **1997**, *10*, 175.

(6)   Anitescu G.; Tavlarides L, L. *J. Supercrit. Fluids* **1997**, *11*, 37.

(7)   Anitescu G.; Tavlarides L, L. *J. Supercrit. Fluids* **1999**, *14*, 197.

(8)   Rodrigues S, V.; Nepamuceno D.; Martins L, V.; Baumann W.; Fresenius J. *Anal. Chem* **1998**, *360*, 58.

(9)   Bartle K, D.; Clifford A, A.; Jafar S, A.; Shilstone G, F. *J. Phys. Chem. Ref. Data* **1991**, *20*, 713.

(10) Stahl E.; Willing E. *Mikrochim. Acta.* **1981**, 465.

(11) Ashraf-Khorassani M.; Combs M, T.; Taylor L, T.; Schweighardt F, K.; Mathias P, S. *J. Chem. Eng. data* **1997**, *42*, 636.

(12) Abbott A, P.; Eardley C, A. *J. Phys. Chem. B* **1998**, *102*, 8574.

(13) Abbott A, P.; Eardley C, A.; Tooth R, J. *J. Chem. Eng. Data* **1999**, *44*, 112.

(14) Abbott A, P.; Eardley C, A. *J. Phys. Chem. B* **1999**, *103*, 2504.

(15) Jackson K.; Bowman L, E.; Fulton J, L. *Anal. Chem.* **1995**, *67*, 2368.

(16) Johnston K, P.; Eckert C, A. *AIChE J.* **1981**, *27*, 773.

(17) van Leer R, A.; Paulaitis M, E. *J. Chem. Eng. Data* **1980**, *25*, 257.

(18) Kurnik R, T.; Holla S, J.; Reid R, C. *J. Chem. Eng. Data* **1981**, *26*, 47.

(19) Fedotov A, N.; Simonov A, P.; Popov V, K.; Bagratashvili V, N. *Russian J. Phys Chem.* **1996**, *70*, 156.

(20) Fedotov A, N.; Simonov A, P.; Popov V, K.; Bagratashvili V, N. *J. Phys. Chem. B* **1997**, *101*, 2929.

(21) Lu B, C-Y.; Zhang D.; Sheng W. *Pure Appl. Chem.* **1990**, *62*, 2277.

(22) Joslin C, G.; Gray C, G.; Goldman S.; Tomberli B.; Li W. *Mol. Phys.* **1996**, *89*, 489.

(23) Harvey A, H. *Fluid Phase Equilib.* **1997**, *130*, 87.

(24) Politzer P.; Murray J, S.; Lane P.; Brinck J. *J. Phys. Chem.* **1993**, *97*, 729.

(25)   Alvarez J, L.; Fernandez-Prini R.; Japas M, L. *Ind. Eng. Chem. Res.* **2000**, *39*, 3625.

(26)   Sedlbauer J.; O'Connell J, P.; Wood R, H. *Chem. Geol.* **2000**, *163*, 43.

(27)   Redlich O.; Kwong J, N, S. *Chem. Rev.* **1949**, *44*, 233.

(28)   Guigard S, E.; Stiver W, H. *Ind. Eng. Chem. Res.* **1998**, *37*, 3786.

(29)   Chrastil J. *J. Phys. Chem.* **1982**, *86*, 3016.

(30)   Peng D-Y.; Robinson D, B. *Ind. Eng. Chem. Fundam.* **1976**, *15*, 59.

(31)   Yu J-M.; Lu B, C-Y. *Fluid Phase Equilib.* **1987**, *34*, 1.

(32)   Adachi Y.; Lu B, C-Y. *Fluid Phase Equilib.* **1983**, *14*, 147.

(33)   Chang H.; Morrell D, G. *J. Chem. Eng. Data* **1985**, *30*, 74.

(34)   Weast R, C.; Astle M, J.; Beyer W, H. *Handbook of Chemistry and Physics*, 68 ed.; CRC Press: Florida, **1988**.

(35)   Le Fevre R, J. W.. *Advan. Phys. Org. Chem.* **1965**, *3*, 1.

(36)   McClellan A, L. *Tables of Dipole Moments*; Freeman: San Francisco, **1963**.

(37)   Stahl E.; Schilz W.; Schutz E.; Willing E. *Angew. Chem. Int. Ed. Engl.* **1978**, *17*, 731.

(38)   Krukonis V, J.; Kurnik R, T. *J. Chem. Eng. Data* **1985**, *30*, 247.

(39)   Taylor L, T. *Supercritical Fluid Extraction*; J. Wiley & Sons: New York, **1996**.

CHAPTER 4

SOLVENT PROPERTIES OF

SUPERCRITICAL

HYDROFLUOROCARBONS

4.1 Introduction

It is known that there are a number of complex solvent effects that have an influence on the kinetics and mechanism of a reaction. In previous studies by Abbott and Eardley the polarisability parameter, π^*, from the theory of Kamlet and Taft were measured for 1,1,1,2-tetrafluoroethane (HFC 134a) and difluoromethane (HFC 32).[1,2] As an extension to this work the hydrogen bond donor (HBD, α) and hydrogen bond acceptor (HBA, β) parameters will be determined by solvatochromic shifts using UV-VIS spectroscopy of a variety of indicator solutes. These properties are essential for understanding reactant association in solution and the acid/base properties of the solvent. These parameters will also be required to model the solubility of the reactants and catalysts in solution.

4.1.1 Solvatochromism

Solvatochromism can be defined as the change in position of an electronic absorption or emission band, accompanying a change in the polarity of the medium. The solvatochromic shift itself is the displacement of an electronic spectrum on going from one solvent to another. Negative solvatochromism corresponds to a hypsochromic shift with increasing solvent polarity and a positive solvatochromism is a bathochromic shift with increasing solvent polarity.

This observed solvatochromic shift could be explained by considering the electronic states of a molecule. Each electronic state has a discrete energy, $\mathbf{E}$, and wavefunction, Ψ, related by the Schrödinger equation[3]

$$\mathbf{H}\Psi = \mathbf{E}\Psi \tag{4.1}$$

where $\mathbf{H}$ is the Hamiltonian operator. In the case of an isolated molecule in quantum mechanics, these electronic states are relaxed states corresponding to the most stable nuclear configurations. From the Franck-Condon principle it is deduced that immediately following an electronic transition the final state, termed the Franck-Condon state, cannot be relaxed because nuclei require considerably more time (around 10^{-12} s) than electrons (around 10^{-16} s) to rearrange to their most stable configurations.[4,5] Hence the nuclear configuration in both the initial relaxed and final Franck-Condon states remains unchanged.

In an absorption or emission process it is a radiative electronic transition that links the initial relaxed and final Franck-Condon states. When considering a molecule

surrounded by a medium, each of its electronic states will be stabilised or destabilised by an amount known as the solvation energy, E_s, which is dependent on the polarity of the medium. Thus it is the influence of this solvating medium on the electronic absorption or emission spectra of the solute that gives rise to the definition of solvatochromism.[4]

The solvatochromic shift between two solvents is the difference in solvation energies between the final (S_1) and initial (S_0) states as shown in Figure 4.1. These shifts are important not only for the description of the relative energies of electronic states of molecules but also for the experimental determination of some important physical properties such as the polarisability and the dipole moment of the molecule in question. However, they can often provide information about specific interactions such as hydrogen bonding and on a microscopic level, solvatochromic shift data can provide information on solvation in the cybotactic region of a solute molecule.

4.1.2 The Kamlet and Taft Polarisability/Dipolarity Parameter, π^*

Solvation is defined quantitatively as the energy of interaction between a solute and a solvent. For non-specific interactions the solvation energy can be expressed as the products of two polarity functions[4]

$$E_{solv} = p_m \times \pi_s \qquad (4.2)$$

where p_m and π_s represent the polarity of the solute and solvent respectively. Attempts at understanding solvent effects in terms of these polarity functions have proved difficult as they are not easy to define precisely or express quantitatively. It has been mostly macroscopic solvent parameters such as dielectric constant, dipole moment, refractive index, or functions thereof, which have been used for the evaluation of medium effects.[6-8] This approach is sufficient in the case of non-specific interactions, however, solute-solvent interactions can also take place on a microscopic level, giving rise to specific interactions such as hydrogen bonding, electron-pair donor or electron-pair acceptor interactions. It is in these cases that this electrostatic approach to medium effects fails in correlating observed solvent effects with physical solvent parameters.[9] To compensate for the failings of this method several empirical solvent polarity scales have been devised,[10,11] which take into consideration the presence, or absence of specific solvent-solute interactions.
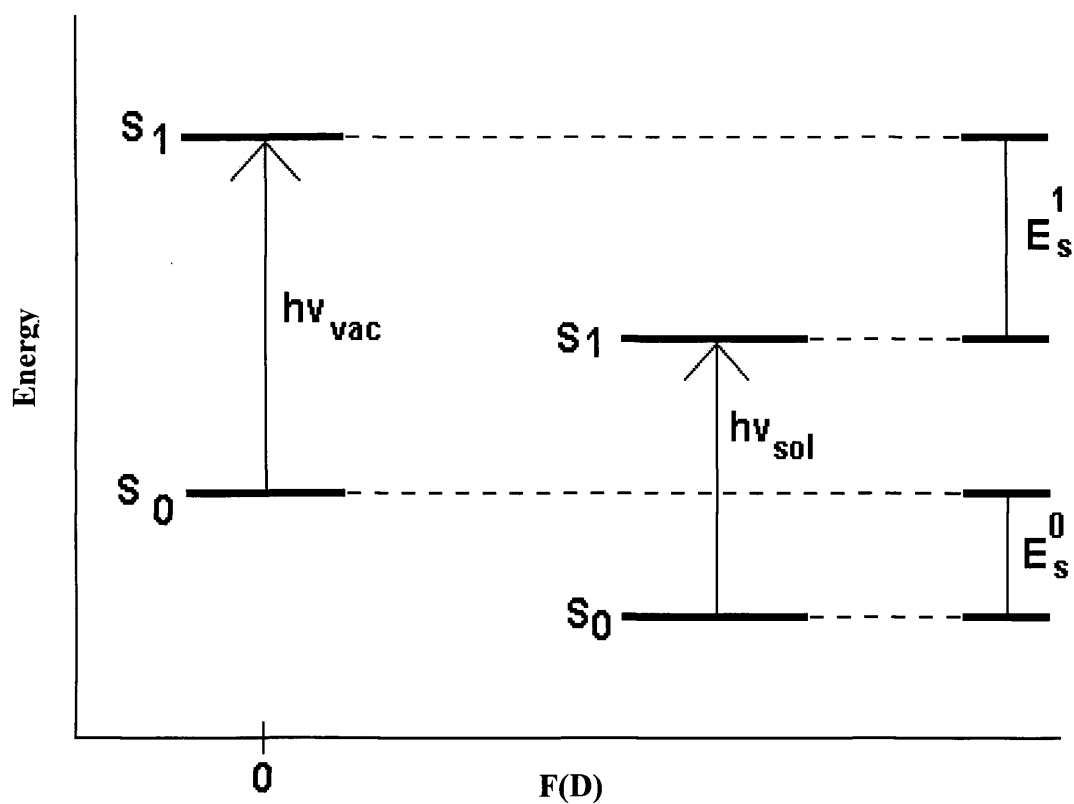
Figure 4.1 A solvatochromic shift energy diagram for the case of a vacuum and a solvent. E^0_s and E^1_s are the solvation energies of the ground and excited states respectively and f(D) is the Onsager solvent polarity function $2(\varepsilon - 1)/(2\varepsilon + 1)$

The first empirical parameter was the Y-scale of solvent ionising power introduced by Winstein *et al.* in 1948.[12] This publication establishing solvent polarities based on Y-values prompted other authors to propose scales of solvent polarities based on a given solvent sensitive property. Brooker and co-workers made the first suggestion that solvatochromic dyes could serve as visual indicators of solvent polarity.[13] However, in 1958 it was Kosower who was first to set up a real spectroscopic solvent polarity scale.[14,15] This was called the Z-scale and was based on the UV-VIS spectra of an *N*-methylpyridinium iodide, where the low energy absorption band in the spectra characterises the charge transfer from iodide to the pyridinium ring. Since then various additional UV/VIS/IR based solvent polarity scales have been developed, for example the $E_T(30)$ scale.[9,16,17]

All these scales are single parameter scales in which the non-specific and specific interactions 'mix' into a single solvent parameter. Obviously, this is an oversimplification and causes serious limitations when applying this single parameter approach to medium effects. A more satisfactory method is to use multi-parameter correlation equations, which may consist of up to four single empirical parameters, each measuring a specific aspect of the overall solvation capability of the medium.[10,18] An example of a commonly used multi-parameter scale is the π^* scale of solvent polarisability/dipolarity.[18-24]

The π^* scale relies on a linear solvation energy relationship (LSER) correlating a number of solvent effects on a solute.[19-21] The relationship has the general form

$$XYZ = XYZ_0 + a\alpha + b\beta + h\delta_H + SPPE \qquad (4.3)$$

where **XYZ** represents a property of the system in a given solvent related to that in the standard **XYZ₀**, such as reaction rate, equilibrium constant or a position or intensity of spectral absorption. The solvatochromic parameter α is a quantitative, empirical measure of the ability of the bulk solvent to act as a hydrogen bond donor (HBD) towards a solute, thus β is the opposite and measures the hydrogen bond accepter (HBA) properties of the solvent.[19,20,25,26] The **a** and **b** parameters are the corresponding hydrogen bonding constants associated with the solute. δ_H is known as the Hildebrand solubility parameter and is a measure of the solvent-solvent interactions that are broken in creating a cavity for the solute and **h** is the corresponding solute parameter.[27] Finally **SPPE** is a parameter that denotes the solvent polarisability/dipolarity effect.

Kamlet, Taft and co-workers developed their π^* scale based on solvent-induced shifts on the peak position of a UV-VIS absorption maximum of an indicator solute in a liquid solvent with characteristic values of the HBD, HBA and SPPE parameters for various solvents.[18,20] Initially using seven nitroaromatics, Kamlet and Taft showed that their UV-VIS spectral data could express the SPPE term by the parameter π^*, a measure of solvent polarisability/dipolarity.[19] This π^* scale is so named as it derives from solvatochromic effects on n $\rightarrow \pi^*$ and $\pi \rightarrow \pi^*$ electronic spectral transition. Over the years from its original construction this π^* scale has been expanded and refined with the addition of other solvatochromic indicators. Hence, an arbitrary π^* scale of solvent polarities has been established, in which for example, non-polar cyclohexane has a π^* value of 0.0 and polar dimethyl sulphoxide has a π^* value of 1.0.

In Equation (4.3) substitution of the π^* parameter for the SPPE term leads to

$$XYZ = XYZ_0 + s\left(\pi^* + \partial\delta\right) + a\alpha + b\beta + h\delta_H \tag{4.4}$$

where s represents the susceptibility of XYZ to changing SPPE and is a constant characteristic of the solute. The quantity δ is a polarisability correction term with dimensions equal to 0.0 for non-halogenated aliphatics, 0.5 for halogenated aliphatics and 1.0 for aromatic solvents. It is observed that when the electronic spectrum is shifted to lower frequencies (bathochromically) with increasing solvent polarity, the coefficient of the δ term, ∂, is equal to zero and, therefore, δ can be neglected.

The LSER in Equation (4.4) can be simplified under a number of conditions. It is notable in the case of UV-VIS spectroscopy that electronic transitions are hardly accompanied by a change in molar volume of the absorbing ground state molecule on excitation. Thus according to the Frank-Condon principle the ground and excited states of the indicator molecule will occupy the same volume and the $h\delta_H$ term in Equation (4.4) can be ignored. If only non-HBD solvents are considered it is the α term that can be ignored. Conversely, if the solutes are non-HBD the β term can be ignored. As a consequence of these simplifications the four-parameter Equation (4.4) can be reduced to a three-, two-, or even a one-parameter equation of the form

$$\upsilon_{max} = \upsilon_0 + s\pi^* \tag{4.5}$$

where ν_{max} is the wavenumber of maximum absorbance in the UV-VIS spectrum and ν_0 is the reference wavenumber of maximum absorbance determined for a standard solvent (cyclohexane).

The success of this π^* scale has led to the characterisation of over 250 liquid solvents.[28] The growth in sc fluids as solvents for extraction processes, chromatography and chemical reactions has led to the interest in the relationship between density and the solvent properties of these fluids. A number of research groups have examined whether the π^* scale introduced by Kamlet and Taft can be used to characterise these solvents.[1,2,29-33] From sc fluid research it is thought that π^* will be affected by density and therefore density will have an impact on both the quantity and the qualitative nature of solute-solvent intermolecular interactions. Thus, both temperature and pressure can have an effect on the peak position of solvatochromic measurements.

Compared to the number of π^* studies in liquid solvents only a small number of investigations have been carried out in sc solvents. Most solvatochromic studies involving sc fluids have been carried out using low polarity solvents, such as CO_2 and NO_2, where the contribution of hydrogen bonding to solvent polarity is small. Sigman et al. have measured π^* values for a number of solvatochromic indicator solutes in sc CO_2.[29] From this work the π^* parameter was shown to increase with the solvent density. However, the values of π^* obtained were found to be less than those for cyclohexane, indicating that sc CO_2 is a very non-polar fluid.

The relationship between π^* and solvent density observed in the work by Sigman et al.[29] have also been reported in other studies. Yonker and co-workers studied numerous sc systems including CO_2, N_2O, CCl_3F and NH_3[30] and later in Xe, SF_6 and ethane.[34] Also a number of fluorinated sc solvents have been studied and π^* values obtained. Bruno et al. used 4-nitroanisole and 4-nitrophenol to calculate the π^* values of ethane and six fluorinated ethane solvents in the sub-sc and sc region.[35] Once again it was found that the π^* parameter increases with solvent density for all of the solvents studied. The trends in the π^* values were related to the degree of fluorination about the ethane molecule. Solvatochromic studies have also been carried out on near critical and sc water and ethanol where it was found that these solvents have a wide range of solvent strength, which can be readily and continuously tuned by temperature and pressure changes.[36,37]

The polarisability parameter π^* has also been studied for HFC 134a[1], HFC 32 and pentafluoroethane (HFC 125)[2] as a function of temperature and pressure, to cover the liquid and sc states over the range 303 to 403 K and 40 to 300 bar. In this work Abbott and Eardley explained the change in π^* with reduced density in terms of local density augmentation and used a van der Waals model to predict the changes in solvent properties. More recently they extended their work to look at CO_2/HFC 134a mixtures.[33] Only a handful of other authors had studied the solvent properties of sc mixtures.[38-41] Research into sc mixtures has shown that there is preferential solvation of the solute by the more polar solvent in the mixture and the local composition of this polar constituent steadily decreases as the pressure is increased. In the work by Abbott *et al.*[33] they discovered that a mixture of 30 mol % HFC 134a in CO_2 has properties similar to those of bulk HFC 134a at high densities. The combination of HFC 134a with CO_2 is found to decrease the critical temperature by 42 K from that of pure HFC 134a making these mixtures more economically attractive solvents especially as the HFC 134a is not left as a residue after depressurisation.

4.1.3 Hydrogen Bonding

The hydrogen bond is an intermolecular or intramolecular interaction, which has a strength of around 20 kJ mol^{-1}. This is similar in strength to a van der Waals force but a hydrogen bond is directional which can give rise to discrete recognisable units consisting of two or more single molecules.

Hydrogen bonds were originally postulated by Latimer and Rodebush in 1920 to explain, among other effects, the high boiling points of compounds containing the groups -OH, $-NH_2$ or >NH compared with isomeric molecules with no hydrogen directly attached to the oxygen or nitrogen.[42] From this initial work it was found that a hydrogen bond is an attractive interaction between two closed shell species, which is represented by the broken line in Figure 4.2. Hydrogen bonding can only occur if A and B in Figure 4.2 are highly electronegative and small for example F, O or N, and B must also possess a lone pair of electrons.
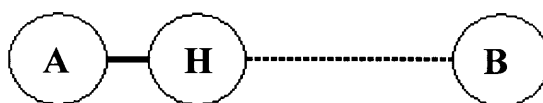
Figure 4.2 Representation of a hydrogen bond

It has been shown that hydrogen bond strengths can be measured via UV-VIS spectral data using a solvatochromic comparison method.[25,26] Initial work by Kamlet and Taft used this method to construct a β-scale of solvent HBA basicities[25] and an α-scale of HBD acidities.[26] These hydrogen bond interactions can be accounted for by modifying Equation (4.5) to

$$\upsilon_{max} = \upsilon_0 + s\pi^* + a\alpha + b\beta \tag{4.6}$$

where α and β are measures of HBD acidity and HBA basicity respectively, and a, b and s are susceptibility constants.

From Equation (4.6) the solvatochromic comparison method can then be used for the determination of α values by comparison of solvent-induced shifts of the longest wavelength $\pi \to \pi^*$ absorption band of two similar probe molecules, one of which cannot act as a HBA towards HBD solvents, whereas the other can. Determination of β values is analogous to the determination of α values, however in this case one of the probe molecules cannot act as a HBD towards solvents, whereas the other one can. Values of α and β for a number of liquid solvents have been reported by Kamlet and Taft[25,26] and more recently by Marcus.[43,44]

Extending the α and β scales to sc fluids has been the focus of more recent work by a number of authors to see how these scales change with density. Kim and Johnston used UV-VIS spectroscopy to characterise the HBD ability of sc fluoroform with the solvatochromic probe phenol blue.[45] It was shown that the hydrogen bond interactions were well developed at the critical density but did not change substantially with pressure up to 350 bar. Bennett and Johnston characterised the HBD strength of sc water with the UV-VIS spectroscopic probes acetone and benzophenone.[46] They also showed that hydrogen bonding can persist in sc media at low densities and specifically as low as 0.1 g cm^{-3} in sc water at 653 K.

Sigman et al. reported β values in sc CO_2 and found a constant value of β over all densities using 4-nitrophenol.[29] The HBD strength of five pure fluids, CO_2, N_2O, $CClF_3$, SF_6 and NH_3 were found using five probe indicators.[32] β values were measured along three isotherms, from atmospheric pressure up to 1000 bar. Of the fluids investigated only NH_3 showed significant basicity under any of the conditions studied. The NH_3 β values were found to be approximately 0.70 at 293 K, 0.65 at 333 K and 0.55 at 413 K and 1000 bar. Lagalante and co-workers have measured β for six

fluorinated ethane solvents in their liquid and sc states.[35] It was found that for the solvents in this work β values were generally negative over the density range studied and could be classed as an average value over the entire density range.

Recently Eckert and co-workers characterised the Kamlet-Taft parameters of near critical and sc ethanol and showed that the HBD properties decrease with increasing pressure and temperature. The HBA properties were found to be small and relatively invariant with pressure in the sc region.[36]

Eardley has reported preliminary results for the determination of α in liquid and supercritical HFC 134a[47] based on the measured Kamlet and Taft parameters, π^* and β, by Lagalante and co-workers using the solvatochromic probe molecule 4-nitroanisole.[48] In the work by Lagalante et al. it was shown that HFC 134a was unable to act as a hydrogen bond acceptor, implying that β is equal to zero. Using this result and assuming the reported π^* values are accurate, Eardley calculated the hydrogen bond donor parameter of HFC 134a as a function of temperature and pressure using Equation (4.6).

Results showed that in liquid HFC 134a at 323 K, α values were widely spread in the range of 0.05 to 0.2 over the pressure range of 60 to 250 bar. The diversity in α values was attributed to the relatively poor accuracy of the 4-nitroanisole solvatochromic measurements. In sc HFC 134a, at 378 K and 393 K, α was found to lie in the range of 0.2 to 0.3 at pressures above 60 bar. Below this pressure α increased dramatically as the pressure tended towards zero. It was thought that if hydrogen bond interactions did exist between HFC 134a and Nile Red (the solvatochromic probe employed by Eardley) they are likely to be relatively consistent over the range of temperatures and pressures studied, as it had previously been shown that there is good correlation between the polarisability function, $\alpha(\varepsilon)$ and π^{*2}. These results had further inconsistencies because α and hence the hydrogen bond donating ability of HFC 134a, increased as the temperature of the system was raised from liquid to supercritical values; generally the hydrogen bond donor strength of a solvent decreases with temperature at a given density.[45,46]

This work looks to quantify the hydrogen bond properties of HFC 32 and HFC 134a over a range of temperatures and pressures. Unlike the preliminary work by Eardley, which relied on results in the literature, this work uses the same instrumentation and technique to measure all the necessary Kamlet and Taft

parameters using three solvatochromic probes, therefore, significantly reducing any sources of error. It is thought that the HBA parameter, β, for these solvents should be zero by analogy with the chlorinated analogues and perfluoroalkanes under ambient conditions[28] but this is yet to be verified. It is also unclear how the α values for these HFC solvents will change as no conclusive comparisons are found in the literature. However, it has been noted that α for pentachloro- and tetrachloroethane is zero, while for dichloromethane α is 0.4.[28]

4.2 Results and Discussion

To obtain the α, β and π^* values for the two HFC fluids the susceptibility constants a, b and s for the three solvatochromic dyes were first obtained by measuring their absorption spectra in 16 liquid solvents of different polarity and solvent type i.e. HBD, HBA and non-hydrogen bonding (NHB). The data obtained were fitted to Equation (4.6) using a multiple regression analysis. Very good correlation was obtained in all cases ($R^2 > 0.95$). The a, b and s values for the three solutes used are listed in Table 4.1 and are in close agreement with those published in the literature.[19] The calculated wavelength of absorption maxima, v_{max}, using the susceptibility constants in Table 4.1 are shown in Table 21 of the appendix along with the measured v_{max} for comparison.

Dye	a value	b value	s value	v_0 (kK)	R^2 value
N,N-dimethyl-4-nitroaniline	-0.562	N/A	-3.326	27.956	0.9757
4-nitroaniline	N/A	-3.484	-2.600	30.820	0.9970
Nile Red	-0.942	N/A	-1.623	19.978	0.9503

Table 4.1 Susceptibility constants for the solvatochromic probes used in this work

4.2.1 Polarisability/Dipolarity Parameter, π^*

Abbott and Eardley previously reported the pressure and temperature dependency of π^* for HFC 134a and HFC 32 using Nile red as an indicator solute.[2] Lagalante and co-workers have also measured the Kamlet-Taft parameters, π^* and β, for six liquid and sc fluorinated ethane solvents, including HFC 134a.[35] The π^* values of HFC 134a previously reported by Abbott were consistently slightly higher ($c.a.$ 0.07) than those determined by Lagalante in both the liquid and sc phases. It was implied that the difference in π^* values results from the neglect of hydrogen bonding interactions between HFC 134a and Nile Red. Similar inconsistencies in π^*, however, have been observed for CO_2 when employing the solvatochromic probes Nile red and 4-nitroanisole[31,33] and hence this may not be the sole reason.

Figures 4.3 and 4.4 show the π^* values calculated for HFC 32 and HFC 134a as a function of temperature and pressure respectively. The first point to note is that
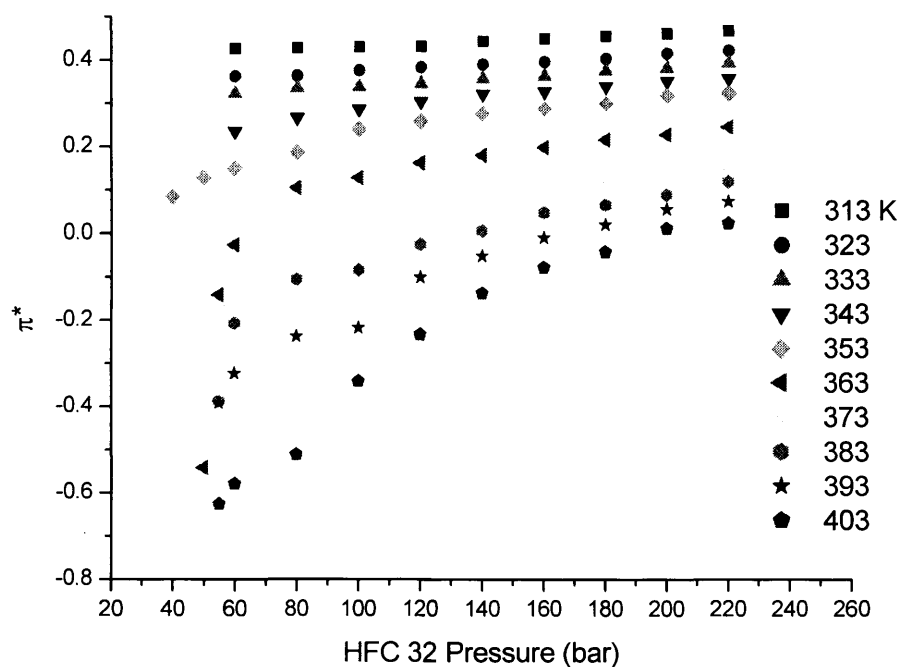
Figure 4.3 The polarisability/dipolarity, π*, values for HFC 32 as a function of temperature and pressure
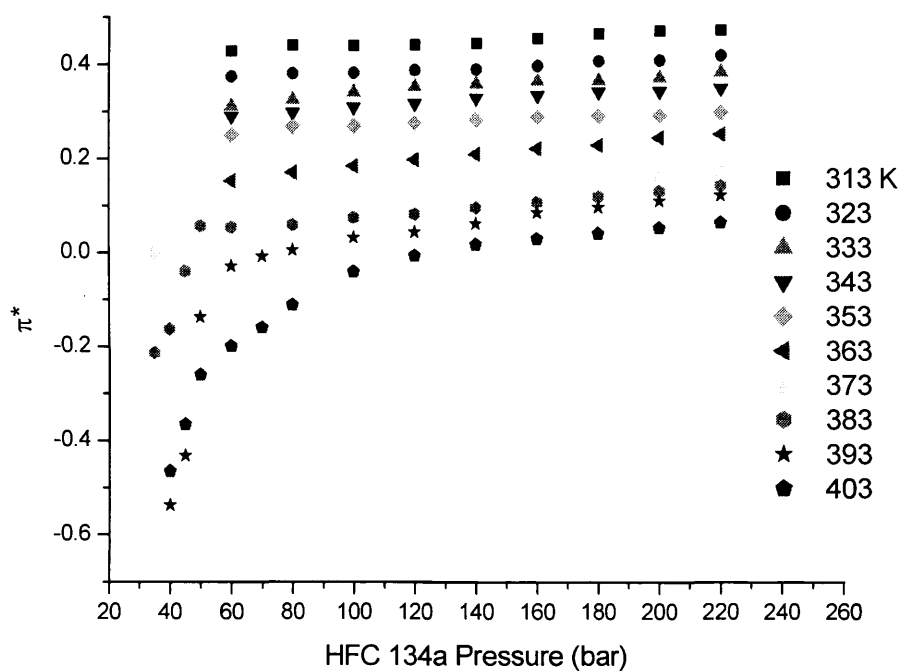
Figure 4.4 The polarisability/dipolarity, π*, values for HFC 134a as a function of temperature and pressure

the π^* values are similar, although slightly lower than those published previously[2] and the agreement with the Lagalante data[35] for HFC 134a is also improved.

Application of the Mean Sphere Approximation (MSA) to these solvents showed π^* and the dielectric constant, ε, to be strongly related in both the liquid and supercritical states.[2] It was shown that π^*, the polarisability/dipolarity, can be related to a complex function of the solution dielectric constant, $\alpha(\varepsilon)$ by

$$\pi^* = \pi^*_{gas} + \frac{2\alpha(\varepsilon)\mu_G(\mu_G - \mu_E)}{s4\pi\varepsilon_o chD^3} \qquad (4.7)$$

where

$$\alpha(\varepsilon) = \frac{8(\varepsilon - 1)}{2uR^3\rho^3 + 2\varepsilon[1 + R(1 - 2u)]^3 + [1 + R\rho]^3} \qquad (4.8)$$

$$R = d / D$$

$$\rho = \frac{(1 - u)}{(1 - 2u)}$$

$$u = \frac{3\xi}{(1 + 4\xi)}$$

$$\xi = \frac{1}{2}\left[1 - \frac{9}{4 + f^{1/3} + f^{-1/3}}\right]$$

$$f = 1 + 54\varepsilon^{1/2}\left[1 - \left[1 + \frac{1}{27\varepsilon^{1/2}}\right]^{1/2}\right]$$

and where π^*_{gas} is the vapor phase limit, R is the ratio of the solvent, d, and solute, D, radii, μ_G and μ_E are the dipole moments of the solute in the ground and excited states, c is the speed of light in a vacuum, ε_0 is the permittivity of free space and h is Planck's constant. Hence, π^* should be proportional to $\alpha(\varepsilon)$. This was shown to be valid for HFCs 134a, 32 and 125 over the temperature range 303 to 403 K and the pressure range 40 to 300 bar.[2] While the slopes of π^* vs. $\alpha(\varepsilon)$ plots were all very similar they were considerably offset from each other in reference to Equation (4.7), which predicts that all the solvents should be coincident since π^*_{gas} should be common to all solvents. It was postulated that this discrepancy may result from hydrogen bonding but the changes in the π^* values from those published previously

are too small to account for this difference. Analysis of Equation (4.8) shows a critical dependence of $\alpha(\varepsilon)$ on the ratio of the solvent and solute radii. The previously reported method[49] for determining the molecular radii was an additive method based upon average atomic Stokes radii that was relatively inaccurate and may result in the previously observed offset. In the current study computer simulation was used to determine the solvent and solute volumes.[50] The equilibrium geometry and charge distributions of the solute and the solvent were calculated using a Hartree-Fock method utilizing an STO-3G model.[50] Figure 4.5 shows plots of π^* vs. $\alpha(\varepsilon)$ for the new π^* data and shows that both solvents are in much closer agreement to Equation (4.7). The model does, however, still assume that the indicator solutes are spherical, which in the case of Nile red is clearly not accurate as it is more oblate. Redefining d and D as the volume/area ratio (rather than the radius) of the solvent and solute respectively, yields a parameter that more accurately accounts for the contribution of molecular geometry to the solvent-solute interaction i.e. an oblate molecule has a larger surface of interaction with the surrounding environment than a spherical molecule of the same formula. Figure 4.5 shows that the modified Mean Sphere Approximation (MMSA) approach yields a much closer agreement between the two solvents and a π^*_{gas} value in close agreement with the theoretical value of -1.06 (π^*_{gas} is -1.10 and -1.22 for HFCs 134a and 32 respectively).[51] The polarisability/dipolarity parameter can accurately be modeled for HFC 32 and HFC 134a using the Mean Sphere Approximation although critical parameters such as molecular radii significantly affect the accuracy of the parameter $\alpha(\varepsilon)$ which is a weakness of this approach.

4.2.2 Hydrogen Bond Acceptor Properties, β

The solvatochromic probes 4-nitroaniline and N,N-dimethyl-4-nitroaniline were used to obtain the basicity parameter based on a comparison method.[25,26] The calculated β values as a function of temperature and pressure for HFC 32 and HFC 134a are shown in Figures 4.6 and 4.7 respectively. The β values for both solvents are small but positive. This is a slight contradiction to the data presented by
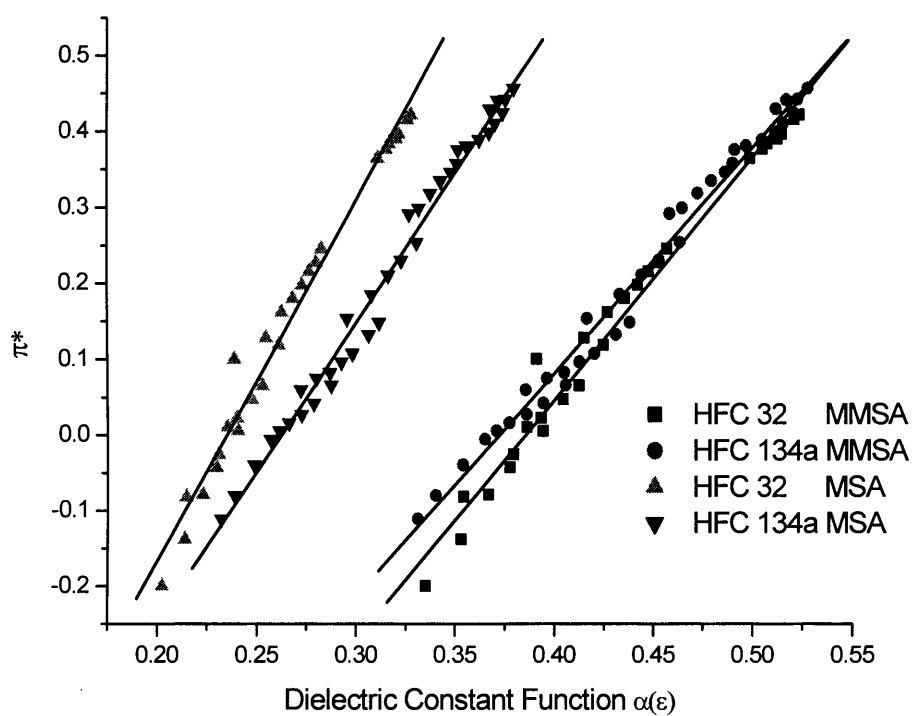
Figure 4.5 Application of the mean sphere approximation (MSA) and modified MSA (MMSA) to the polarisability/dipolarity, π^*, data shown in Figures 4.3 and 4.4
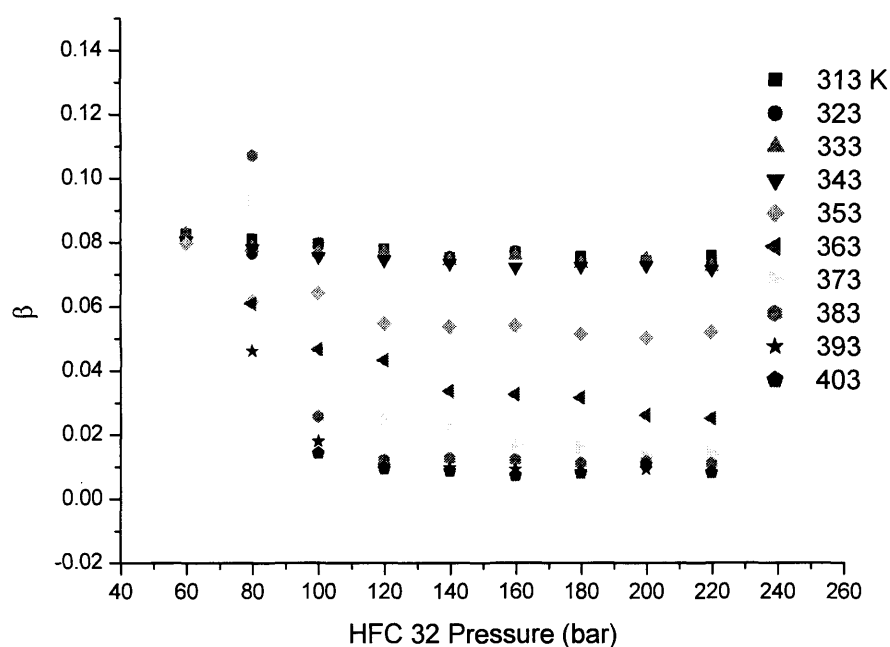
Figure 4.6 Hydrogen bond acceptor basicity, β, values for HFC 32 as a function of temperature and pressure
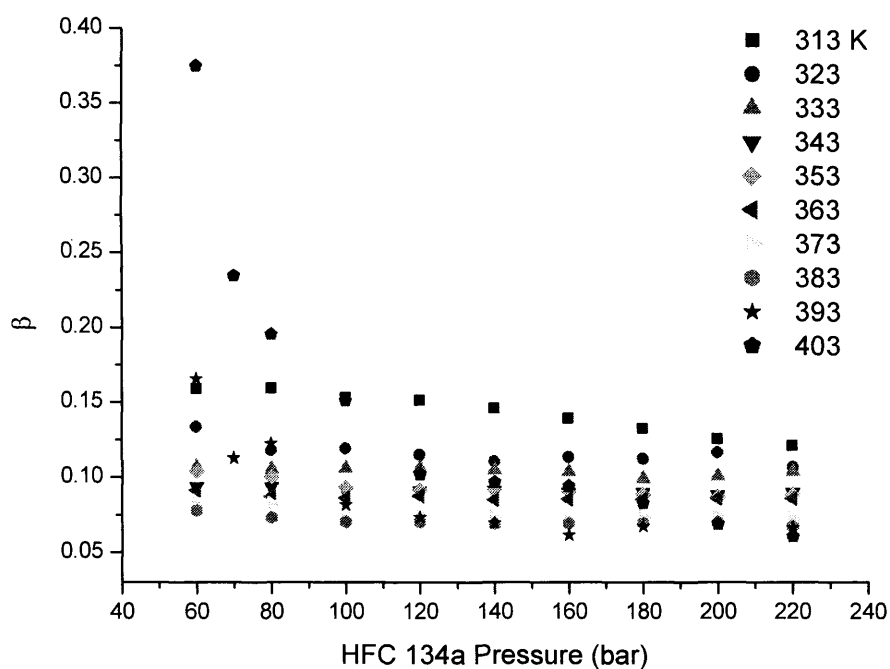
Figure 4.7 Hydrogen bond acceptor basicity, β, values for HFC 134a as a function of temperature and pressure

Lagalante *et al.*[35] who showed that HFC 134a is a poor hydrogen bond acceptor, since β was found to be slightly negative.

The results presented in Figure 4.7 do seem logical since the β value should be greater than that for cyclohexane ($\beta = 0$) since the fluorine atoms will be relatively good HBAs. The discrepancy probably occurs from the assumption made by Lagalante that the indicator solute, 4-nitroanisole, does not act as a hydrogen bond acceptor. For HFC 32 the β value is almost invariant with either temperature or pressure in the liquid state (i.e. below 351 K). At $T \geq T_c$ a decrease in β with increasing temperature and pressure is observed. At sc temperatures the β values for HFC 134a are slightly larger than those for HFC 32. From the β values at low pressures it can be seen that both solvents are relatively good HBAs. The β values for both fluids are similar to those reported recently for sc ethanol by Lu *et al.*[36]

4.2.3 Hydrogen Bond Donor Properties, α

Figures 4.8 and 4.9 present, for the first time, the α values for these solvents. Given the relatively acidic protons on both solvents it would be expected that they would be relatively good HBDs. The magnitude of the α values are comparable with related compounds e.g. dichloromethane at ambient conditions where $\alpha = 0.4$ and similar to the value reported by Corr[52] for liquid HFC 134a ($\alpha = 0.48$) at ambient temperature and an approximate density of 1.22 g cm^{-3}. The decrease in α with increasing pressure in the sc state is consistent with the data presented recently for ethanol.[36] The α values for both solvents are shown to be almost constant with increasing pressure in the liquid state and decrease with increasing pressure in the sc state. Similar results were also obtained using the previously published data.[47]

At higher pressures (> 100 bar) the α value decreases with increasing temperature as would be expected. However, at lower pressures when $T > T_c$ the α value increases with increasing temperature. This is an unusual result and is observed for both solvents. Lu *et al.*[36] suggested that for ethanol the change in α with temperature was due to the change in the equilibrium between solvent-solvent and solvent-solute interactions with the latter dominating at high temperature.
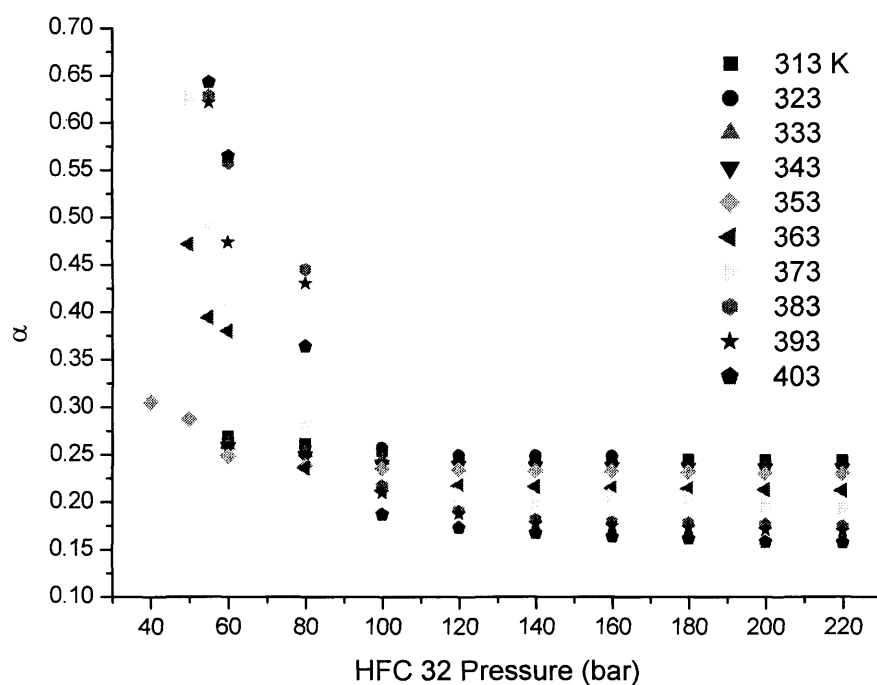
Figure 4.8 Hydrogen bond donor acidity, α, values for HFC 32 as a function of temperature and pressure
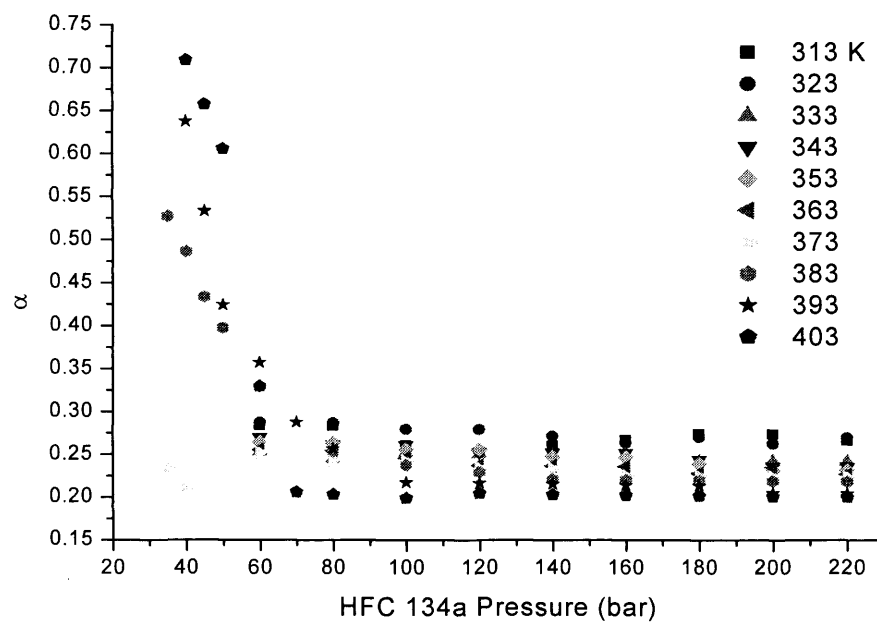
Figure 4.9 Hydrogen bond donor acidity, α, values for HFC 134a as a function of temperature and pressure

It can be argued that because the α parameter gives a measure of the equilibrium constant, K, between the solvent-solvent and solvent-solute interactions in a liquid, then at low density it can be used to obtain an apparent enthalpy of hydrogen bond formation $\Delta H'$ since

$$\frac{d \ln K}{d(1/T)} = \frac{\Delta H'}{R} = \frac{d\alpha}{d(1/T)}$$

(4.9)

where R is the gas constant and T in the temperature in Kelvin. Hence when p < 100 bar and T > T_c, $d\alpha/dT$ is negative and hydrogen bond formation is exothermic. At 55 bar, for example, the data obeys Equation (4.9) well and yields an apparent enthalpy of hydrogen bond formation of -9.2 kJ mol^{-1}. The exothermic behavior is also observed for HFC 134a although less data display this characteristic because of the higher T_c. It is interesting to note that for all the data where $d\alpha/dT$ is negative the density of the solvent is less than the critical density, ρ_c. It is around this density that the solvation sheath is assumed to be complete and hence the decrease in hydrogen bonding is most probably due to the competing solvent-solvent interactions with neighbouring solvent molecules. This suggests that the same three-region density model should also be evident for α as is observed for π^*.[2]

Figure 4.10 shows the α, β and π^* values for HFC 32 as a function of solvent density. The first point to notice is that HFC 32 is such an excellent solvent due in part to the high density exhibited in the sc state. The density in the sc state is higher than many common solvents in the liquid state at ambient conditions. It is also clear from Figure 4.10 that this three-region density model does indeed exist for the α parameter. Unfortunately it was not possible to confirm this for the β parameter although the trend observed over the obtainable density range is remarkably linear suggesting that density augmentation has little effect on the HBA properties of the solvent. Figure 4.10 shows that at low density the polarity of this HFC is dominated by hydrogen bond donor properties, which suggests that in the low density region the solvent interaction is different to that at higher densities. Analogous results were obtained for HFC 134a.

Figure 4.11 compares the polarity parameters for HFCs 32 and 134a as a function of reduced density at a reduced temperature of 1.128 (HFC 32: T = 373 K; HFC 134a: T = 403 K). It can be seen that at a given reduced density the HBA and HBD parameters for HFC 134a are larger than those for HFC 32, which may be
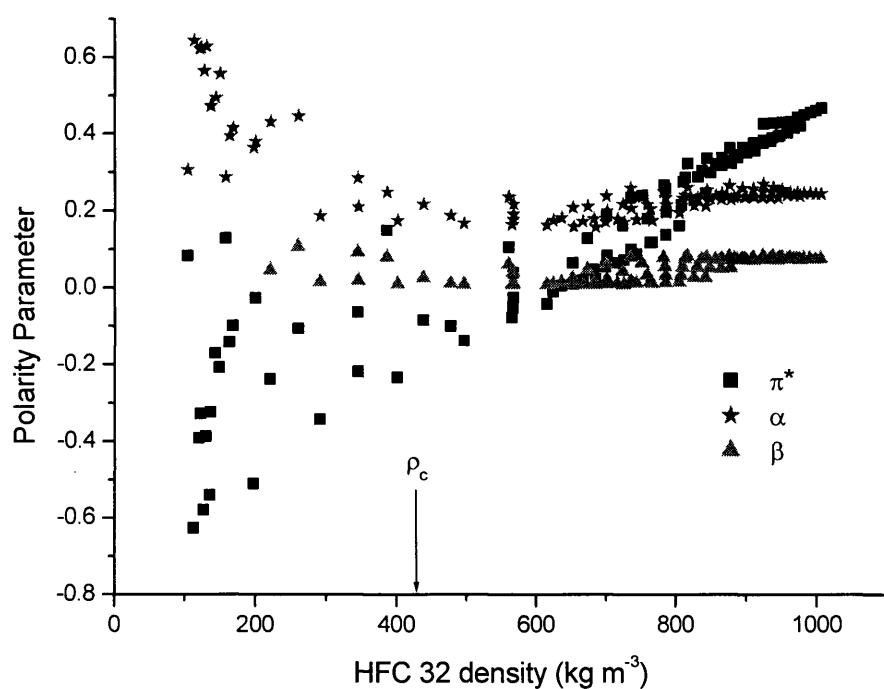
Figure 4.10 Polarity parameters for HFC 32 as a function of reduced density
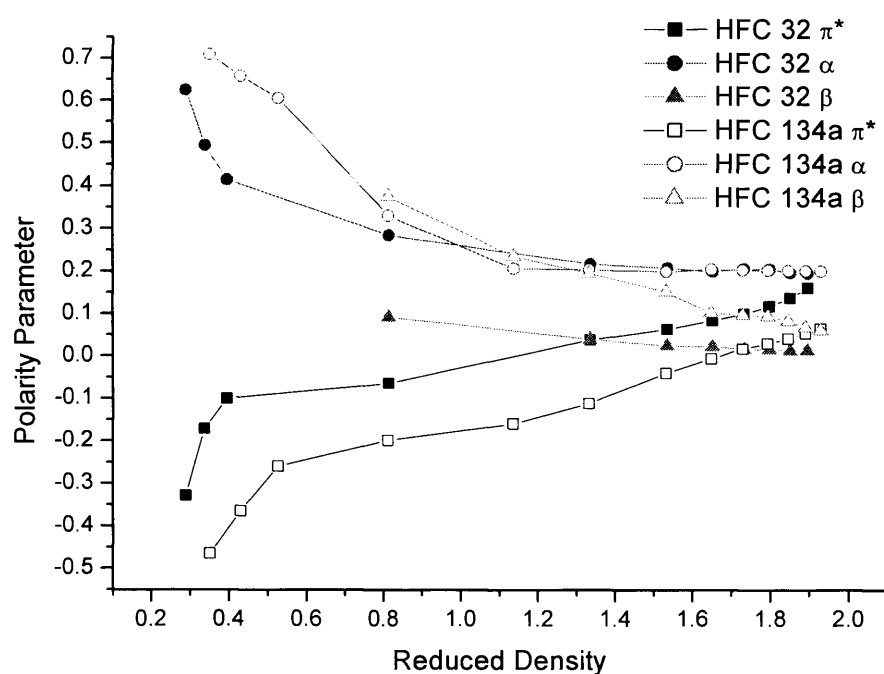
Figure 4.11 Polarity parameters for HFC 32 and 134a as a function of reduced density at a constant reduced temperature (1.128)

expected given the differences in dipole moment (2.058 and 1.987 D respectively). In contrast the π^* for HFC 32 is larger than that for HFC 134a possibly due to the difference in size and the ability to pack more of the smaller solvent molecules around the indicator solute. The two solvents show points of inflection for all three parameters at approximately the same reduced density confirming that they both obey the same three-region density model.

Cross correlation of the parameters presented above also yields some interesting results. Figure 4.12 shows the correlation between α and π^* for HFC 32 as a function of reduced density. Two distinct regions are observed, one with a positive and one with a negative correlation between the parameters. At high densities in the 'liquid-like' region ($\rho_r > 1$) there is a small, positive correlation of α and π^* and this is linearly dependent on density, suggesting it is just the packing of solvent molecules around the solute that affects these two parameters. In the 'gas-like' region ($\rho_r < 1$) both parameters change more significantly with density. Importantly, a negative correlation is observed between the parameters and $d\alpha/d\pi^*$ increases with increasing temperature. Exactly the same trend is observed for HFC 134a shown in Figure 4.13. The two solvents differ only in the reduced density at which the point of inflection occurs (for HFC 32 it is $c.a.$ 0.4 whereas for HFC 134a it is $c.a.$ 0.6).

There are two possible scenarios that could lead to this effect; either the solvent-solvent interactions are weakened as the inter-solvent separation increases (allowing the solvating molecules to interact more strongly with the solute) or the solvation sheath is incomplete and the solvent molecules cluster preferentially around the hydrogen bonding moieties. To analyse these scenarios it is important to determine the local solvent density by assuming that if local density augmentation did not occur then π^* would increase linearly with density as it does in the liquid state (and the sc state at high pressures).[53] Figure 4.14 shows the value of the α parameter as a function of the average local intermolecular separation for HFC 32. Increasing the distance between the solvating molecules to about 5 to 6 Å causes a significant increase in α suggesting that decreased solvent-solvent interactions play a key role in influencing solvent-solute interactions. However, since under the low-density conditions, where α increases significantly, the solvation sheath is incomplete, hydrogen bond interactions will be larger than dipole-dipole or dipole-induced dipole
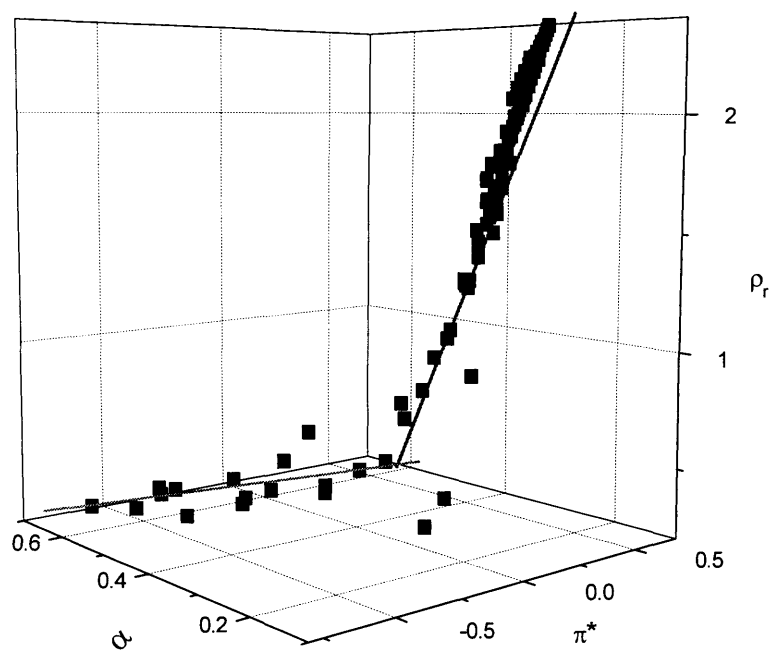
Figure 4.12 Cross-correlation between hydrogen bond donor acidity, α, the polarisability/dipolarity, π*, and the reduced density, ρ_r for HFC 32
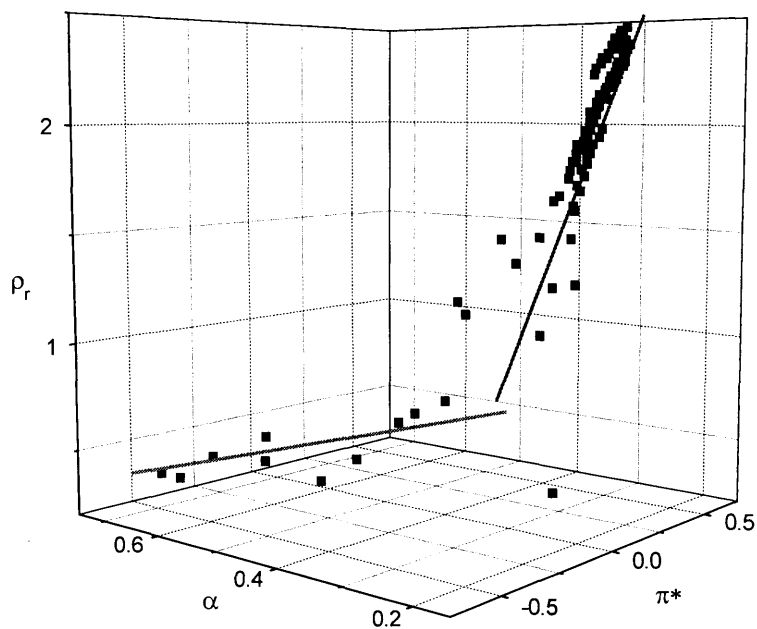
Figure 4.13 Cross-correlation between hydrogen bond donor acidity, α, the polarisability/dipolarity, π*, and the reduced density, ρ_r for HFC 134a
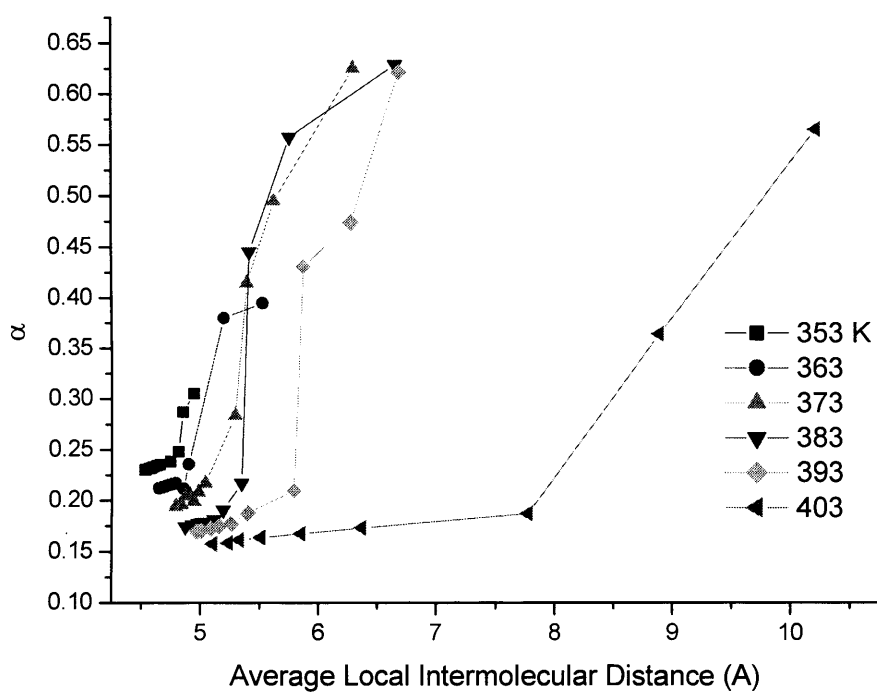
Figure 4.14 Change in hydrogen bond donor acidity, α, with intermolecular distance for HFC 32

interactions and it is probable that the solvent interacts with the indicator solute preferentially at the polar groups. The computer simulation by Tucker[54] showed that the local solvent density around a solute was larger around a polar functional group and supports this idea.

Figure 4.15 shows the correlation between α and β for both solvents and while this cannot interrogate the low-density region because of the lack of β data it is clear that the two parameters are related. For HFC 32 a well defined correlation is observed where $d\beta/d\alpha$ is small under liquid and sc conditions and larger in the near critical regime. Considerably more scatter is seen for HFC 134a, although a general positive correlation is observed which would be expected. The difference between the two solvents is difficult to rationalize although the generally larger β value for HFC 134a suggest that solvent-solvent interactions through hydrogen bonding may be more important than in HFC 32.

4.2.4 Solubility Modelling

The ability to predict accurately the solubility of a molecule in a sc fluid is of great industrial importance. There have been many studies dedicated to the prediction of solubilities employing for example computer simulation,[55-57] equations-of-state[55] and linear solvation energy relationships (LSER).[55,58] The LSER is based on that first developed by Kamlet et al.[59] As there is a plethora of solubility data in the literature using sc CO_2 the construction of these models has been carried out to a high degree of accuracy. This work looks to model the solubility data in Chapter 3 using a LSER of the form shown in Equation (4.3).

The LSER used to model **Log S** (in mole fraction) incorporates the solvent properties measured earlier in this chapter and is given by

$$LogS = LogS_0 + s\pi * + a\alpha + b\beta \qquad (4.10)$$

where s, a and b are coefficients relating to the solute interactions and π^*, α and β relate to the solvent interactions. A data set of 11 molecules, at a constant temperature of 363 K and varying pressures in the range 70 to 270 bar, totalling 53 data points was used. The coefficients were calculated using a multiple regression analysis and from this the following LSER was obtained
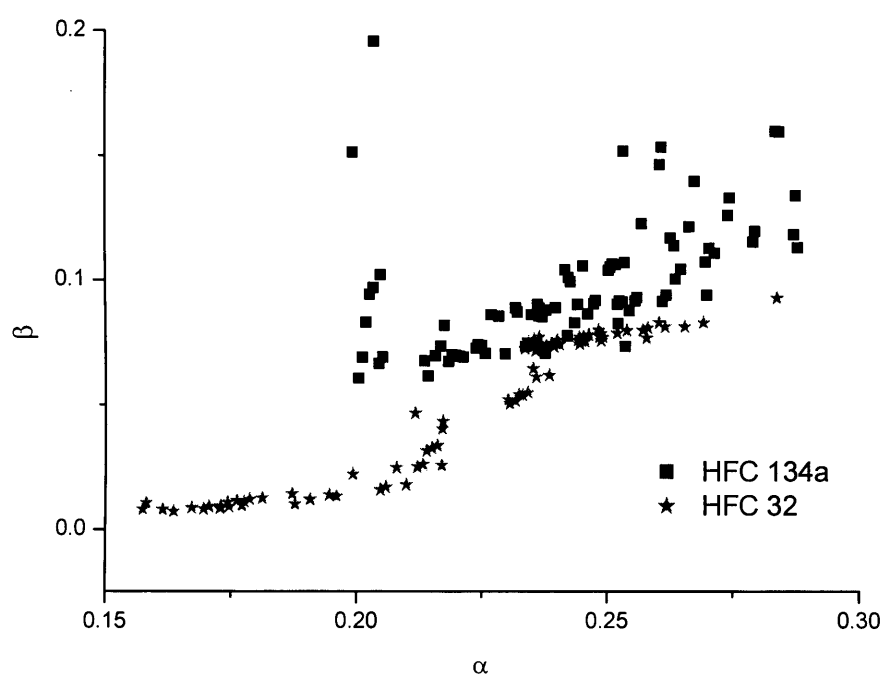
Figure 4.15 Cross-correlation between the hydrogen bond donor acidity, α, and the

hydrogen bond acceptor basicity, β, for HFC 32 and 134a

$$LogS = 2.13574 - 8.12413\pi * -6.86849\alpha - 57.50452\beta \qquad \text{(4.11)}$$

n = 53,   r = 0.39364,   sd = 0.31216,   % AARD = 27.03

The correlation statistics obtained from using this model are also shown where r is the correlation coefficient of the regression, sd is the standard deviation of the LSER equation and % AARD is the percentage average absolute relative deviation in predicting the reported values. Figure 4.16 shows the correlation for this model between the predicted and measured results. On inspection of this and the statistics presented above it can be seen that these solvent properties alone do not form an accurate LSER for the prediction of solubilities. This may be due to the fact that the data set is too small and/or there are numerous properties of the solutes that also influence their solubilities that have to be taken into consideration.

Abraham[60] used five physicochemical properties in a LSER that also include solute properties to describe solubility as shown in Equation (4.12).

$$LogS = LogS_0 + s\pi * +a\alpha + b\beta + rR + vV \qquad \text{(4.12)}$$

where R is the excess molar refraction and V is the McGowens characteristic volume of the solute. To apply this LSER these extra solute descriptors must be known or estimated. For the majority of the solutes studied in this work these were available and are shown in Table 4.2.[60,61] The solute descriptors were measured at 278 K but it has been assumed that the values, relative to each other, remain constant up to 363 K. Due to the lack of data on certain solutes the data set for this LSER was reduced to 9 molecules and 46 data points. The coefficients were once again obtained by a multiple regression analysis and the LSER obtained is shown below.

$$LogS = 44.03802 - 1.33824\pi * +2.68406\alpha - 18.87531\beta +$$
$$2.32781R - 52.83497V \qquad \text{(4.13)}$$

n = 46,   r = 0.96515,   sd = 0.23694,   % AARD = 9.157

Figure 4.17 shows the correlation using this LSER and it can be seen from the graph and the correlation statistics that including these solute properties dramatically improves the LSER model.
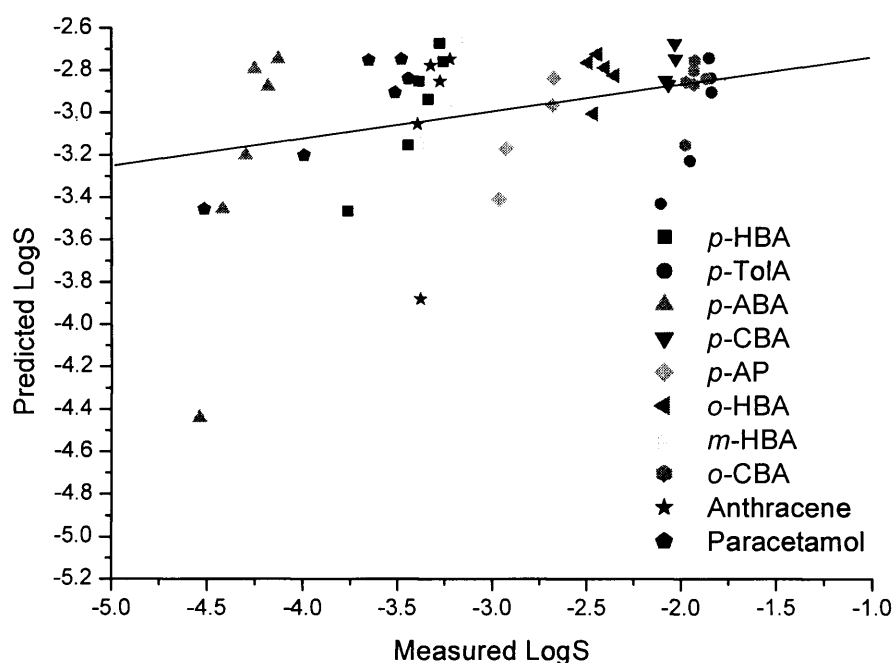
Figure 4.16 Comparison of measured Log solubility and those predicted by the LSER of Equation (4.11)
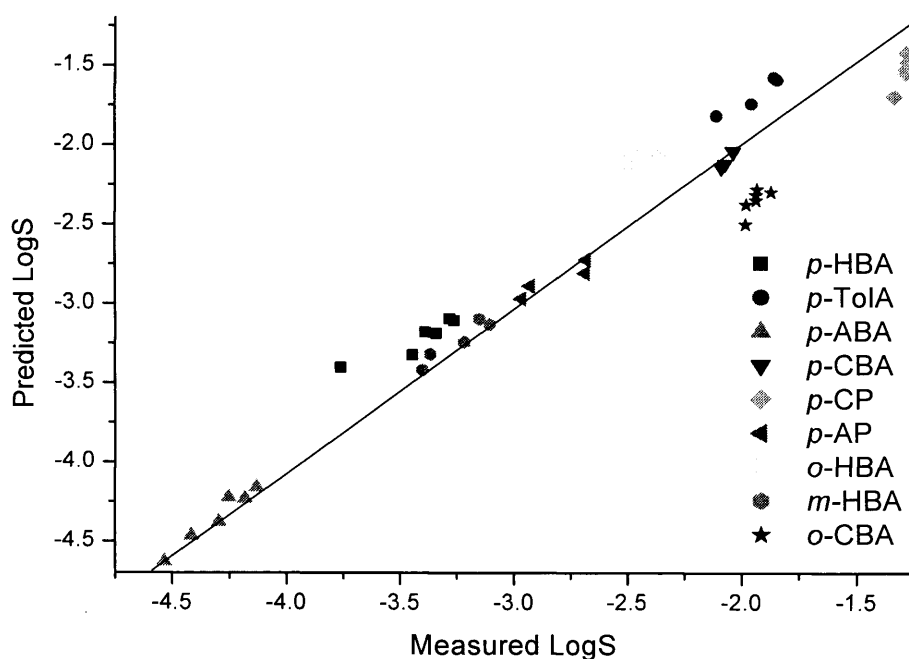
Figure 4.17 Comparison of measured Log solubility and those predicted by the LSER of Equation (4.13)

Solute	R	V	π_2	α_2	β_2
p-hydroxybenzoic acid (HBA)	0.73	0.92	1.00	0.70	0.45
p-toluic acid (TolA)	0.73	0.89	0.90	0.60	0.38
p-aminobenzoic acid (ABA)	0.73	0.94	1.02	0.80	0.42
p-chlorobenzoic acid (CBA)	0.73	0.90	0.90	0.60	0.38
p-chlorophenol (CP)	0.92	0.89	1.08	0.67	0.20
p-aminophenol (AP)	0.92	0.92	1.12	0.90	0.32
o-hydroxybenzoic acid (HBA)	0.73	0.90	0.90	0.55	0.42
m-hydroxybenzoic acid (HBA)	0.73	0.92	0.95	0.62	0.43
o-chlorobenzoic acid (CBA)	0.63	0.90	0.80	0.30	0.43

Table 4.2 Solute descriptors used in the LSER models

The LSER model in Equation (4.13) can be improved further still if more solute descriptors are taken into account.[58,62,63] In this case a total of eight physicochemical properties are used to describe the LSER as shown in Equation (4.14).

$$LogS = LogS_0 + s\pi * + a\alpha + b\beta + rR + vV + s_2\pi_2 + a_2\alpha_2$$

$$+ b_2\beta_2 \qquad (4.14)$$

where π_2 is the polarisability/dipolarity of the solute, α_2 is the solutes effective hydrogen bond acidity and β_2 is the solutes effective hydrogen bond basicity.

Table 4.2 lists the solute descriptors used as the solute independent variables in the LSER. Using these solute descriptors and the solvent descriptors presented earlier in this chapter the following LSER was obtained.

$$LogS = 29.211 - 1.79689\pi * -0.79703\alpha - 15.85885\beta + 2.9612R$$

$$- 31.6557V - 1.6839\pi_2 - 1.6225\alpha_2 - 4.0266\beta_2 \qquad (4.15)$$

n = 46,   r = 0.99272,   sd = 0.11215,   % AARD = 3.856

The correlation for this LSER is shown in Figure 4.18 where an excellent agreement between predicted and measured values is observed.

It can be seen that for the solutes under investigation in this study, these models allow the possibility of predicting their solubilities with an accuracy of, at maximum, around 0.3 mole fraction units. The accuracy of these models is found to be highly dependent on the number of descriptors used. The coefficients of these LSER should give an indication of the relative importance of each descriptor when a solute is solved in HFC 32. Tables 4.3 - 4.5 list the coefficients, standard errors (S.E.) and the t-values for the LSER in Equations (4.11), (4.13) and (4.15) respectively. The t-value is the ratio of the regression coefficient to its standard error and this can be used to test the significance of each coefficient.

Variable	Coefficient	S.E.	t-value
π^*	-8.12413	9.46636	-0.85821
α	-6.86849	18.36068	-0.37409
β	-57.50452	50.89429	-1.12989

Table 4.3 Coefficients, S.E. and t-values for the variables in Equation (4.11)

On inspection of the t-values in Table 4.3 the most significant term is the β term. This β variable has the largest t-value and because it is negative, it shows that the stronger a solutes hydrogen bond acceptor basicity, the less it will be solvated by the HFC 32.

When solute descriptors are added to the LSER it can be seen from Tables 4.4 and 4.5 that the standard errors associated with the coefficients decrease. From these LSER it is observed that the variable V dominates the solubility in both models. The t-values for V in both cases are large and negative, which, as expected, indicates that the solubility of solutes in HFC 32 is favoured if it is small.

Figure 4.18 Comparison of measured Log solubility and those predicted by the LSER of Equation (4.15)
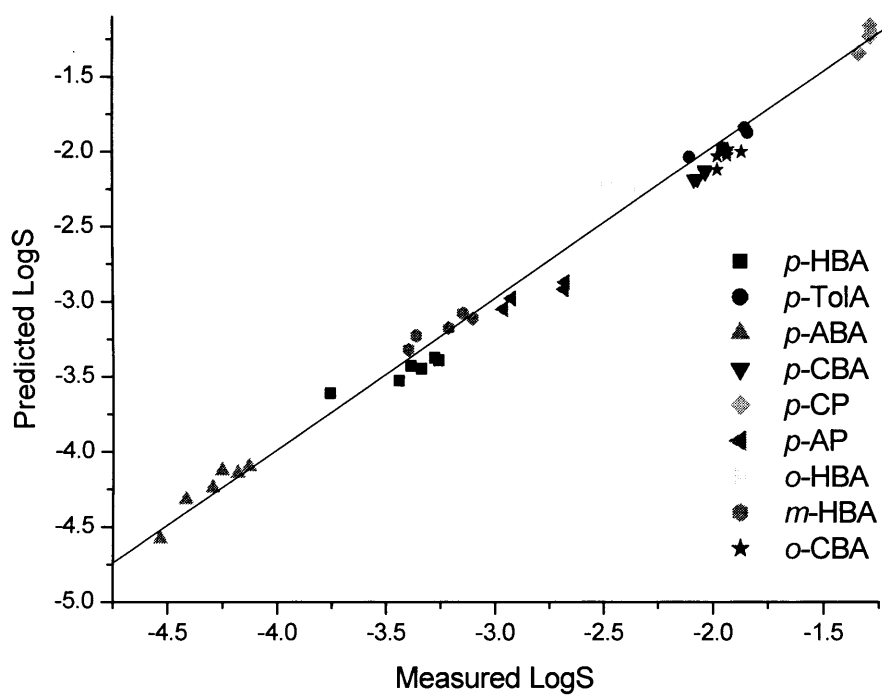
The data sets used in these LSER are not sufficiently large to draw accurate conclusions about the applications of these models. The LSER formed here are only likely to be applicable to similar aromatic solutes for the prediction of solubilities, until the data in the literature is extended. The LSER could be a useful alternative to traditional equation of state methods for correlating solubility. The computational time with the LSER is minimal and reliance on estimated critical parameters is not required.

Variable	Coefficient	S.E.	t-value
π^*	-1.33824	3.68224	-0.36343
α	2.68406	6.16832	0.43514
β	-18.87531	19.74355	-0.95602
R	2.32781	0.44116	5.27655
V	-52.83497	2.61186	-20.22888

Table 4.4 Coefficients, S.E. and t-values for the variables in Equation (4.13)

Variable	Coefficient	S.E.	t-value
π^*	-1.79689	1.77453	-1.01260
α	-0.79703	3.03008	-0.26304
β	-15.85885	9.53659	-1.66295
R	2.96120	1.21755	2.43211
V	-31.65570	3.21690	-9.84042
π_2	-1.68390	1.21637	-1.38437
α_2	-1.62250	0.35652	-4.55103
β_2	-4.02660	0.74562	-5.40440

Table 4.5 Coefficients, S.E. and t-values for the variables in Equation (4.15)

4.2.5 Partition Coefficient Modelling

Bruno and co-workers measured the water-HFC 134a partition coefficients for a set of 11 organic solutes in the gas and sc phases of HFC 134a.[62] They then developed a LSER to predict the measured partition coefficients using the Kamlet and Taft descriptors of the solvent and solute molecules as independent variables.

The LSER was similar in form to Equation (4.14) but the solubility, S, is substituted by the partition coefficient, K, and the solvent α and β terms are omitted from the equation. In this work the same data set is used but the solvent π^* value used by Bruno *et al.* is substituted for those calculated for HFC 134a earlier in this chapter. Incorporating all this data found the following LSER.

$$LogK = -0.35771 + 3.91812\pi^* - 0.50712R + 2.8837V$$
$$- 0.29097\pi_2 - 2.53015\alpha_2 - 2.63785\beta_2 \qquad \textbf{(4.16)}$$

$$n = 102, \qquad r = 0.966, \qquad sd = 0.19227, \qquad \% AARD = 29.09$$

The correlation statistics are also reported and in Figure 4.19 where the correlation between predicted and measured values of the water-HFC 134a partition coefficient is shown. Using the values of π^* from this work it can be seen that the correlations have been slightly improved from the LSER of Bruno. The predictive ability from this model is within the acceptable error range for measurements in sc fluids and is comparable to EOS uncertainties.

Direct comparison of the coefficients in Equation (4.16) should give an indication of the relative importance of each descriptor. Table 4.6 shows the coefficients, S.E. and t-values for the coefficients in this equation. The t-value gives the best indication of coefficient significance and it can be seen that π^* is the most significant descriptor with the largest value. This value is positive, indicating that the higher the density of the sc HFC 134a, the higher the solvent strength and the greater the partitioning of the organic solvent.

Table 4.6 also shows that the partition coefficients strongly depend on the solutes hydrogen bond donor ability, hydrogen bond acceptor ability and the volume, with the other descriptors being less significant. The large positive t-value displayed by V means that larger molecules prefer water to HFC 134a. The large negative t-
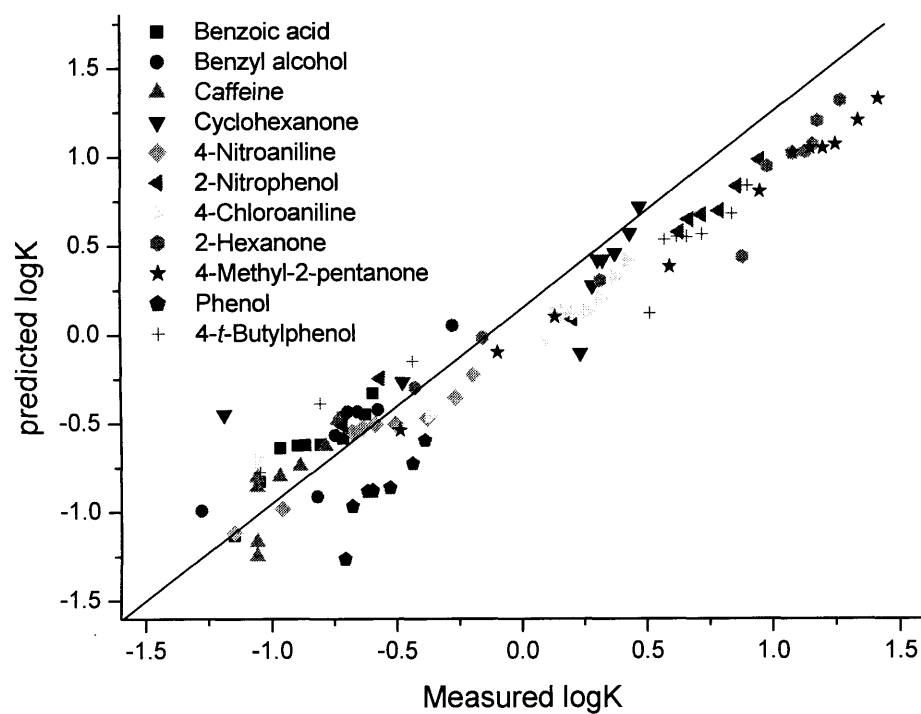
Figure 4.19 Comparison of measured water-HFC 134a partition coefficients and those predicted by the LSER of Equation (4.16)

value for the β_2 coefficient means that the stronger a solutes hydrogen bond basicity the less it will be partitioned into the HFC 134a and the α_2 term is analogous to this but represents the solutes hydrogen bond acidity.

Variable	Coefficient	S.E.	t-value
π^*	3.91812	0.18304	21.40523
R	-0.50712	0.10068	-5.03703
V	2.88370	0.15857	18.18538
π_2	-0.29097	0.10171	-2.86092
α_2	-2.53015	0.11908	-21.24675
β_2	-2.63785	0.12622	-20.89853

Table 4.6 Coefficients, S.E. and t-values for the variables in Equation (4.16)

This model successfully predicts water-HFC 134a partition coefficients. The relative size of the coefficients allow the importance and influence of each descriptor to be determined and in the case of these partition coefficients the main contributing factor was π^*, which means that partitioning into the HFC 134a is increased if the density of the HFC 134a is increased.

4.3 Conclusions

This work has shown that HFCs 32 and 134a have significant hydrogen bond donor characteristics, particularly in the sc state. The hydrogen bond donor properties of the solvents decrease with increasing pressure and this trend is suggested to be due to a decrease in solvent-solvent interactions and an increase in the preferential solvation around the polar moieties as the local solvent density decreases.

The Log solubility of aromatic solutes in HFC 32 was modelled using the solvent properties obtained in this study and published solute descriptor data. The LSER approach was found to be successful for the solutes under investigation and can rival equation of state methods. The accuracy of this LSER model was found to increase with the addition of a number of solute descriptors but the data set was not large enough to draw any accurate conclusions about the applicability of this model to predict other solute solubilities. It is thought however, that it would be successful for the prediction of solubilities with similar aromatic solutes.

Using π^* values from this work a slightly improved LSER was observed for the water-HFC 134a partition coefficients of organic solutes. This model had a % AARD of 29.09, which means the accuracy of this model rivals equation of state methods. The t-value for the descriptor coefficients gave an indication of the relative importance and influence of each descriptor. It was found that π^* dominates and partitioning into the HFC 134a phase increases as the density, and hence solvent strength increases.

4.4 References

(1)   Abbott A, P.; Eardley C, A. *J. Phys. Chem. B* **1998**, *102*, 8574.

(2)   Abbott A, P.; Eardley C, A. *J. Phys. Chem. B* **1999**, *103*, 2504.

(3)   Atkins P, W. *Physical Chemistry*, 5 ed.; Oxford University Press: Oxford, **1996**.

(4)   Suppan P.; Ghoneim N. *Solvatochromism*; Royal Society of Chemistry: Cambridge, **1997**.

(5)   Hollas J, M. *Modern Spectroscopy*; Wiley: Chichester, **1992**.

(6)   Abraham M, H. *J. Am. Chem. Soc.* **1982**, *104*, 2085.

(7)   Battino R.; Clever H, L. *Chem. Rev.* **1966**, *16*, 395.

(8)   Davies M. *Molecular Behaviour*; Pergamon Press: Oxford, **1965**.

(9)   Reichardt C. *Chem. Rev.* **1994**, *94*, 2319.

(10)   Reichardt C. *Solvents and Solvent Effects in Organic Chemistry*, 2 ed.; VCH Publishers: Weinheim, **1988**.

(11)   Reichardt C. *Angew. Chem.* **1965**, *77*, 30.

(12)   Grunwald E.; Winstein S. *J. Am. Chem. Soc.* **1948**, *70*, 841.

(13)   Brooker L, G, S.; Craig A, C.; Heseltine D, W.; Jenkins P, W.; Lincoln L, L. *J. Am. Chem. Soc.* **1965**, *87*, 2443.

(14)   Kosower E. *J. Am. Chem. Soc.* **1958**, *80*, 3253.

(15)   Kosower E. *Physical Organic Chemistry*; Wiley: New York, **1968**.

(16)   Dimroth K.; Reichardt C.; Siepmann T.; Bohlmann F. *Lieb. Ann. Chem.* **1963**, *661*, 1.

(17)   Reichardt C. *Angew. Chem.* **1979**, *91*, 119.

(18)   Taft R, W.; Abboud J-L, M.; Kamlet M, J.; Abraham M, H. *J. Soln. Chem.* **1985**, *14*, 153.

(19)   Kamlet M, J.; Abboud J-L, M.; Taft R, W. *J. Am. Chem. Soc.* **1977**, *99*, 6027.

(20)   Kamlet M, J.; Taft R, W.; Abboud J-L, M. *Prog. Phys. Org. Chem.* **1981**, *13*, 485.

(21)   Bekarek V, J. *J. Phys. Chem.* **1981**, *85*, 722.

(22)   Brady J, E.; Carr P, W. *J. Phys. Chem.* **1985**, *89*, 1813.

(23)   Nicolet P.; Laurence C, J. *J. Chem. Soc., Perkin Trans.* **1986**, *2*, 1071.

(24)   Laurence C, J.; Nicolet P.; Dalati M, T.; Abboud J-L, M.; Notario R. *J. Phys. Chem.* **1994**, *98*, 5807.

(25)   Kamlet M, J.; Abboud J-L, M.; Taft R, W. *J. Am. Chem. Soc.* **1976**, *98*, 377.

(26) Kamlet M, J.; Abboud J-L, M.; Taft R, W. *J. Am. Chem. Soc.* **1976**, *98*, 2886.

(27) Hildebrand J, H.; Scott R, L. *The Solubility of Non-Electrolytes*, 3 ed.; Dover Publisher: New York, **1964**.

(28) Kamlet M, J.; Taft R, W.; Abboud J-L, M.; Abraham M, H. *J. Org. Chem.* **1983**, *48*, 2877.

(29) Sigman M, E.; Lindley S, M.; Leffler J, E. *J. Am. Chem. Soc.* **1985**, *107*, 1471.

(30) Yonker C, R.; Frye S, L.; Kalkwarlf D, R.; Smith R, D. *J. Phys. Chem.* **1986**, *90*, 3022.

(31) O'Neill M, L.; Kruus P.; Burk R, C. *Can. J. Chem.* **1993**, *71*, 1834.

(32) Maiwald M.; Schneider G, M. *Ber. Bunsen. Phys. Chem.* **1998**, *102*, 960.

(33) Abbott A, P.; Eardley C, A.; Scheirer J, E. *J. Phys. Chem. B* **1999**, *103*, 8790.

(34) Smith R, D.; Frye S, L.; Yonker C, R.; Gale R, W. *J. Phys. Chem.* **1987**, *91*, 3059.

(35) Lagalante A, F.; Hall R, L.; Bruno T, J. *J. Phys. Chem. B* **1998**, *102*, 6601.

(36) Lu J.; Boughner E, C.; Liotta C, L.; Eckert C, A. *Fluid Phase Equilib.* **2002**, *198*, 37.

(37) Lu .J; Brown J, S.; Boughner E, C.; Liotta C, L.; Eckert C, A. *Ind. Eng. Chem. Res.* **2002**, *41*, 2835.

(38) Yonker C, R.; Smith R, D. *J. Phys. Chem.* **1988**, *92*, 2304.

(39) Kim S.; Johnston K, P. *AIChE J.* **1987**, *33*, 1603.

(40) Sun Y, P.; Bennett G.; Johnston K, P.; Fox M, A. *J. Phys. Chem.* **1992**, *96*, 10001.

(41) Zhang .J; Lee L, L.; Brennecke J, F. *J. Phys. Chem.* **1995**, *99*, 9268.

(42) Latimer W, M.; Rodebush W, H. *J. Am. Chem. Soc.* **1920**, *42*, 1419.

(43) Marcus Y. *Chem. Soc. Rev.* **1993**, *22*, 409.

(44) Marcus Y. *J. Soln. Chem.* **1991**, *20*, 929.

(45) Kim S.; Johnston K, P. *Ind. Eng. Chem. Res.* **1987**, *26*, 1206.

(46) Bennett G, E.; Johnston K, P. *J. Phys. Chem.* **1994**, *98*, 441.

(47) Eardley C, E. PhD, University of Leicester, **2000**.

(48) Lagalante A, F. *Private Communication*.

(49) Edwards J, T. *J. Chem. Educ.* **1970**, *47*, 261.

(50) Spartan Pro, W. I., Irvine, CA, USA.

(51) Essfar M.; Guiheneuf G.; Abboud J-L, M. *J. Am. Chem. Soc.* **1982**, *104*, 6786.

(52) Corr S. *J. Fluor. Chem.* **2002**, *118*, 55.

(53)   Johnston K, P.; Kim S.; Combes J. *ACS Symp. Ser.* **1989**, *406*, 52.

(54)   Tucker S, C. *Chem. Rev.* **1999**, *99*, 391.

(55)   Saunders R, A.; Platts J, A. *J. Phys. Org. Chem.* **2001**, *14*, 612.

(56)   Famini G, R.; Wilson L, Y. *J. Phys. Org. Chem.* **1993**, *6*, 539.

(57)   Politzer P.; Lane P.; Murray J, S.; Brinck T. *J. Phys. Chem.* **1992**, *96*, 7938.

(58)   Catchpole O, J.; Proells K. *Ind. Eng. Chem. Res.* **2001**, *40*, 965.

(59)   Kamlet M, J.; Taft R, W.; Abboud J-L, M. *J. Am. Chem. Soc.* **1977**, *91*, 8325.

(60)   Abraham M, H. *Chem. Soc. Rev.* **1993**, *22*, 73.

(61)   Abraham M, H.; Haftvan J, A.; Whiting G, S.; Leo A. *J. Chem. Soc., Perkin Trans.* **1994**, *2*, 1777.

(62)   Lagalante A, F.; Clarke A, M.; Bruno T, J. *J. Phys. Chem.* **1998**, *102*, 8889.

(63)   Lagalante A, F.; Bruno T, J. *J. Phys. Chem.* **1998**, *102*, 907.

CHAPTER 5

EQUILIBRIUM REACTIONS IN

SUPERCRITICAL MEDIA

5.1 Introduction

An increase in environmental awareness has led to stringent regulations on the use and disposal of hazardous materials by the chemical industry. There are a number of reaction components that could be replaced to make the chemical industry 'greener' and more environmentally friendly. An obvious target for replacement is the solvent and supercritical (sc) fluids are one of a number of possible alternatives to conventional organic solvents.

This work studies the esterification and aldol equilibrium reactions in sc HFC 32. HFC 32 is used as the reaction solvent rather than the traditionally used sc solvent CO_2 as it has a much higher dielectric constant and density. The higher dielectric constant value means that reactions will not be limited by the solubility of the reagents and catalysts. Other environmental benefits including the fact that HFC 32 is non-toxic, ozone friendly and recyclable add to the attractiveness of using it as a sc solvent.

The dielectrometry technique, used in Chapter 3 to measure solubilities, is shown in this work to be suitable to follow the progress of the esterification and aldol reactions. This technique can be used to follow changes in reactant/product concentration with time. These measurements show when the equilibrium condition is attained and then equilibrium constants for the reaction can be calculated. Dielectrometry is found to be a quick, simple, *in situ* method for following equilibrium reactions and is not limited by the concentration of species in solution.

The first equilibrium reactions in sc HFC 32 are reported in this work and by using the newly proposed dielectrometry technique, for the first time it is possible to follow the extent of these equilibrium reactions and calculate equilibrium constants. In particular, the effect of pressure on the progress of these equilibrium reactions is discussed.

5.1.1 Chemical Equilibrium Constants

Many chemical processes exist in a state of balance in which the starting material is not completely converted to products so both reactants and products are present. This state of balance is called an equilibrium. At this equilibrium state the reactants and products have no further tendency to undergo net change so the quantities of all species present in the mixture remain constant, although the reaction

is still continuing. This is because the rates of the forward and back reactions are equal.

For example, looking at a general reaction written in the form

$$aA + bB \leftrightarrow cC + dD$$

If the reaction is allowed to reach equilibrium and then the equilibrium concentrations are measured, these can be combined into an expression for the equilibrium constant as shown below

$$K = \frac{[C]^c [D]^d}{[A]^a [B]^b} \tag{5.1}$$

where A, B, C and D are the equilibrium concentrations of reactants and products and a, b, c and d are the stoichiometric constants in the chemical equation.

In a sc fluid the pressure of the system affects the activity of reactants and products, therefore, the equilibrium constant should be expressed in terms of mole fraction instead of concentration giving

$$K = \frac{\gamma_C X_C \gamma_D X_D}{\gamma_A X_A \gamma_B X_B} = K_\gamma K_X \tag{5.2}$$

and

$$K_\gamma = \frac{\gamma_C \gamma_D}{\gamma_A \gamma_B} \tag{5.3}$$

$$K_X = \frac{X_C X_D}{X_A X_B} \tag{5.4}$$

where X_A, X_B, X_C and X_D are the mole fractions of A, B, C and D at equilibrium conditions respectively. K_X is the apparent equilibrium constant and γ_A, γ_B, γ_C and γ_D are the activity coefficients, which have not yet been thoroughly researched in sc fluids. To my knowledge, the only study on measuring activity coefficients in sc fluids has been carried out by Abbott and Durling.[1] In this work it was shown that the activity coefficients for ferrocene carboxylic acid, in HFC 32 at 363 K, behaved ideally at low pressures but decreased as the pressure was increased.

The equilibrium constant for a particular reaction has the same value irrespective of the initial amounts of A, B, C and D, provided the temperature is kept constant. If the value of $K_X < 1$ then mostly reactants are present and if $K_X > 1$ then mainly products are present at equilibrium.

5.1.2 Dependence of Equilibrium & Rate Constants on Temperature & Pressure

The temperature and pressure dependency of the equilibrium (K) and rate (k) constants is reviewed in detail by Blandamer *et al.*[2] In this review it is found that there is no universally correct method of analysing kinetic data. The conclusions reached about the chemistry are found to depend on the model adopted and the method of analysis used on the kinetic data. Approximately 80 % of this review is dedicated to describing the dependence of ln K and ln k on temperature with the remaining 20 % describing the pressure dependence. These percentage values accurately reflect data published to date with research on the dependence of temperature far exceeding that of pressure.

The pressure dependence ln K or ln k is not defined by thermodynamics so often the aim is to analyse the pressure dependence to extract further information. Usual practice is to adopt a simple description for the chemical processes where a reactant, *A*, goes to products, *B*, as shown below.

$$A \xleftrightarrow{K} B \tag{5.5}$$

$$A \xrightarrow{k} B \tag{5.6}$$

It is then possible to estimate the activation volume, ΔV^K or ΔV^k, because

$$\left[\frac{\partial \ln K}{\partial p}\right]_T = \frac{-\Delta V}{RT} \tag{5.7}$$

The simplest equation expresses ln K and ln k as a linear function of pressure

$$\ln K = a_1 + a_2 p \qquad \Delta V^K = -a_2 RT \tag{5.8}$$

$$\ln k = a_1 + a_2 p \qquad \Delta V^k = -a_2 RT \tag{5.9}$$

From this it is found that ΔV is independent of pressure and a_1 is the value of ln K or ln k when the pressure is zero. If this simplest equation is found to be inadequate for describing the dependence of measured ln K and ln k values on pressure, other methods have been reported in the literature. These include polynomial dependences[2-4] and non-linear least squares techniques,[2,5] however, the models and analysis methods become increasingly more complex.

To describe temperature dependencies it is assumed that the K and k values have been measured for a series of temperatures, T. Once again the first task is to formulate an equation to describe the observed dependence. One suggested approach is to assume that ln K and ln k are linear functions of T so

$$\ln K = a_1 T + a_2 \qquad (5.10)$$

$$\ln k = a_1 T + a_2 \qquad (5.11)$$

and differentiation of this equation yields an expression for the enthalpy, ΔH^K or ΔH^k that is dependent on temperature.

$$\left[\frac{\partial \ln K}{\partial T} \right]_p = \frac{\Delta H^\theta}{RT^2} \qquad (5.12)$$

Another approach treats ΔH^K or ΔH^k as independent of T to give an equation that relates $\ln K$ or $\ln k$ to T^{-1}

$$\ln K = a_1 T^{-1} + a_2 \qquad (5.13)$$

$$\ln k = a_1 T^{-1} + a_2 \qquad (5.14)$$

where a_2 is the value of $\ln K$ or $\ln k$ when T^{-1} is zero. From this equation it is found that the Gibbs free energy, ΔG, is a simple linear function of temperature because

$$\Delta G = -RT \ln K \qquad (5.15)$$

These are the simplest models for describing the temperature dependency of equilibrium and rate constants. When these simple models become inadequate there are numerous other, more complex models that can be applied.[2,6,7] It can be seen from the models described here that it is possible to extract various thermodynamic information depending on whether $\ln K$ or $\ln k$ is dependent on T or T^{-1}.

5.1.3 Equilibrium Reactions in Supercritical Fluids

The recent growth in the use of sc fluid solvents as media for chemical synthesis[8] has inspired several research groups to examine chemical equilibria in order to probe intermolecular interactions in sc fluids. The solvent influences reaction thermodynamics through the environment it produces around the solutes. Among the most important solvent properties that characterise this reaction environment are the polarity and the polarisability. The solvent polarity corresponds to the permanent dipole-dipole interactions, whereas polarisability is indicative of inductive forces, where the solute molecule induces a dipole in the solvent. Thus, measuring equilibria in sc fluids can give insight into molecular interactions.

Kimura et al.[9-11] addressed the problem of how fluid structure influences chemical reactions by examining the effect of solvent density on the equilibrium

constant for the dimerisation of 2-methyl-2-nitrosopropane in CO_2, $CClF_3$, CHF_3, Ar, and Xe. Their studies were typically carried out at sc temperatures and the densities ranged from the gas to the sc phase. The experimental results showed that the equilibrium constant in CO_2, $CClF_3$ and CHF_3 increased with density in the low-density region (gas-phase). Further increases in density caused the equilibrium constant to decrease into the high-density region. However, once in the high-density region the equilibrium constant increased once more with density. The authors argued that these observations were due to the different dominant molecular interactions of the fluid within each of these density regions.

Chemical equilibria have also been related to hydrogen bonding in sc fluids. Gupta and co-workers[12] studied the hydrogen bonding between methanol and triethylamine in sc SF_6 where a pronounced solvent effect was observed. The equilibrium for methanol-triethylamine association increased as the pressure decreased towards the critical point, with the pressure effect being most dominant around the critical point.

O'Shea et al.[13] probed the hydrogen bonding and polar interactions in sc ethane, fluoroform and CO_2 by measuring the tautomeric equilibrium of 4-(phenylazo)-1-napthol in these solvents as shown in Scheme 1.

$\mu = 1.79$ D $\mu = 5.03$ D
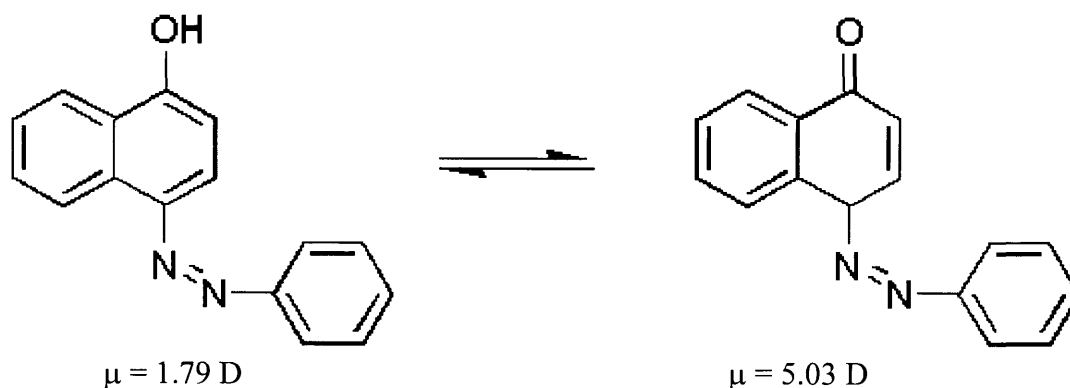
Scheme 1 Equilibrium between the tautomers of 4-(phenylazo)-1-naphthol

The least polar tautomer ($\mu = 1.79$ D) was dominant in ethane, nearly equal amounts of the tautomers were seen in CO_2 and in fluoroform it was found that the most polar tautomer ($\mu = 5.03$ D) was dominant. These shifts in equilibrium composition favouring the more polar tautomer were attributed to the large quadrupole moment of CO_2 and hydrogen bond donor ability of fluoroform. From these results it is

suggested that pressure can be used to control processes involving polar molecules in some sc fluids.

Studies in the literature on aldol and esterification reactions in sc fluids are very limited. Ikariya and co-workers have reported the catalytic asymmetric Mukaiyama aldol reaction of a ketene silyl acetal of thioester in sc CHF_3 and CO_2.[14] The reaction proceeded to give the silylated aldol product in moderate yields. The yield and enantioselectivity of the reaction were found to be influenced by the solvent used. A maximum in enantioselectivity and yield of 88 % and 46 % respectively was observed for the reaction in sc CHF_3. On comparison with CO_2 the reaction was found to proceed only slightly to give an aldol product yield of 8 % and also a reduced enantioselectivity of 72 %. The low yield in sc CO_2 was reported to be due to its low polarity that results in the low solubility of the acid catalyst in this medium.

Ellington et al.[15] and Ellington and Brennecke[16] have used UV-VIS spectroscopy to find the apparent bimolecular rate constant for the esterification of phthalic anhydride with methanol in sc CO_2 at 313 and 323 K and pressures from 97.5 to 166.5 bar. This reaction was chosen as a representative reaction between a dilute solute (phthalic anhydride) and a typical co-solvent (methanol) in sc CO_2. At 313 K the calculated bimolecular rate constants exhibited a 4-fold increase with a decrease in pressure from 145.8 to 97.5 bar. Along the 323 K isotherm a 25-fold increase in the rate constant was observed when the pressure was decreased from 166.5 to 97.5 bar. The 25-fold decrease in the rate constant at low pressures and 323 K greatly exceeded what the authors expected from the estimated activation volumes of the reaction. Thus, the authors attributed the enhanced reaction rate constants at lower pressures to the local concentration of methanol around the phthalic anhydride molecules exceeding the average, bulk methanol concentration. By using estimated local densities and local compositions they showed that this explanation was reasonable.

The esterification of acetic acid and ethanol in compressed CO_2 has been studied at 333 K and at pressures up to 160 bar.[17] From conversion verses time experiments they found that the reaction had reached equilibrium in 3 hours under sc conditions and could be reached in 6 hours under sub-critical conditions. They calculated the apparent equilibrium constant, K_x, from the conversion of ethanol at a reaction time of 6 hours. Results showed that K_x increased with pressure at low pressures and reached a maximum in the critical region where the system becomes one phase. Once past the critical point K_x was found to decrease with increasing

pressure. The observed increase in K_x at low pressures was explained with respect to the degree of clustering/local density enhancement at these pressures. At high pressures, where clustering is insignificant, K_x for the reaction was found to be close to that of the reaction in the absence of CO_2.

5.2 Results and Discussion

5.2.1 Esterification Reaction

For the first time an esterification reaction is reported in sc HFC 32. The dielectrometry technique, employed in Chapter 3 to measure solid solubilities, was used to follow the esterification reaction by measuring the change in capacitance as the reaction proceeded. This dielectrometry technique is a quick, simple, *in situ* method for measuring capacitance changes of reaction systems. Dielectrometry is not affected by solution concentration, high pressure and turbidity restraints that are present with spectroscopic techniques.

As with most analytical techniques there are always some limitations. Firstly, this technique can only be used with reagents that are readily soluble because accurate capacitance measurements can only be obtained in homogeneous solutions. It is also necessary to have a large difference in dielectric constant between the reactants and products so that product formation produces a change in the capacitance of the solution. For this to occur it is also necessary for the products to remain in solution as the reaction proceeds.

With these limitations in mind the esterification reagents employed were benzoic acid, 1-butanol and *p*-toluenesulphonic (*p*Tos) acid as the catalyst. Benzoic acid is known to have reasonable solubility in some non-polar solvents (sc CO_2) and from the solubility measurements of some benzoic acid derivatives reported in Chapter 3, it can be assumed that the solubility of benzoic acid will be greater than these. A quick gravimetric solubility study carried out using sc HFC 32 at 363 K justified this assumption. At 100 bar and below the solution saturation limit it was found that a solubility of 0.542 mol dm^{-3} could be obtained. The alcohol was observed to readily go into solution, which was expected because it is a liquid, and the catalyst has been observed in earlier work to have a high solubility in sc HFC 32.[18]

The dielectrometry technique had to be assessed to see whether it could be used to follow this esterification reaction. To do this the reaction was carried out in dichloroethane, as this has a similar dielectric constant to sc HFC 32 at 363 K (DCE, ε = 10.37 at 278 K; HFC 32, ε = 8.99 at 363 K and 200 bar). The reaction was followed over a 2 hour time period by using dielectrometry and GC-MS. Dielectrometry measurements were measured *in situ* and for the GC-MS measurements, 2 ml aliquots of the reaction solution were taken. The actual reaction conversion was obtained from

the GC-MS results at specific time intervals. The conversion value from the dielectrometry measurements was calculated from a knowledge of the final conversion of the reaction, from GC-MS, and the capacitance value at a given time interval. The measured (GC-MS) and calculated (dielectrometry) conversions for this esterification reaction are shown in Figure 5.1. It can be seen from Figure 5.1 that very close agreement between the measured and calculated ester conversion values is observed, signifying that the dielectrometry technique is suitable for following the process of this reaction.

The esterification reaction was then carried out in the presence of sc HFC 32 as the reaction solvent. From previous esterification studies in sc fluids it is assumed that this esterification reaction follows the mechanism shown in Scheme 2.

$R = CH_3CH_2CH_2CH_2$

$R = CH_3CH_2CH_2CH_2$
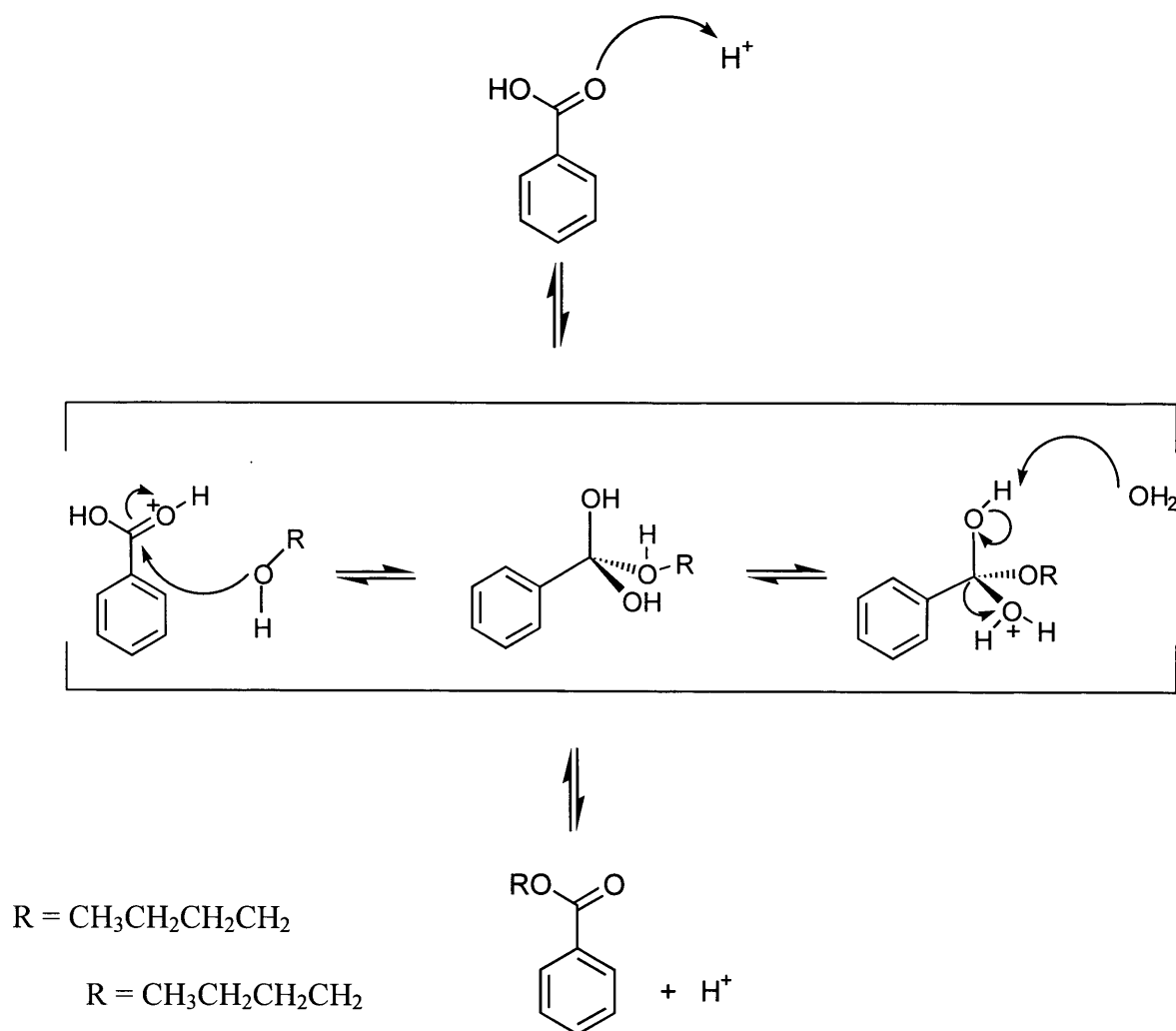
Scheme 2 The mechanism for esterification between benzoic acid and 1-butanol

107
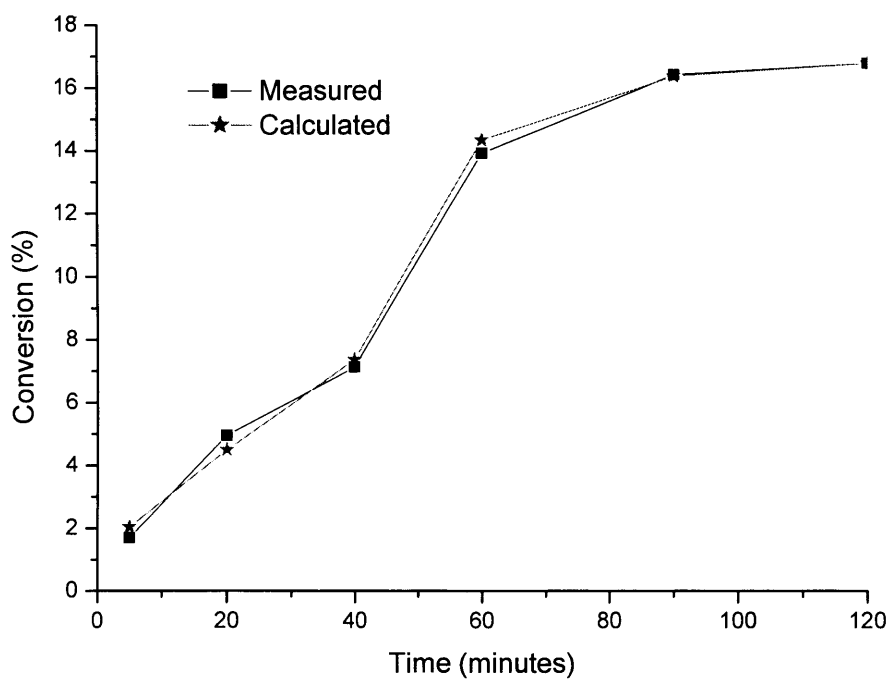
Figure 5.1 Comparison of measured and calculated conversion for the esterification reaction

Using an optical cell it was visually observed that the reaction was homogeneous under all conditions studied in this work. The dielectrometry technique was used to follow the progress of the benzoic acid esterification reaction as a function of time. This is shown in Figure 5.2 at some selected pressures. The uncertainty of the conversion is found to be no greater than ± 2 %. From Figure 5.2 it can be seen that this dielectrometry technique is useful for following equilibrium reactions as it can be easily seen when the reaction has reached equilibrium. Figure 5.2 shows that the reaction has reached equilibrium in two hours or less under the conditions studied. Therefore, in the rest of this work a reaction time of 2 hours was taken to ensure that the system had reached equilibrium.

The apparent equilibrium constant, K_X, calculated using Equation (5.4) and the equilibrium mole fractions of the reactants and products are shown as a function of pressure in Figure 5.3 and Table 22 of the appendix. K_X increases with decreasing pressure and a sharp increase is observed as the critical point is approached. The increase in the K_X value with decreasing pressure signifies that K_γ must be decreasing because the equilibrium constant, K, is independent of pressure (see Equation (5.2)). However, the lack of activity coefficient data reported in the literature makes it impossible to justify this observation.

A 14-fold decrease in the apparent equilibrium constant is observed when the pressure is increased from 70 to 220 bar. Ellington et al. have reported a decrease in an esterification reaction rate constant previously.[15] They suggested that a significant portion of the large reaction rates at low pressures is most likely to be due to local composition enhancements of the alcohol about the acid. To verify this they measured the local composition enhancements of the alcohol about a solvatochromic probe. It is assumed that the same reasons apply to the high reaction rates observed in this work, which means that K_x must increase with the increased degree of local composition enhancement at low pressure and vice versa for K_γ. The results presented here for this reaction in HFC 32 also clarify the points made by Hou et al. on the effect of pressure on the reaction equilibrium of an esterification reaction in sc CO_2.[17]
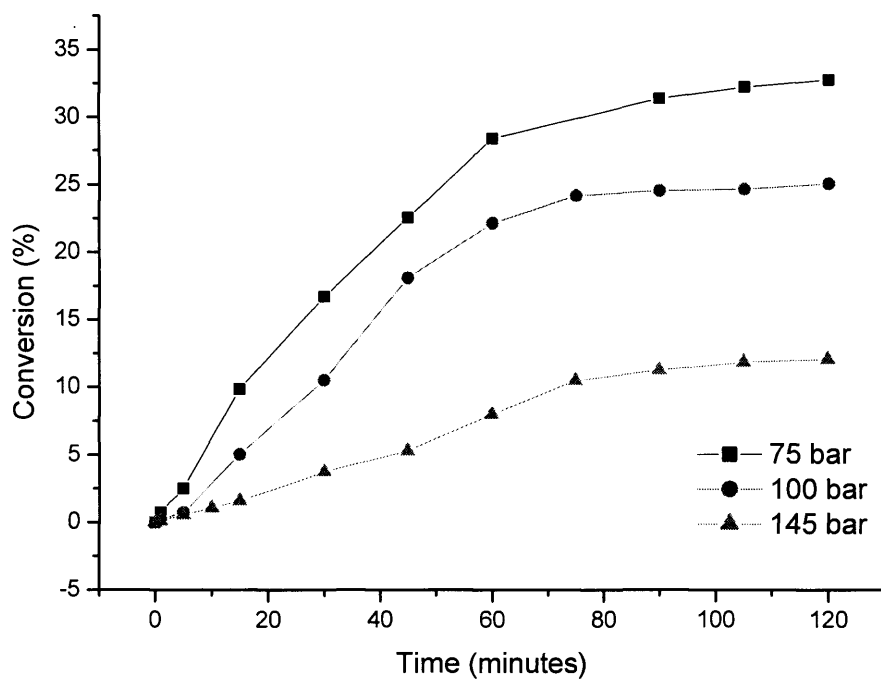
Figure 5.2 Ester conversion with time for a variety of pressures in HFC 32 at 363 K
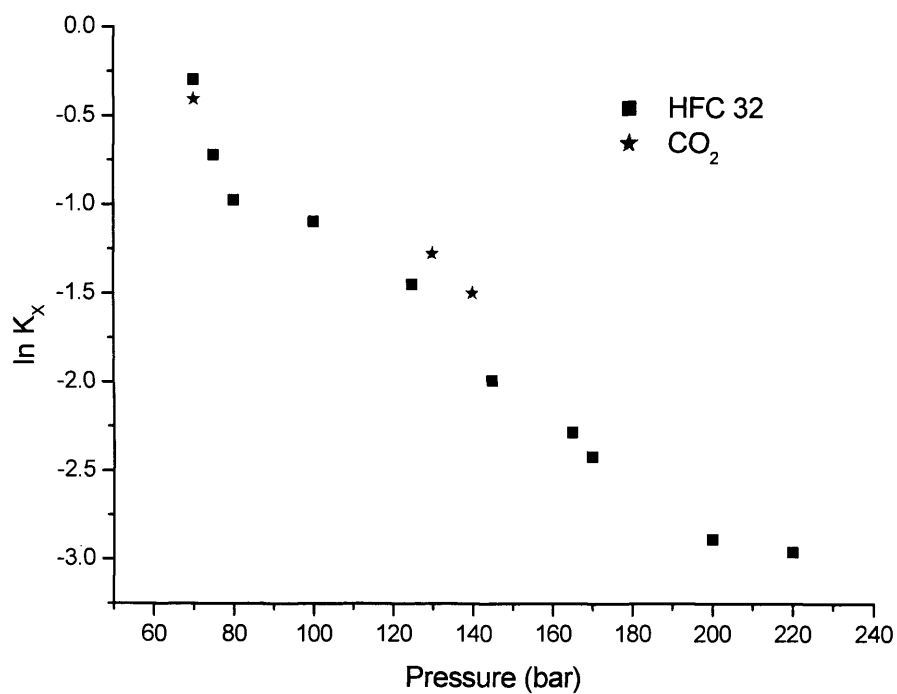
Figure 5.3 The change in ln K_X with pressure for the benzoic acid esterification reaction at 363 K

To verify that it is an enhancement in the local composition of 1-butanol about benzoic acid that gives rise to the increase in K_x at low pressure, the measurement of local composition of 1-butanol about a solvatochromic probe is the topic of future work.

This esterification reaction was also carried out in conventional liquid solvents for comparison. Dichloroethane (DCE) was chosen as it has the closest dielectric constant to HFC 32 at 363 K. The apparent equilibrium constant, calculated from dielectrometry measurements, for this reaction in DCE at 363 K was calculated to be 0.201, which is similar to the K_X values in HFC 32 at moderate pressures (K_x = 0.23 at 125 bar) where local composition enhancement is less important. The reaction was also carried out in cyclohexane (CH), which has a much lower dielectric constant than DCE or HFC 32 (CH, ε = 2.02 at 273 K). However, the K_X value was calculated to be 0.192, which is very similar to that in DCE considering the large difference in dielectric constant and density between the two solvents.

To assess whether the solution dielectric constant has this effect in a sc fluid, the esterification reaction was carried out in sc CO_2 at 363 K (CO_2, ε = 1.2 at 363 K and 200 bar). Carbon dioxide under these conditions has a considerably lower dielectric constant than HFC 32. Results obtained for K_X are shown on Figure 5.3, where within experimental error, the K_X values for CO_2 fall onto the same line as those for HFC 32. This is a remarkable observation considering the vast differences between the two solvents.

In the low dielectric media under liquid and sc conditions it is surprising that the reaction progresses at all as the dissociation of the acid catalyst should be negligible. This suggests that the catalyst activity is not a factor affecting the reaction rate. It is interesting to note that the starting dielectric constant of the solution containing reagents in CO_2 is *c.a.* 5, which is much higher than the dielectric constant for the pure solvent (ε < 1). So even though the reagents are present in less than 1 mol % they have a marked effect on the dielectric constant of the solution. This result suggests that to gain a better understanding of the process of a reaction it is necessary to measure the solution dielectric constant and not assume that it is the solvent dielectric constant that influences a reaction.

5.2.2 Aldol Condensation Reaction

The first acid catalysed aldol condensation in sc HFC 32 is reported in this work. The aldol equilibrium is studied by applying the dielectrometry technique and equilibrium constants are calculated as a function of pressure. In an aldol reaction it is the α carbon of an aldehyde or ketone molecule that adds to the carbonyl carbon of another molecule of the aldehyde or ketone. Base catalysed aldol reactions are most common but acid catalysed reactions are known.[19,20] Under acidic conditions the alcohol almost always undergoes acid catalysed dehydration to yield the α,β-unsaturated ketone. Scheme 3 shows the mechanism of the acid catalysed reaction of the ketone, cyclohexanone (1), which is used in this work.
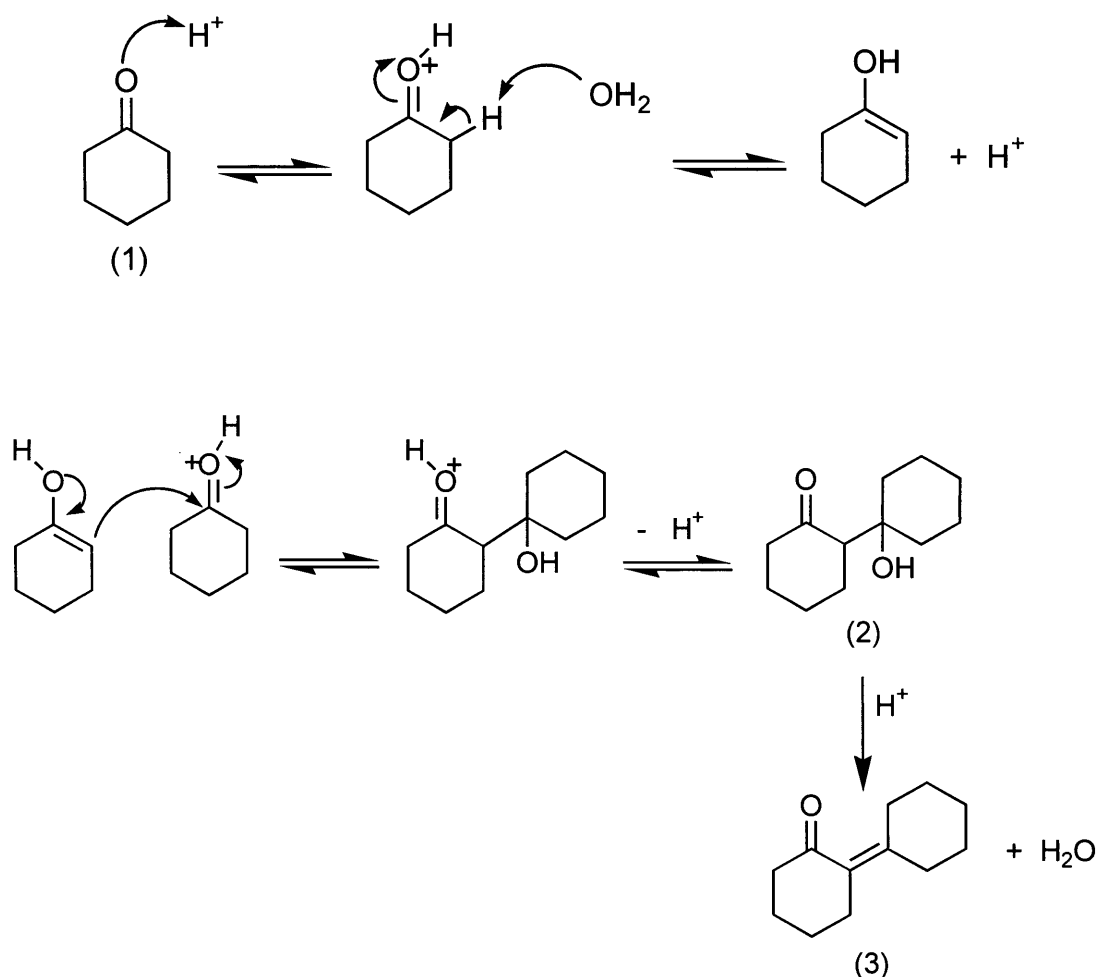
Scheme 3 The mechanism for the acid catalysed aldol reaction of cyclohexanone

Cyclohexanone was chosen for environmental and handling reasons and also because it is a liquid, which readily solves into solution allowing the reaction to be followed by dielectrometry. Aldol condensation reactions using ketones are known to be less feasible than those using aldehydes. However, due to handling reasons aldehydes could not be employed in this work. The acid catalyst employed was once again pTos as this has been found to have a high solubility in HFC 32 at 363 K.

As expected, analysis of the product showed that the dehydration product (3) was isolated rather than the aldol dimerisation product (2). Analogous to the esterification reaction the dielectrometry technique was assessed to see whether it was suitable for use with the aldol condensation reaction. The change in dielectric constant accompanying the formation of products for this reaction was found to be sufficiently large so that dielectrometry could be used. Initial experiments involved conversion versus time analysis and it was found that this reaction had reached equilibrium in less than 2 hours. The mole fraction of reactants and products at 2 hours were therefore taken to be the equilibrium values in the rest of this work.

Figure 5.4 and Table 23 in the appendix show the calculated apparent equilibrium constants for this reaction as a function of pressure. The K_X values shown in Figure 5.4 follow the same trend observed with the esterification reaction described earlier, where K_X increases with decreasing pressure. A sharp increase in K_x can be seen as the pressure decreases towards the critical pressure. The arguments applied to the esterification reaction also apply to the results observed here for the aldol reaction, where the increased value of K_x at low pressures is thought to be due to local composition enhancements.

The values for the apparent equilibrium constants for the aldol reaction are lower than those observed for the esterification reaction and the rate of the aldol reaction showed only a 4-fold increase when decreasing the pressure from 200 to 70 bar. At higher pressures it should be noted that both the esterification and aldol reactions have similar K_x values, so the main factor in causing only a 4-fold change in rate is due to the much lower K_x values observed for the aldol reaction at low pressures. For the esterification reaction at 70 bar, K_x is 0.743 whereas for the aldol reaction at 70 bar, K_x is 0.121. It is proposed that this large difference in K_x at low pressures is due to lower local composition enhancements bought about by weaker solute-solute interactions between reagents for the aldol reaction. For example, in the
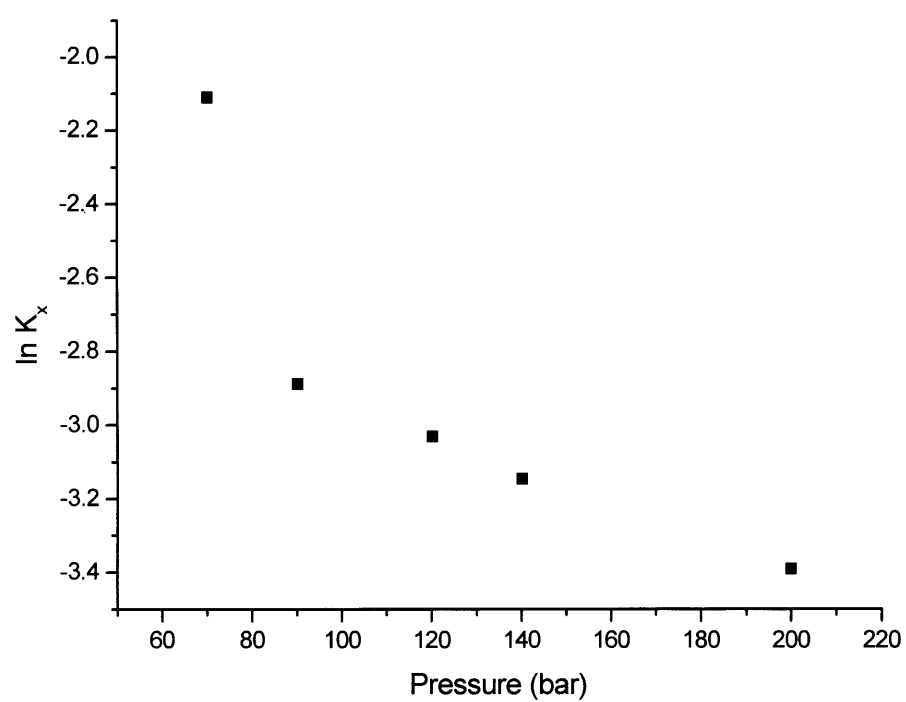
Figure 5.4 The change in ln K_X with pressure for the aldol condensation reaction of cyclohexanone in HFC 32 at 363 K

esterification reaction it is possible for the reagents to be in close proximity due to hydrogen bonding. This however, is not possible for the cyclohexanone in the aldol reaction.

5.3 Conclusions

The first examples of an esterification and aldol condensation reaction in sc HFC 32 are presented here. By using these reactions as examples the successful application of the *in situ* dielectrometry technique to follow equilibrium reactions was demonstrated. The advantages and disadvantages of applying this technique to follow reactions were discussed but it could be seen that when it is possible to apply this technique, it is a quick and simple method. From the measured capacitance values using dielectrometry it was possible to tell when the reaction has reached equilibrium and also the concentrations of reactants or products could be measured as a function of time. This data then presented the opportunity to calculate equilibrium constants.

Equilibrium constants were calculated for both reactions using dielectrometry as a function of pressure. For both reactions it was found that the apparent equilibrium constant decreased with increasing pressure. The enhanced equilibrium constants observed at low pressure were thought to be due to local composition enhancements. The lower observed apparent equilibrium constants for the aldol reaction compared to those for the esterification reaction are thought to be due to lower local composition enhancements. This situation may arise because of the lower polarity solute employed in the aldol reaction giving a reduced ability to form solute-solute interactions.

5.4 References

(1)   Abbott A, P.; Durling N, E. *Phys. Chem. Chem. Phys.* **2001**, *3*, 579.

(2)   Blandamer M, J.; Burgess J.; Robertson R, E.; Scott J, M., W,. *Chem. Rev.* **1982**, *82*, 259.

(3)   Ives D, J, G.; Marsden P, D. *J. Chem. Soc.* **1965**, 649.

(4)   Golinkin H, S.; Lee I.; Hyne J, B. *J. Am. Chem. Soc.* **1907**, *89*, 1307.

(5)   Jones W, R.; Carey L, R.; Swaddle T, W. *Can. J. Chem.* **1972**, *50*, 2739.

(6)   Harned H, S.; Embree N, D. *J. Am. Chem. Soc.* **1934**, *56*.

(7)   Heppolette R, L.; Robertson R, E. *Can. J. Chem.* **1966**, *44*, 677.

(8)   Jessop P, G.; Leitner W. *Chemical Synthesis using Supercritical Fluids*; Wiley-VCH: Weinheim, **1999**.

(9)   Kimura Y.; Yoshimura Y.; Nakahara M. *J. Chem. Phys.* **1989**, *90*, 5679.

(10)   Kimura Y.; Yoshimura Y. *J. Chem. Phys.* **1992**, *96*, 3085.

(11)   Kimura Y.; Yoshimura Y. *J. Chem. Phys.* **1992**, *96*, 3824.

(12)   Gupta R, B.; Combes J, R.; Johnston K, P. *J. Phys. Chem.* **1993**, *97*, 707.

(13)   O'Shea K.; Kirmse K, M.; Fox M, A.; Johnston K, P. *J. Phys. Chem.* **1991**, *95*, 7863.

(14)   Mikami K.; Matsukawa S.; Kayaki Y.; Ikariya T. *Tetrahedron Lett.* **2000**, *41*, 1931.

(15)   Ellington J, B.; Park K, M.; Brennecke J, F. *Ind. Eng. Chem. Res.* **1994**, *33*, 965.

(16)   Ellington J, B.; Brennecke J, F. *J. Chem. Soc., Chem. Comm.* **1993**, 1094.

(17)   Hou Z.; Han B.; Zhang X.; Zhang H.; Z, L. *J. Phys. Chem. B* **2001**, *105*, 4510.

(18)   Lange S. University of Leicester *unpublished results* **2000**.

(19)   Mahrwald R.; Gundogan B. *J. Am. Chem. Soc.* **1998**, *120*, 413.

(20)   Simth M, B.; March J. *March's Advanced Organic Chemistry*, 5th ed.; Wiley & Son: New York, **2001**.

CHAPTER

6

RATES OF REACTION IN

SUPERCRITICAL MEDIA

6.1 Introduction

Supercritical (sc) fluids are attractive media for chemical synthesis because of their unique properties. One of the attractive features of a sc fluid as a medium for chemical reactions is that its properties e.g. viscosity, dielectric constant and diffusivity vary with density, which is a strong function of temperature and pressure. Consequently, sc fluids provide the opportunity to engineer the reaction environment by manipulating temperature and pressure and this in turn may have an effect on selectivity and rate of reaction.

This work reports the first Friedel-Crafts (FC) alkylation study in sc HFC 32 and compares the results to the commonly employed sc solvent CO_2. The kinetics of the reaction is measured by application of the newly proposed dielectrometry technique and the first rate constants of a FC reaction in a sc fluid are presented. The effect on the reaction selectivity and rate to changes in the reagent/catalyst concentration, time, temperature and pressure are also addressed.

6.1.1 Reaction Kinetics

It is useful to study chemical kinetics as it can give mechanistic information for the reaction. In a sc fluid, by measurement of the kinetics, it has been found that reaction rates, yields and selectivity can be adjusted by varying the pressure without the need for harsh chemical changes.[1]

A common observation of reactions in sc fluids is that local density and/or local composition enhancements are found to affect the reaction thermodynamic and kinetic properties and therefore influence reaction rates. Effects observed include local density augmentation[2-5] and preferential solvation on the addition of co-solvents.[6,7] Many papers have been published in this area and there have been some review papers on the topic.[8-10] These local solvation effects are in addition to the fluctuations of the properties of sc fluids normally observed near the critical point.

Reaction kinetics in sc fluids is a relatively new area and therefore the mechanism by which a sc fluid controls a reaction is still unclear. Some studies have been carried out but conclusions drawn by the authors are often contradictory due, in part, to the complexity of the parameters that change with pressure in the sc state.

The majority of kinetic measurements in the literature have been achieved by application of time-resolved spectroscopic techniques where the reaction rate can be determined directly by monitoring the intensity of absorption in a spectral region of a

reactant or product.[11] Spectroscopic techniques used to measure both the solvation of the reactants and the kinetics of a reaction in a sc fluid can give detail on whether and to what extent the solvation influences reactivity.

Most research on chemical kinetics studies that employ spectroscopic techniques, which measures the change in absorption/emission peak height of a reactant or product as the reaction proceeds, has involved the use of non-polar sc fluids e.g. CO_2 and ethane.[12-16] Research in the literature involving more polar sc solvents is much more limited. Rhodes *et al.* used the more polar solvent fluoroform and compared their results to those obtained in the non-polar solvent ethane.[17] The basis of their work was to see how solvent-solute and solute-solute interactions affect the rate of Michael addition of piperidine to methyl propiolate in sc fluoroform and sc ethane at 310 K and pressures between 48.3 and 213.8 bar. This reaction had been studied previously and a mechanism was proposed in which the reaction proceeds through a highly zwitterionic intermediate.[18] Therefore, a change in the polarity of the medium (from non-polar to polar) and the change in polarity induced by varying pressure in a sc fluid would dramatically stabilise this intermediate and thus increase the rate constant for the reaction. It was observed that the kinetics in the two sc solvents were distinctly different, which was attributed to a strong density dependent dielectric constant in fluoroform, whereas in ethane the dielectric constant is regarded as approximately constant over the density range studied. The observed rate constants were related to the changes in solvent dielectric with pressure, which result from the increased stabilisation of a highly polar zwitterionic transition state.

In sc ethane the Michael addition reaction kinetics were largely unaffected by changes in pressure and thus density, as the polarity of ethane is only weakly affected by density. However, it was observed that near the critical point the reaction rate increased due to solute-solute clustering. As solvent density had little effect on the kinetics of the reaction this observed increase could not be due to solvent-solute clustering. The Michael addition in sc fluoroform exhibited different trends. The rate constant is linearly related to pressure above 82 bar due to the pressure dependence of solvent polarity and thus the stabilisation of the transition state. Rhodes and co-workers attributed the changes in rate constant near the critical point to solvent-solute clustering, indicating that the reaction occurs in an environment different from the rest of the bulk. Their work illustrates how the polarity of a solvent can greatly affect the solubility and stability of a reaction species in an organic reaction. It was also shown

that altering the pressure could favour one interaction type, providing a means of kinetic control for a reaction.

Kinetic measurements can also be made via product analysis and this has been the method of choice of a number of investigators. A variety of organic reactions have been analysed and the affect of local composition on the reaction kinetics is often considered.

The Diels-Alder reaction has been the focus of a number of studies by various investigators in sc CO_2 and sc propane.[19-23] In 1987, Paulaitis and Alexander used transition state theory to explain the reaction kinetics for the Diels-Alder reaction of maleic anhydride with isoprene in CO_2 near the CO_2 critical point.[23] Later work by Reaves and Roberts examined the same system but in sc CO_2 at 308 K and sub-critical propane at 353 K.[20] Their experiments were carried out over a range of pressures and bimolecular rate constants were calculated. Values for the experimental rate constants were compared to predications from the thermodynamic pressure effect using transition state theory and the Peng-Robinson equation-of-state. The rate constants in sc CO_2 were in good agreement with predicted values over the pressure range studied and it was also observed that the rate constants varied linearly with the density of solution. However, in sub-critical propane, rate constants diverged from the predictions made and the system lost its density dependence at lower pressures.

Weinstein *et al.* carried out the Diels-Alder reaction of cyclopentadiene and ethyl acrylate in sc CO_2 from 311 to 361 K and pressures from 80 to 210 bar.[22] Results were related to a simple second-order rate law and used to construct a linear Arrhenius plot at a constant density of 0.5 g cm^{-3}. Over the temperature range studied the density independent activation energy was calculated to be 40 ± 2 kJ mol^{-1}. By application of transition state theory the effects of temperature and density on the reaction rate was considered. When the rate constants were normalised at various temperatures to a fixed density, the data fell on to a single line. Results from other researchers were also shown to fit this trend, giving rise to a possible global rate law, where all that is required to predict the rate constant is the activation energy and a pre-exponential term with a linear dependence on the density of solution.

6.1.2 Friedel-Crafts Reaction

The FC reaction first introduced in 1877 by Charles Friedel and James Crafts,[24] reported that benzene rings could be alkylated by reaction with an alkyl chloride in the presence of aluminium chloride as the catalyst.

Since its discovery the FC alkylation has been recognised as one of the most important tools for introducing alkyl substituents onto the ring of aromatic compounds. Friedel and Crafts could not have foreseen the countless applications, theoretical discussions and reviews that have followed their pioneering work. The original scope of their research has been extended continuously over more than 120 years to cover every conceivable variation of reagent, catalyst and affiliated reactions. Therefore, over the years, the amount of material in both scientific and patent literature has grown tremendously. Due to the vast amount of data available it is not feasible to attempt to survey the entire FC reaction background. Much of the earlier FC studies are reviewed in the comprehensive treatise compiled by Olah.[25] This monograph was published in four volumes (six parts) with about 20,000 references. In these books Olah provides a summary of data and attempts to achieve some evaluation of the data to formulate a general picture of a specific field from both a theoretical and preparative chemical point of view.

From this published literature a general picture of the mechanism for FC alkylation can be achieved. Depending on the reactants employed it is commonly accepted that the reaction can go through either a carbocation or nucleophilic displacement mechanism. Tertiary alkyl halides have the highest tendency to ionise. Secondary halides are intermediate and primary halides are least prone to such transformations. As the ability of the alkylating agent to ionise declines the mechanism by which the reaction proceeds will tend to move away from the ionic mechanism and change more and more to a reaction involving nucleophilic substitution.

The widely accepted carbocation mechanism for a general FC reaction is shown in Scheme 1. The reaction proceeds initially by addition of a catalyst that enables the alkyl halide to ionise to a carbocation. Once this carbocation is formed an electrophilic substitution then takes place. The reaction is completed by loss of a proton to form the substituted aromatic compound.

$$RX \xrightleftharpoons{H^+} R^+ + X^-$$
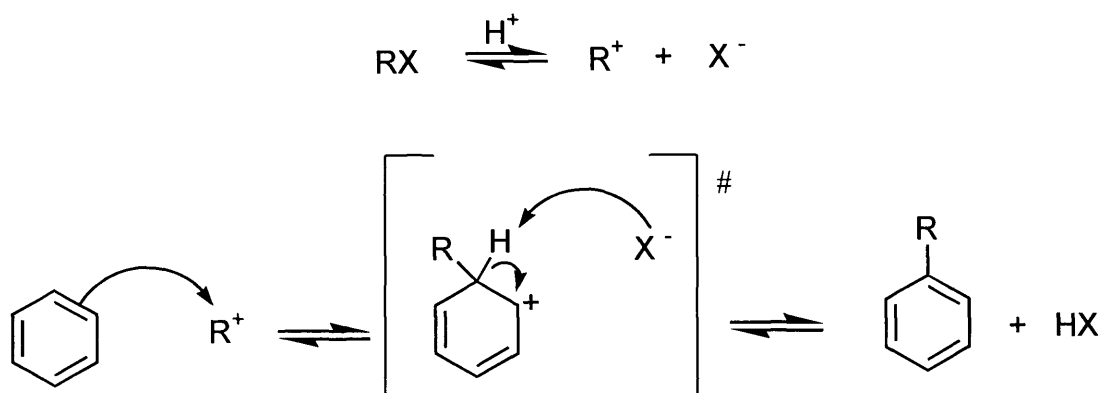
Scheme 1 The carbocation mechanism for a FC alkylation reaction

When ionisation is unfavourable it then becomes possible for the reaction to proceed through a nucleophilic displacement reaction in which no carbocation is involved. Scheme 2 shows an example of a general FC nucleophilic displacement reaction. The reaction takes place in a single step in which the transition state involves a partially formed C – C bond and a partially broken C – X bond.
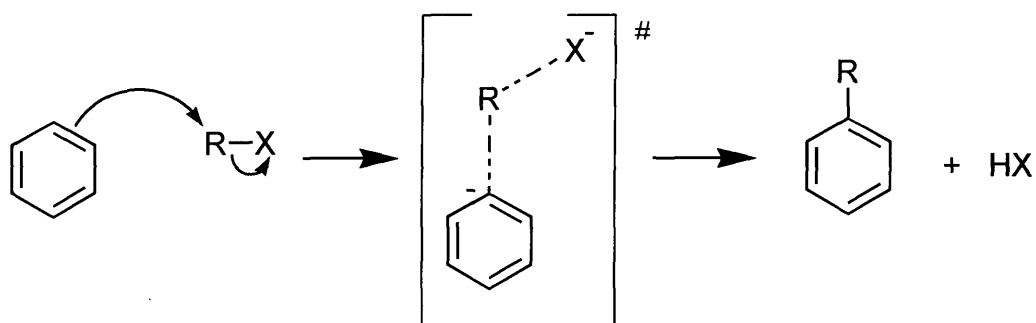
Scheme 2 The nucleophilic displacement mechanism for a FC alkylation reaction

There are several problems associated with reactions, including the FC reaction, in conventional solvents both from an environmental and a practical standpoint.

• Reactions are usually carried out batch wise

• A large excess of the substrate is needed or the reaction is carried out in an organic solvent.

- These reactions typically use more than one stoichiometric equivalent of a liquid acid (e.g. H_2SO_4) or Lewis acid (e.g. $AlCl_3$) catalyst.

- To maintain selectivity a long reaction time at low temperature is necessary.

- After the reaction the catalyst and solvent have to be separated from the reaction mixture.

The conditions of the reaction are not ideal because under these conventional conditions large quantities of waste are produced that cause problems associated with separation, cost, apparatus and the environment. As a result FC reactions are far from being atom efficient or environmentally friendly. Therefore, the development of environmentally more benign FC processes is a high priority.

One recently explored area that may present possible solutions to some of these problems is the use of sc fluids.[26-31] Using sc fluids allows reaction conditions to be tuned to get high product selectivity. It is hoped that relatively small amounts of FC catalyst can be used due to higher solubilities and depressurisation of the reaction vessel easily separates the solvent, products and acid catalyst. The majority of the sc fluid and acid catalyst can then be recycled for further use.

These sc fluid properties and reaction conditions sound very promising at overcoming some of the problems associated with conventional reactions but only on a few occasions have sc fluids been utilised for such a reaction. Poliakoff *et al.* introduced the sc phase to the FC alkylation reaction by using CO_2 and propene as the sc fluid.[30] They carried out a continuous FC reaction of mesitylene and anisole with propene or propan-2-ol employing a heterogeneous Deloxan® catalyst in a small fixed bed reactor. By optimising the conditions they managed to achieve 100 % selectivity for mono-alkylated products with 50 % conversion. Their work clearly demonstrates the feasibility of continuous and sustainable FC alkylation in sc fluids but no comparison was made with conventional continuous alkylation in conventional solvent using the same catalyst. A few other research groups have also looked at applying solid acid catalysts such as zeolites[26,29] and fixed bed catalysts[32] to FC reactions.

Research into the use of sc fluids as homogeneous reaction media for the FC reaction is much more limited. The main reason behind this is that sc CO_2 is usually the fluid of choice and conventional FC catalysts have very low solubility in this non-polar medium. FC reactions have been reported in near critical water[27,31] where it was

found that phenol and *p*-cresol could be alkylated with *t*-butyl alcohol and 2-propanol in the absence of added acid catalyst. Under the reaction conditions it was found that the water acted as both the solvent and catalyst.

Chateauneuf and Nie carried out the FC alkylation of triphenylmethanol with anisole in sc and sub-critical CO_2 employing a small amount of trifluoroacetic acid (TFA) as the catalyst.[28] Their work in the sc state was found to be homogeneous but the product yield was low, at approximately 3 to 4 %. They concluded that for this particular FC reaction the TFA initiated homogeneous reaction conditions do not appear suitable for synthesis. It is their aim to build on these initial studies and investigate other FC alkylations and explore the kinetics of these reactions using *in situ* optical spectroscopy. To my knowledge no kinetic studies on the FC reaction in sc fluids appear in the literature.

6.1.3 Determination of a Rate Law

The rate of a chemical reaction may depend upon reactant concentrations, temperature, and the presence of catalysts. It is often found that the rate of reaction is proportional to the concentrations of the reactants raised to a power. For example, if it is found that the rate is proportional to the concentration of two reactants A and B, the rate can be expressed as

$$rate = k[A]^a[B]^b \qquad (6.1)$$

where the concentration of *A* and *B* are raised to the *a* and *b* power respectively. The coefficient *k* is the rate constant for the reaction that is independent of the concentration of reactants but depends on temperature. The quantities *a* and *b* are called the order of reaction with respect to that species and the sum of the orders equals the overall reaction order. An experimentally determined equation of this kind is called the rate law.

The rate law can be deduced directly from the rate-determining step (RDS) of the reaction. The RDS is the slowest elementary step in a sequence of reactions. For example if we take a two-step reaction

$$A + B \leftrightarrow C + D \quad \text{(fast)}$$
$$C + E \rightarrow F + B \quad \text{(slow, RDS)}$$
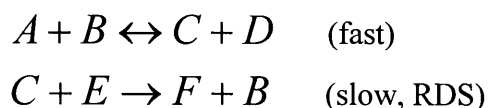
in which the second step is much slower than the first step it is found that the second, slow RDS governs the rate of the overall reaction. Figure 6.1 shows pictorially the

hypothetical reaction steps above. The first step, on going from reactants to intermediates, is fast because it has a low activation barrier and a large proportion of the reactants have enough energy to overcome this barrier. Once the intermediates have been formed, Figure 6.1 shows that the activation barrier for conversion to products is high. The number of molecules with an energy high enough to overcome this barrier will be far less so this step will be slow and rate-determining.
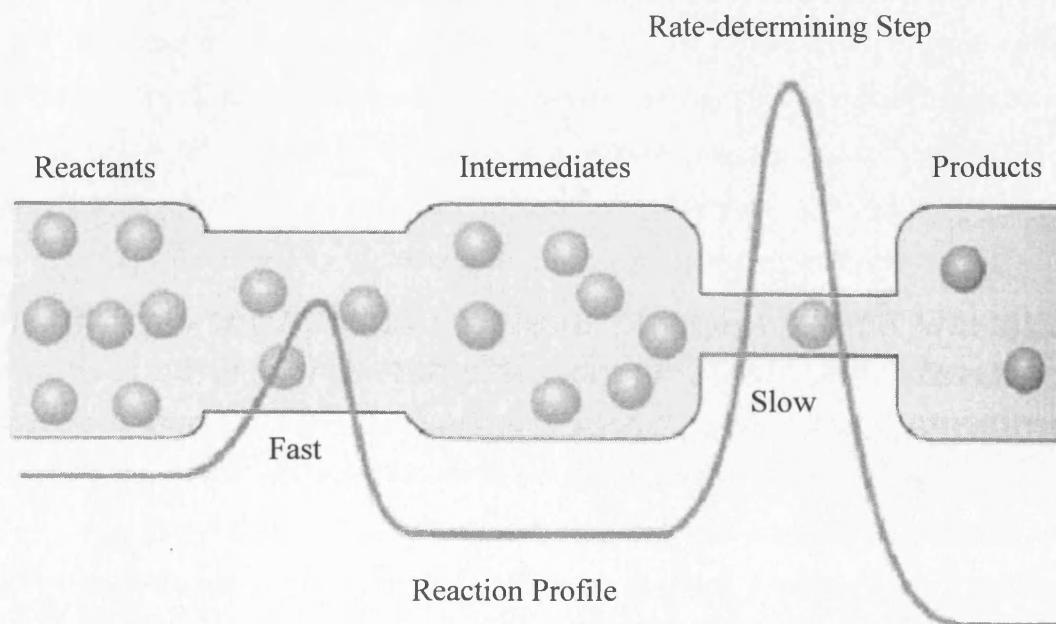
Figure 6.1 Reaction profile of a 2-step reaction in which the second step is rate-determining

The method of initial rates[11] is a useful technique for determining the order of a reaction. The assumption is made that the initial rate of reaction is proportional to the initial concentrations of reagents before measurable amounts of products are formed. Thus, in a reaction with 2 reactants where the rate law is shown in Equation (6.1) a "pseudo-first order rate constant" can be defined so that

$$rate(initial) = k[A_0]^a[B_0]^b \qquad (6.2)$$

To find the reaction order b, with respect to the reactant B, Equation (6.2) can be rearranged assuming the initial concentration of reactant A (= A_0) is held constant:

$$k' = k[A_0]^a \qquad (6.3)$$

$$rate(initial) = k'[B_0]^b \qquad (6.4)$$

By taking the logarithm of both sides the order of reaction with respect to B is found as the slope of a Log-Log plot.

$$Log(rate(initial)) = Logk' + bLog[B_0] \qquad (6.5)$$

The same substitution can then be repeated for reactant A by defining another "pseudo-first order rate constant". Once the order of reaction with respect to each reactant is known the rate law for the reaction can be written.

6.2 Results and Discussion

6.2.1 Rate Law of the Friedel-Crafts Reaction

The acid catalysed FC alkylation reaction has been extensively studied in the liquid state.[25] However, considering the fact that the FC reaction is one of the most important tools for introducing alkyl substituents into an aromatic compound it seems strange that studies on this reaction in the sc state are limited.[1,28,30] This work looks to widen the knowledge of the FC alkylation reaction in the sc state and presents the first acid catalysed FC reaction in sc HFC 32. The aim of this work was not to find optimum operating conditions for the reaction but to achieve a knowledge of the manner in which changes in sc solvent, temperature, pressure and reagents affect the kinetics and therefore the yield and selectivity of the reaction.

The dielectrometry technique has been shown to be applicable to follow the progress of certain equilibrium reactions (Chapter 5). The change in dielectric constant of general FC reagents and products (Scheme 1 and 2) is thought to be large enough so that dielectrometry could be used to follow this reaction. Reagents for this reaction then had to be chosen which would dissolve rapidly in the sc medium.

Traditionally, the FC reaction employs Lewis acid catalysts such as $AlCl_3$ and BF_3 or uses highly reactive organometallic reagents.[25] It is widely known that these catalysts have some unfavourable properties such as limited solubility in organic solvents, sublimation at higher temperatures and they can cause undesirable side reactions. A number of organic sulphonic acids have also been employed as catalysts in FC alkylations, including pTos acid. Recent work by Mahindaratne and Wimalasena[33] demonstrated that pTos acid is a very effective environmentally friendly catalyst for the alkylation of aromatic rings because it can be recovered, reused and has a low cost. They also discovered that the formation of undesired products from side reactions was minimised. It has also been reported previously that pTos has a high solubility in HFC 32.[34] These results made pTos a very attractive catalyst for use in this work.

Anisole and toluene were chosen as the aromatic compounds in this work because they are both liquids and they were observed to solve into solution quickly. There were also no environmental issues with these two reagents and it was hoped that a direct comparison between the results of the two reagents could be made.

Tert-buytlchloride (*t*-BuCl) and *tert*-butylalcohol (*t*-BuOH) were chosen as the alkylating agents because, firstly, they are liquids and it was observed that they solve

into solution readily and, secondly, they are tertiary compounds so rearrangement to a more stable carbocation will not occur. It is therefore likely that a carbocation will be formed when a tertiary alkylating agent is used and it is probable that the reaction will follow a mechanism similar to that shown in Scheme 1.

To assess whether the dielectrometry technique is applicable to following the progress of a FC reaction it was used to follow the alkylation of anisole (R = OCH3) (1) with t-BuCl (X = Cl) (2) using pTos as the catalyst, as shown in Scheme 3. The reaction was carried out over a 1 hour time period in DCE at 363 K and followed by dielectrometry and GC-MS.
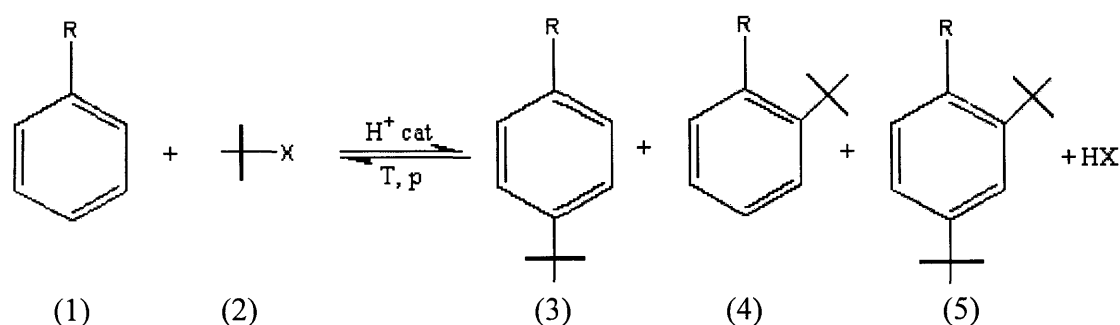
where R = CH3 or OCH3
and X = Cl or OH

Scheme 3 The acid catalysed FC alkylation reaction of PhR with t-BuX used in this work

As with the previously described equilibrium reactions in Chapter 5, the dielectrometry measurements were taken *in situ* and for the GC-MS measurements, 2 ml aliquots of the reaction solution were taken. The actual reaction conversion was obtained from the GC-MS results at specific time intervals. The conversion value from the dielectrometry measurements was calculated from a knowledge of the final conversion of the reaction, from GC-MS, and the capacitance value at a given time interval. Three products were isolated in this reaction as shown in Scheme 3. It was found that *ortho-*, *para-* and *di*-butylated substitution could occur on the aromatic compound. The isolation of these products has been reported previously.[35]

The measured (GC-MS) and calculated (dielectrometry) conversions for this FC reaction are shown in Figure 6.2. Very close agreement is once again observed
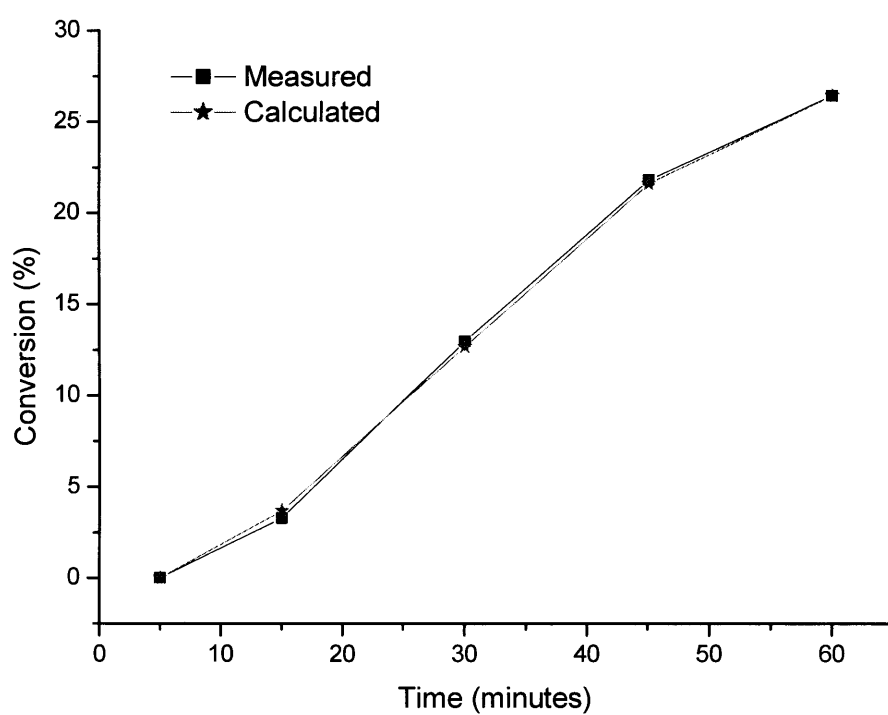
Figure 6.2 Comparison of measured and calculated conversions for the FC reaction of anisole and *t*-BuCl in DCE at 363 K

between the measured and calculated conversion values, signifying that the dielectrometry technique is applicable to following the progress of this reaction.

The FC reaction is actually an equilibrium reaction therefore equilibrium constants can be calculated if the reaction is left long enough so an equilibrium is reached. In Chapter 5 it has been shown that equilibrium constants could be calculated using dielectrometry. The aim of this section however, is to study the FC alkylation reaction under non-equilibrium conditions and from this get an appreciation of the mechanism and rate of reaction under various conditions.

Initially the time taken for this reaction to reach equilibrium had to be determined. To achieve this the FC reaction of anisole (0.16 M) and t-BuCl (0.16 M) was carried out at 363 K and 235 bar in HFC 32. Taking capacitance measurements at time intervals up to 20 hours enabled the reaction to be followed. Figure 6.3 shows the measured changes in capacitance as the FC reaction proceeds. The increase in capacitance is rapid at first and begins to plateau after 5 to 6 hours indicating that the reaction is approaching equilibrium. To calculate rate constants, instead of equilibrium constants, reactant or product concentrations need to be calculated under non-equilibrium conditions. To fulfil this a reaction time of 1 hour was taken for the calculation of rate constants because at this time the reaction will be far from equilibrium under all conditions studied.

The reproducibility of this dielectrometry technique was assessed with this FC reaction. Five separate FC reactions were carried out under the same conditions of temperature, pressure and reagent concentrations in HFC 32. These five reactions were left to proceed for different times lengths ranging from 30 minutes up to 20 hours. Figure 6.4 shows the change in anisole concentration (calculated from the capacitance of the reaction medium) as a function of time. Within experimental error all reactions are in agreement with each other over the same measured time lengths indicating that dielectrometry is highly reproducible.

Before attempting to obtain rate constant information it is important to elucidate the mechanism. To achieve this for the FC reaction of anisole with t-BuCl using pTos in sc HFC 32 at 363 K in this work, the method of initial rates as explained in section 6.1.3 is applied. By varying the initial concentration of a reactant, whilst keeping the concentrations of the other reagents in excess, the initial rate for that reactant can be calculated from dielectrometry measurements. The order of reaction with respect to that reactant can then be calculated. This then needs to be
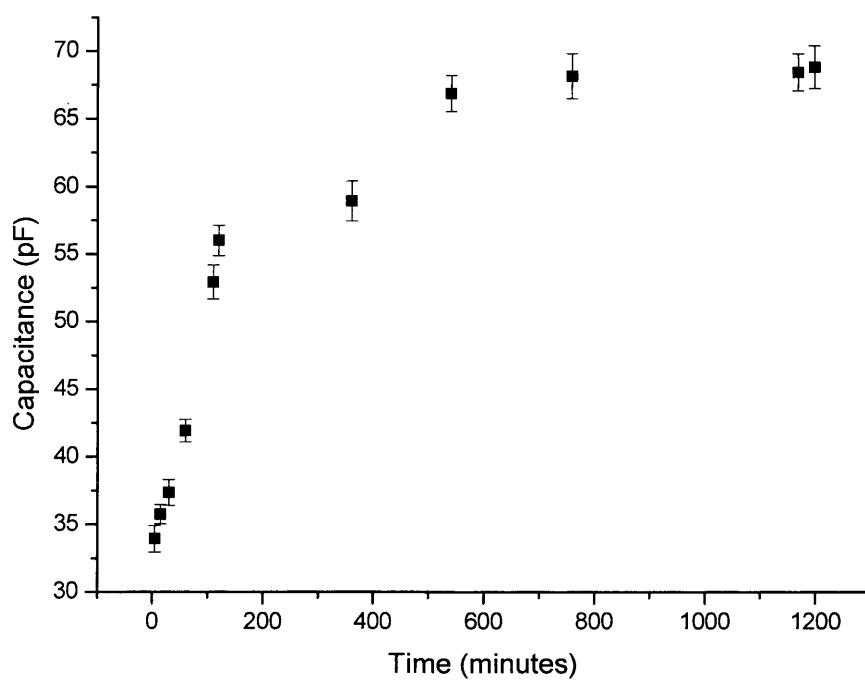
Figure 6.3 Change in capacitance for the FC reaction of anisole and *t*-BuCl in HFC

32 at 235 bar and 363 K over 20 hours
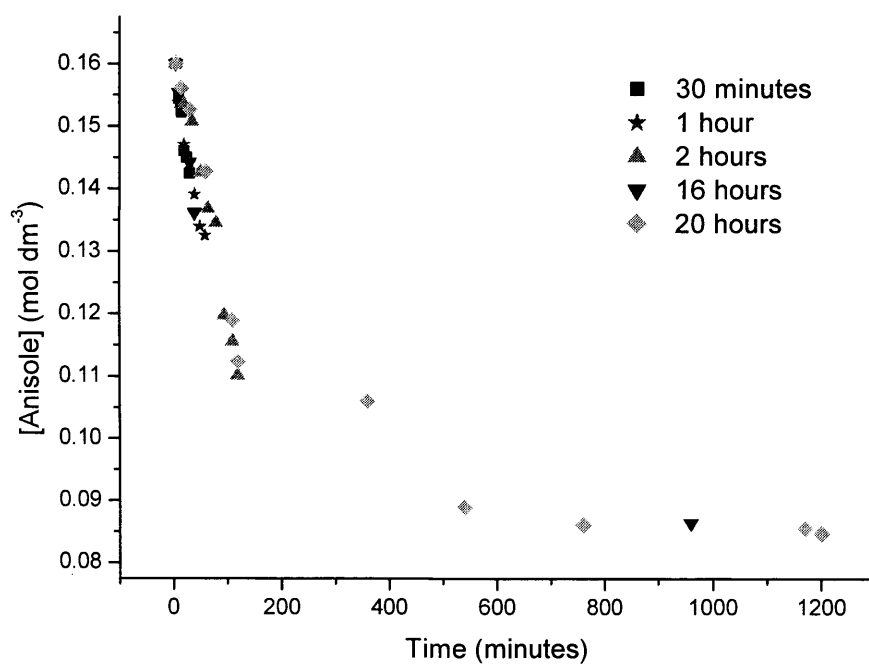
Figure 6.4 Change in anisole concentration for the FC reaction in HFC 32 at 363 K at

250 ± 10 bar as a function of time

repeated for the other reactants, so the order of reaction with respect to each reactant can be found and then the rate law can be written. This rate law will then be a guide to the mechanism of the reaction.

It has been reported previously that for active halides, like t-BuCl employed here, a trace amount of catalyst will be enough to initiate the reaction.[36] If this is observed in this work then differing pTos concentrations will not have an effect on the initial rate. Table 6.1 and Figure 6.5 show the affect of different initial pTos concentrations on the initial rate of FC alkylation in HFC 32 at 363 K and 140 bar.

Entry	Anisole (M)	t-BuCl (M)	pTos (M)	Initial Rate (Mol dm^{-3} s^{-1})
1	0.08	0.16	0.04	1.423×10^{-5}
2	0.08	0.16	0.08	1.427×10^{-5}
3	0.08	0.16	0.16	1.461×10^{-5}

Table 6.1 Effect of the acid catalyst on the initial rate of the FC alkylation of anisole with t-BuCl in HFC 32 at 363 K and 140 bar

It can be seen that the initial rate remains unchanged and the reaction order from the slope of the Log-Log plot is zero. Entry 3 in Table 6.1 cannot be included in the method of initial rates as the anisole concentration is not in excess of the pTos under investigation. However, from these results it can reasonably be assumed that as the initial rate is unchanged the catalyst does not appear in the RDS and is not in the rate law for this reaction.

The method of initial rates was then repeated for anisole as shown in Table 6.2 and Figure 6.5. On analysis of Figure 6.5 and Table 6.2 it is noted that the initial rate increases as the concentration of anisole increases under the conditions studied. The concentration of pTos shown in Table 6.3 as entry 2 and 3 can be seen not to be in excess compared to the concentration of anisole. It was found previously that the acid catalyst is not included in the rate law so it can be assumed that it does not affect the initial rate of these reactions and therefore it does not need to be in excess. From the Log-Log plot the order is calculated from the slope of the graph, which is found to be 1.215. Within experimental error it can be assumed that the reaction is first order with
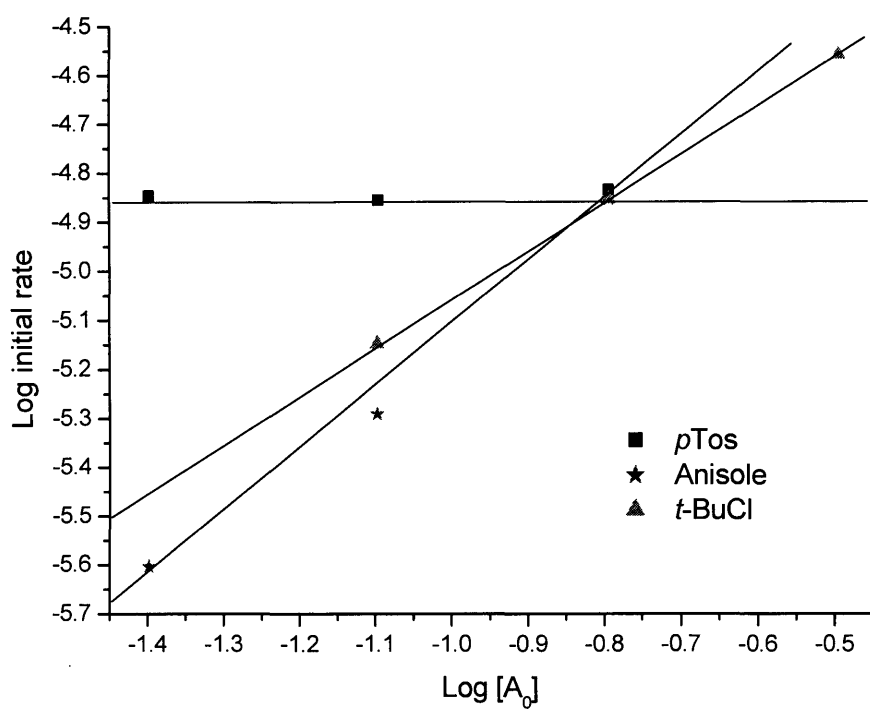
Figure 6.5 Log-Log plot to calculate the reaction order of the acid catalyst, anisole and t-BuCl in the FC reaction

respect to anisole. This result indicates that anisole will be involved in the RDS and will, therefore, appear in the rate law for the reaction raised to the power of 1.

Entry	Anisole (M)	t-BuCl (M)	pTos (M)	Initial Rate (Mol dm^{-3} s^{-1})
1	0.04	0.16	0.08	2.491 x 10^{-6}
2	0.08	0.16	0.08	5.117 x 10^{-6}
3	0.16	0.16	0.08	1.398 x 10^{-5}

Table 6.2 Effect of anisole concentration on the initial rate of FC alkylation in HFC 32 at 363 K and 260 bar

The method of initial rates was then repeated for t-BuCl as shown in Table 6.3 and Figure 6.5. Similar analysis of Table 6.3 and Figure 6.5 for various t-BuCl concentrations shows that doubling the t-BuCl concentration the initial rate also doubles. The slope of the Log-Log plot was found to be 0.9784 and therefore within experimental error it can be assumed that the reaction is first order with respect to t-BuCl. From this result it is deduced that t-BuCl will be involved in the RDS and therefore appears in the rate law for the reaction raised to the power of 1.

Expt	Anisole (mols)	t-BuCl (mols)	pTos (mols)	Initial Rate (Mol dm^{-3} s^{-1})
1	0.16	0.08	0.08	7.108 x 10^{-6}
2	0.16	0.16	0.08	1.398 x 10^{-5}
3	0.16	0.32	0.08	2.762 x 10^{-5}

Table 6.3 Effect of t-BuCl concentration on the initial rate of FC alkylation in HFC 32 at 363 K and 260 bar

Using the method of initial rates on each reactant in turn, the rate law for this pTos catalysed FC alkylation of anisole and t-BuCl in HFC 32 at 363 K has been determined to be

$$rate = k[tBuCl]^{1}[Anisole]^{1} \qquad (6.6)$$

From the addition of the individual orders it can be seen that the rate of the overall reaction is second order

The method of initial rates might not reveal the full rate law for a reaction because the products formed may participate in the reaction and affect the rate. To assess this possibility the rate law should be fitted to the data obtained for the duration of the reaction not just at initial time lengths. Rate laws are differential equations so by integration it is possible to find the concentrations of reactants/products as a function of time. Anisole and t-BuCl are formed in the same stoichiometric amounts in the chemical equation so it can be assumed that [anisole] $\equiv$ [t-BuCl] so the integrated form of the second order rate law in Equation (6.6) becomes

$$\frac{1}{[A]} - \frac{1}{[A]_0} = kt \tag{6.7}$$

This equation signifies that if 1/[concentration] is plotted against time a straight line will be observed if the reaction is second order. Figure 6.6 shows the change in 1/[anisole] versus time for the FC reaction in HFC 32 at 363 K. A straight line is observed in accordance to Equation (6.7) with a correlation of 0.9937. This result verifies that this FC reaction is indeed second order. It is noted however that a limitation of this approach is that if the data for the FC reaction are fitted to the integrated rate law of a first order reaction a linear plot may also be observed that is a consequence of experimental error.

6.2.2 Effect of Temperature and Pressure on the Friedel-Crafts Reaction Rate

For an organic reaction there are a number of variables that can be adjusted e.g. reactant concentrations, solvent, catalyst, time and temperature and these will have an effect on the rate and maybe the selectivity of the reaction. In a sc fluid, the same organic reaction can also be affected by alteration of the pressure because above the critical point a small change in pressure can result in a change in a number of the solvent properties including density, viscosity, hydrogen bonding and dielectric constant.

It is found that the majority of reaction rates depend on the temperature at which the reaction is run. As the temperature increases the molecules carry more kinetic energy, resulting in faster movement of molecules and more frequent
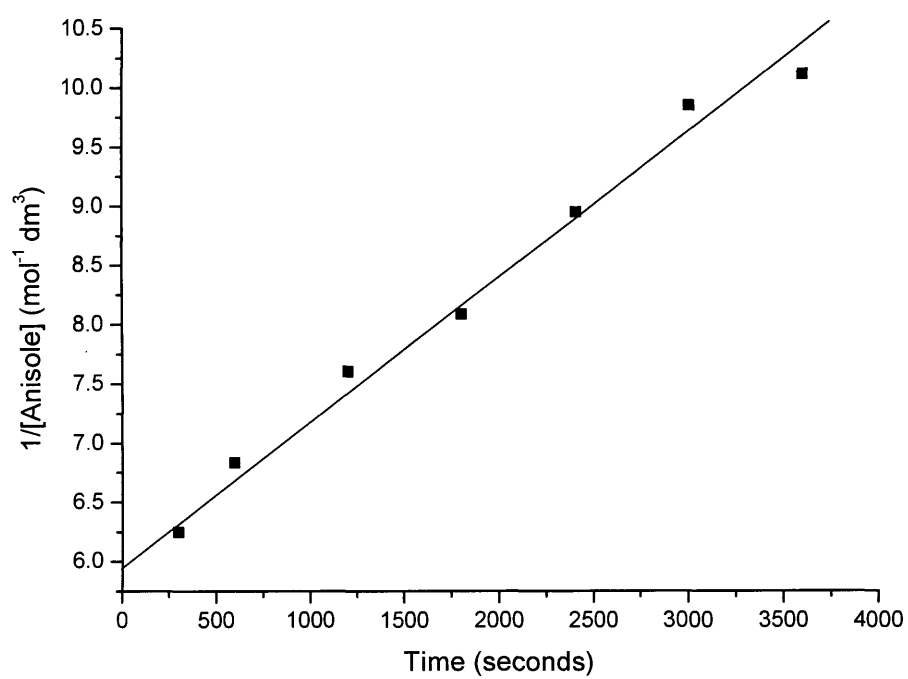
Figure 6.6 The change in 1/anisole concentration with time for the FC reaction in HFC 32 at 363 K

collisions. Thus, the proportion of collisions that can overcome the activation energy for the reaction increases with temperature.

The simplest model to explain the relationship between temperature and rate of reaction is the Arrhenius equation.

$$k = Ze^{\frac{-E_a}{RT}} \tag{6.8}$$

Where, k is the rate constant for the reaction, Z is a proportionality constant that varies from one reaction to another, E_a is the activation energy for the reaction, R is the ideal gas constant and T is the temperature in Kelvin.

The Arrhenius equation can be used to determine the activation energy for a reaction. By taking the natural logarithm of both sides the equation becomes

$$\ln k = \ln Z - \frac{E_a}{RT} \tag{6.9}$$

A plot of ln k against 1/T according to Equation (6.9) should give a straight line with a slope of $-E_a/R$.

The Arrhenius plot in Figure 6.7 is compiled from the data in Table 24 of the appendix for the FC reaction of anisole (0.16 M) and t-BuCl (0.16 M) at 260 ± 10 bar. Rates of reaction were measured at three different temperatures and from the linear relationship seen in Figure 6.7 the activation energy is found to be 93.6 kJ mol^{-1}. A direct literature comparison for this reaction in a liquid solvent could not be found. DeHaan et $al.$ have reported the activation energy for the FC reaction of benzene with t-BuCl in nitromethane.[37] In this work they calculated the activation energy to be 76 ± 13 kJ mol^{-1}. The activation energy reported in this study is the same order of magnitude.

To assess the effect of pressure on the FC alkylation of anisole (0.16 M) with t-BuCl (0.32 M) using pTos (0.08M) in HFC 32 at 363K a number of reactions were conducted at differing pressures over a 1 hour time period. The total conversion of the reaction at a variety of pressures is shown in Figure 6.8 and Table 25 of the appendix. At low pressures the conversion increases and as the critical pressure is reached a maximum in conversion is observed. Further increases in pressure result in a decrease of the observed conversion.
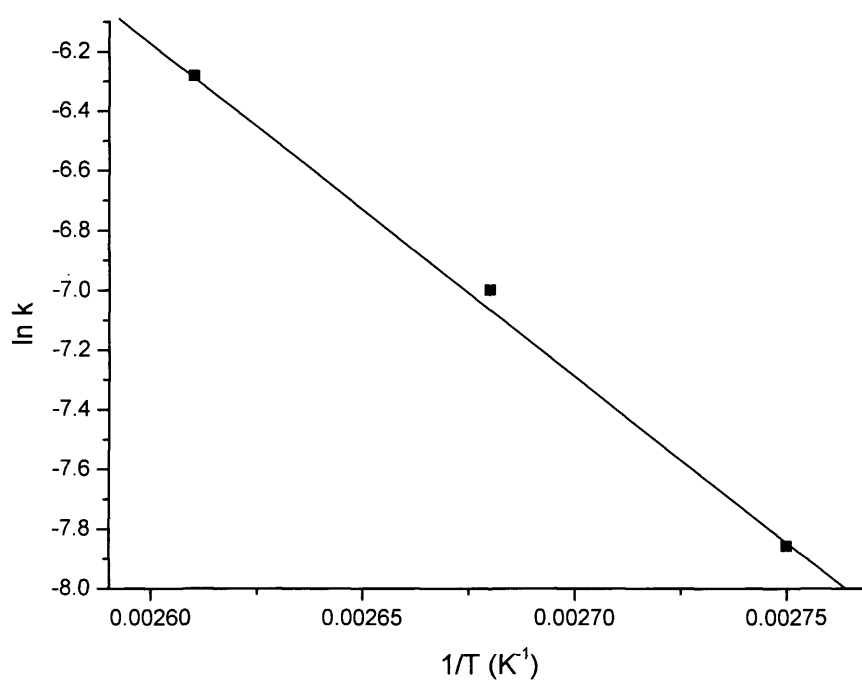
Figure 6.7 Arrhenius plot for the FC alkylation of anisole with *t*-BuCl in HFC 32 at

260 ± 10 bar
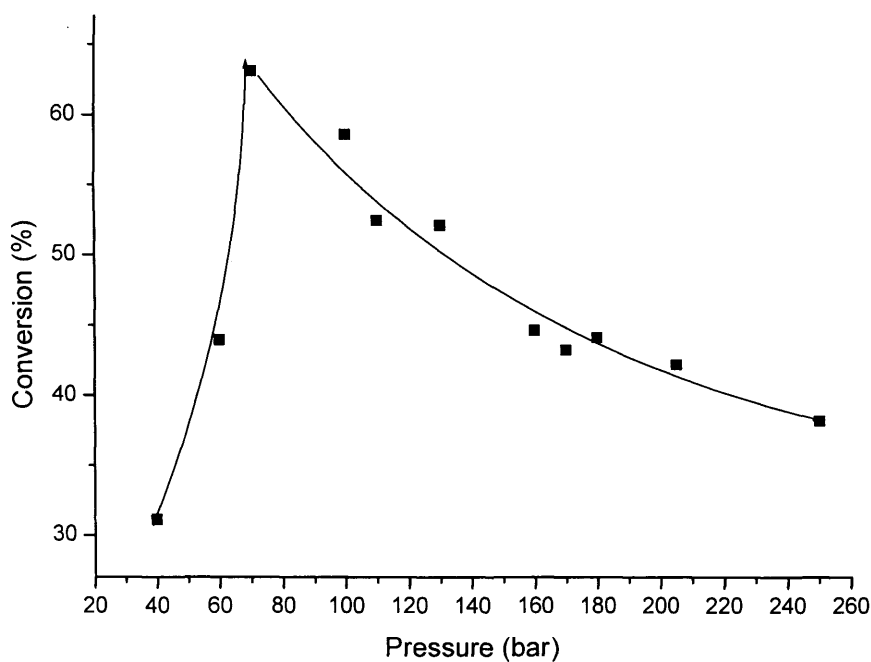
Figure 6.8 Change in conversion for the FC alkylation of anisole and *t*-BuCl in HFC

32 at 363 K after 1 hour at a variety of pressures

Second order rate constants can be calculated for each pressure by measuring the gradient of a 1/[anisole] against time plot, as shown previously in Figure 6.6. This process was carried out for all pressures and the results are shown in Figure 6.9 and Table 26 of the appendix. It is observed that the rate constant increases with pressure and reaches a maximum at the critical point. From this point a further increase in the pressure results in a decrease in the rate of reaction. In these reactions the number of reactant molecules stays constant but as the pressure increases the number of solvent molecules in the reaction system will increase. Thus, an increase in the pressure of the reaction system results in an increase in the ratio of solvent molecules to starting reagent molecules. Therefore it is necessary to see whether the observed change in rate with pressure is actually a result of a pressure affect or whether it is due to a dilution effect.

To remove the possibility of dilution affecting the rate as the pressure is increased, FC reactions were carried out with the same mole fraction of solute and solvent molecules at various pressures. To achieve this, different amounts of starting reagents had to be used in each reaction for a given pressure. The reaction of anisole and t-BuCl in HFC 32 at 363 K was once again used for this study.

The results in Table 27 of the appendix were obtained from the reactions at the same mole fraction of solute and solvent but at different pressures. It can be seen from Table 27 that these rates of reaction do not have such a large dependency on pressure (c.f. Table 26 of the appendix). Also shown in Table 27 is a second order rate constant for this FC reaction in a liquid solvent. Dichloroethane was chosen as it has a similar dielectric constant to HFC 32 at 363 K. The reaction in DCE was carried out under reflux using the same number of moles of solvent and reagents as the FC reaction at 180 bar and 363 K in HFC 32. The calculated second order rate constant in the liquid solvent is an order of magnitude lower than that in the sc state. The number of molecules used in the liquid state was the same and the dielectric constant between the two solvents is very similar so the difference in the rate is thought to be due to the difference in density and viscosity between the two solvents In the sc fluid the density and the viscosity is lower which means that diffusion of the reactant species should be greater and therefore the reaction should be faster than that in the liquid solvent.
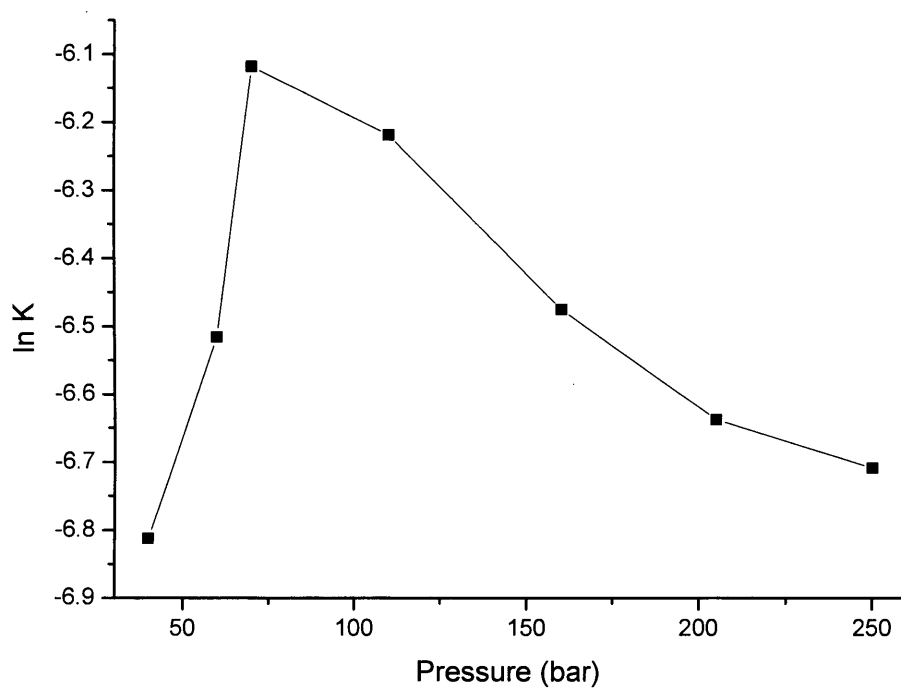
Figure 6.9 The change in ln second order rate constant for the FC reaction of anisole with t-BuCl as a function of pressure in HFC 32 at 363 K

The results in Table 27 are plotted in Figure 6.10, where it can be seen that ln k increases at low pressures as observed earlier in Figure 6.9. However, it should be noted that the difference in the second order rate constant at low pressures is an order of magnitude lower than the difference at low pressures shown in Figure 6.10.

From the experimental results at constant mole fraction the actual affect of pressure on the FC reaction can be ascertained. The increase in rate at low pressures, albeit small, may be due to local composition enhancements, which have been observed previously for other reactions in sc fluids. As sc HFC 32 has the ability to form hydrogen bonds at low pressures as shown in Chapter 4, the increase in rate may also be due to hydrogen-bonding affects

If we take a closer look at the results at higher pressures in Figure 6.10, when the effect of local composition enhancement and hydrogen-bonding ability is minimal, it can be seen that the rate increases slightly with pressure. In the review by Blandamer et al.[38] it was stated that thermodynamics does not define how ln k depends on pressure but often the aim is to analyse the dependence to extract further information. Usual practice is to adopt a simple description for the chemical processes and estimate the activation volume, ΔV^k, because

$$\left[\frac{\partial \ln k}{\partial p} \right]_T = -\frac{\Delta V^k}{RT} \tag{6.10}$$

where R is the gas constant and T is the temperature.

From the gradient of the slopes in Figure 6.10 the volume of activation calculated for this reaction in the sc state at low pressures (70 to 120 bar) was found to be 84 cm^3 mol^{-1}. At higher pressures where local composition enhancement can be ignored (120 bar to 210 bar) the activation volume was found to be -3.2 cm^3 mol^{-1}. The large change in the activation volume observed at low pressures is positive, which suggests that there is an expansion in the solvent as the reaction proceeds to products. The expansion of the solvent may be a consequence of the lower polarity of the products when compared to that of the transition state, which is charged. The increase in activation volume may also be brought about by a decrease in hydrogen bonding of the solvent. The solvent is able to form hydrogen bonds with the reactants but because the products are substituted the hydrogen bonding sites are not available due to steric hindrance.
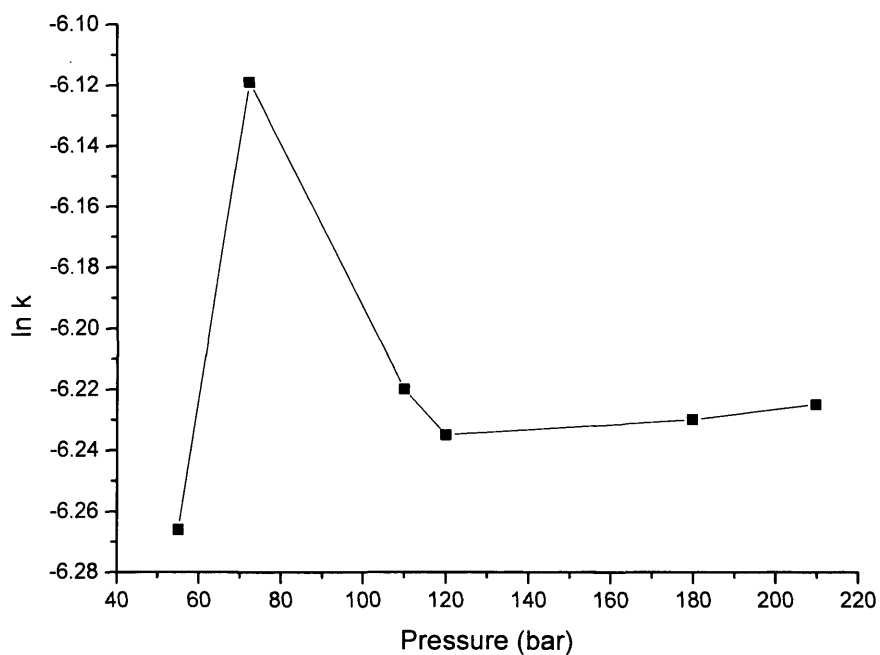
Figure 6.10 The change in ln second order rate constant for the FC reaction of anisole with t-BuCl at constant mole fraction as a function of pressure in HFC 32 at 363 K
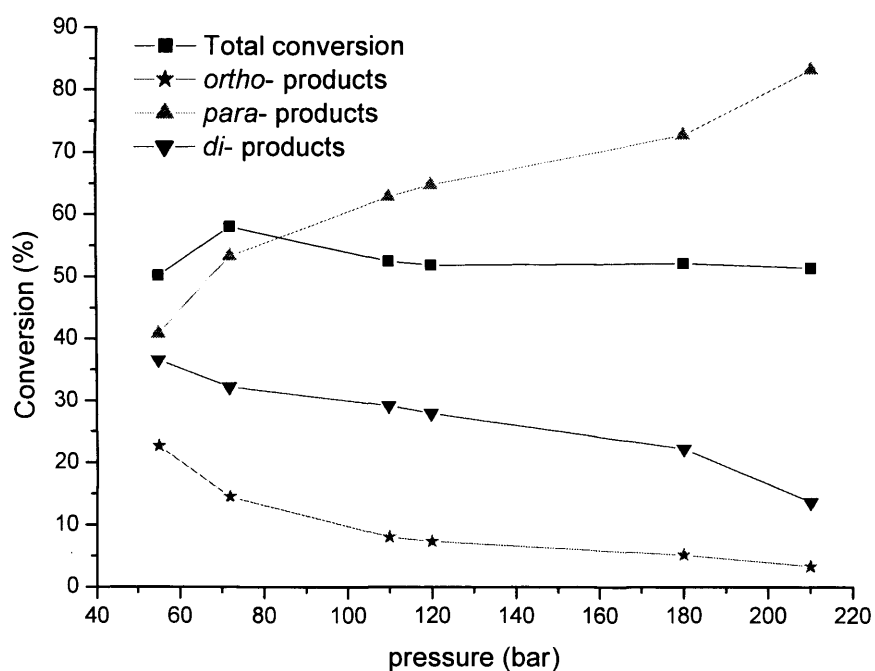
Figure 6.11 Conversion for the FC reaction of anisole with t-BuCl in HFC 32 at 363 K for a variety of pressures at constant mole fraction

143

CHAPTER 6. Rates of Reaction in Supercritical Media

From this work it has been found that pressure has only a small affect on the rate of FC alkylation so under the pressures studied the yield (total conversion) for the reaction is approximately constant as shown in Figure 6.11 and Table 28 of the appendix. On analysis of the products from the FC alkylation of anisole with *t*-BuCl it was found that 3 products were observed, the *ortho*-, *para*- and *di*- butyl substituted anisole, as shown in Scheme 3.

In Figure 6.11 the change in conversion of these three products is displayed as a function of pressure at constant mole fraction. Compared to the total conversion for the reaction it is seen that the product selectivity has a large dependency on the pressure. As the pressure is increased the amount or *ortho*- and *di*- products decreases and the amount of *para*- product increases. The methoxy group on anisole is *ortho*- and *para*- directing so substitution at both these positions is to be expected. The observation that the amounts of these products varies with pressure is an interesting one and presents the opportunity to change the selectively of the FC reaction by manipulation of the pressure.

The observed changes in the product ratio with pressure may be due to the change in hydrogen bonding of the solvent as the pressure is increased. It has been shown in Chapter 4 that the ability of HFC 32 to form hydrogen bonds decreases with increasing pressure. The observed decrease in the *ortho*- and *di*- (both products involve *ortho*- substitution) products as pressure is increased so it is possible that this is related to the decrease in hydrogen bonding ability of the HFC 32 solvent. The FC reaction in the commonly employed sc solvent CO_2 was carried out for a comparison because CO_2 cannot form hydrogen bonds. In this reaction it was found that the selectivity of the reaction is independent of pressure (see section 6.2.4 later) and therefore it may be possible that the observed changes in product distribution are somehow connected to hydrogen bonding effects. Further investigations will be carried out in future work to assess this possibility.

To assess the true affect of pressure on a reaction it can be seen that it is necessary to keep the mole fraction of all the reagents and the solvent constant as the pressure is increased. In this work it has been shown that the rate of the FC reaction can easily be calculated by application of the dielectrometry technique. Even though the FC reaction between anisole and *t*-BuCl has not been optimised, good yields are observed. The rate of this reaction is found to be only slightly dependent on pressure

but the selectivity of the reaction can be tuned by small changes in pressure due to the hydrogen bonding ability of HFC 32.

6.2.3 Effect of Reagents on the Friedel-Crafts Reaction Rate

It has been shown that the FC alkylation of anisole using t-BuCl proceeds with moderate yields in sc HFC 32. The selectivity was also found to be a function of pressure due to the presence of hydrogen bonds between the anisole oxygen and the solvent. In this work anisole is replaced by toluene in the FC alkylation reaction in HFC 32. Toluene differs from anisole in that the functional group on the benzene ring is missing an oxygen atom. The lack of this oxygen atom results in a lower dielectric constant for toluene (ε = 2.38 at 278 K, whereas for anisole ε = 4.33 at 278 K) and also toluene is unable to form hydrogen bonds. The effect that the loss of this oxygen atom has on the rate, yield and selectivity of FC alkylation is assessed.

The conversion for the FC reaction of toluene (0.16 M) with t-BuCl (0.16 M) at 260 bar is shown in Figure 6.12 as a function of time. The results for anisole at the same concentrations are also shown for comparison. It can easily be seen that conversion is greater for the FC reaction employing anisole than toluene. It is interesting to note that on analysis of the product distribution for the toluene reactions, only the *para*-substituted product was isolated. This is surprising because it is known that under kinetic control anisole and toluene are both *ortho*- and *para*- directing.[35] The reason for this observation is unknown but it may be possible that the sc solvent is inhibiting substitution at the *ortho*- position. It is possible that the *ortho*- product is formed in the very early stages of the reaction at time lengths shorter than those studied here. If this is so and the amount of *ortho*- product is low, the rapid *ortho-para* interconversion[35] observed with these t-butylated products may account for the lack of *ortho*- product isolated at longer time lengths. Experimental work to explain the observed product distribution for the FC reaction of toluene is the focus of future research.

To assess the affect of pressure on the FC alkylation of toluene (0.16 M) with t-BuCl (0.32 M) using pTos (0.08M) in HFC 32 at 363K, a number of reactions were conducted at differing pressures over a 1 hour time period. The total conversion of the reaction at a variety of pressures is shown in Figure 6.13 and Table 29 of the appendix. At low pressures the conversion increases and a maximum is observed
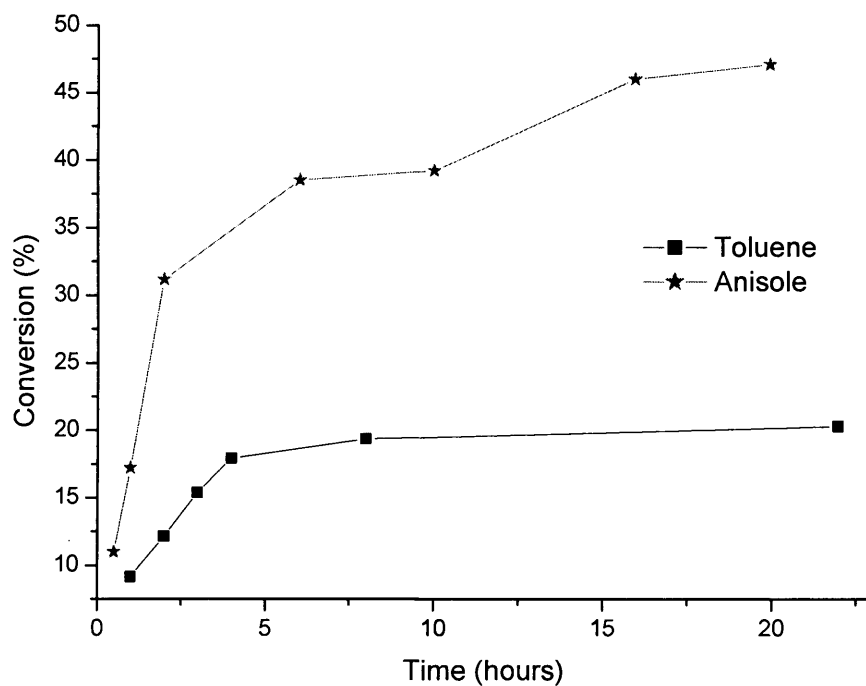
Figure 6.12 Change in conversion with time for the FC reaction of toluene compared to anisole in HFC 32 at 260 bar and 363 K
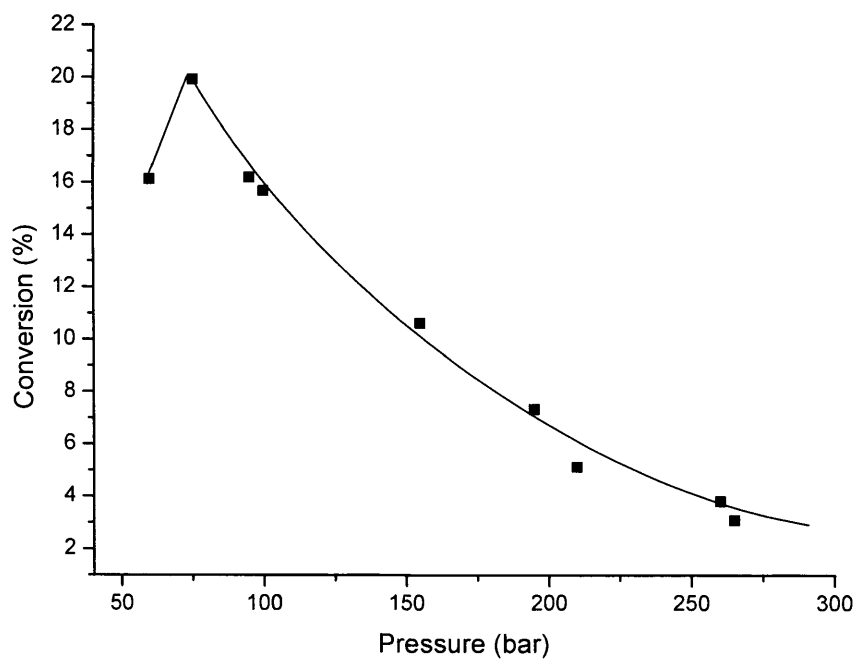
Figure 6.13 Change in conversion for the FC alkylation of toluene and *t*-BuCl in HFC 32 at 363 K after 1 hour at a variety of pressures

146

at the critical pressure. Further increase in the pressure results in a decrease of the observed conversion. Results for the reaction with anisole presented earlier follow the same trend observed here but the observed conversions are considerably higher for the anisole reaction.

Second order rate constants can be calculated for each different pressure by measurement of the gradient of a 1/[toluene] against time plot, as shown previously for anisole in Figure 6.6. This process was carried out for all pressures and results are shown in Figure 6.14 and Table 30 of the appendix. It is observed that the rate constant increases with pressure up to a maximum at the critical point. From this point a further increase in the pressure results in a decrease in the rate of reaction. In these reactions the number of reactant molecules stays constant but as the pressure increases the number of solvent molecules in the reaction system will increase. An 8-fold decrease in the rate is observed in the sc region when the pressure in increased from 75 to 265 bar. The resulting rate decrease observed in these studies is once again thought to be due to a dilution effect as the increase in pressure increases the ratio of solvent to solute molecules increases. The actual affect of pressure on the FC reaction of toluene would need to be found from constant mole fraction studies. These have not been carried out at this time and will be the focus of future work.

To explain the relationship between temperature and rate of reaction it is commonly assumed that the rate constant depends on the temperature at which the reaction is run as explained earlier. To assess the affect of temperature on the rate of FC alkylation reactions of toluene (0.16 M) and t-BuCl (0.16 M) at 260 ± 20 bar were carried out at 363, 373 and 383 K in HFC 32. The results are shown on the Arrhenius plot in Figure 6.15 and in Table 31 of the appendix. From the gradient of the plot in Figure 6.15 the activation energy is found to be 139.8 kJ mol^{-1}. If this is compared to the result obtained for anisole under the same conditions it is observed that the activation energy for the toluene reaction is approximately 40 kJ mol^{-1} higher. The higher activation energy for these reactions explains the lower yields obtained for the FC reaction involving toluene. As the activation energy is higher there are less reaction molecules that have sufficient energy to overcome the activation barrier and so less molecules will have the ability to react.
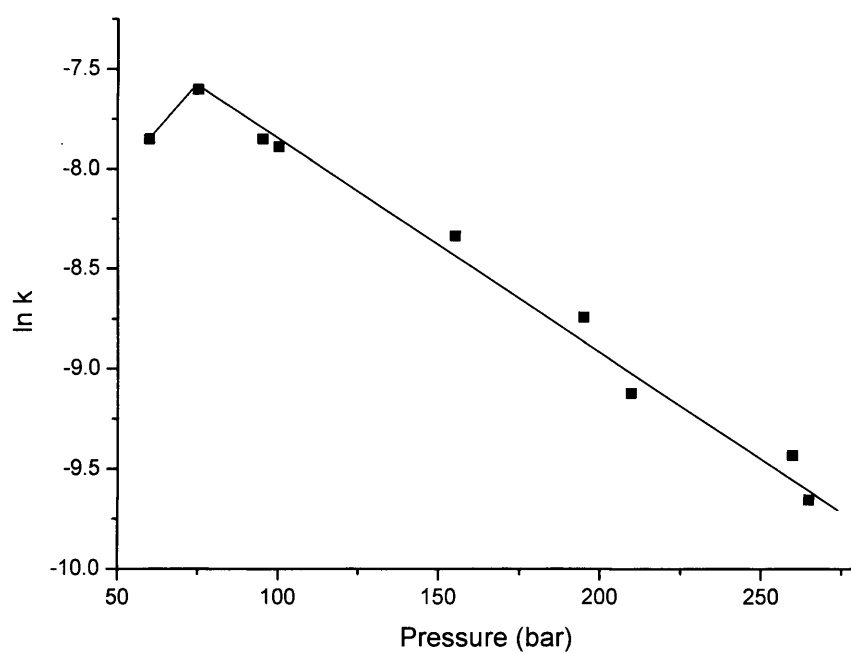
Figure 6.14 The change in ln second order rate constant for the FC reaction of toluene with t-BuCl as a function of pressure in HFC 32 at 363 K
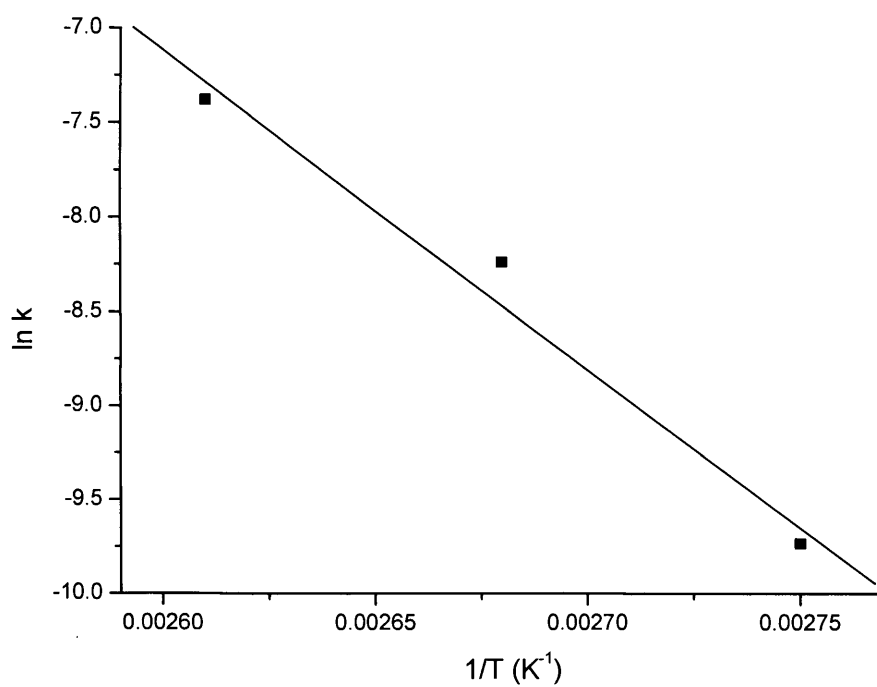
Figure 6.15 Arrhenius plot for the FC alkylation of toluene with t-BuCl in HFC 32 at 260 ± 20 bar

By changing the aromatic reagent to toluene in the FC reaction a change in the reaction yield, selectivity and rate is observed, which further supports the inclusion of the aromatic species in the rate law. The anisole reaction is favoured over that of toluene due to the greater stabilisation of the transition state. The oxygen on the methoxy group is a good electron donor so it is able to donate electrons to the ring, thereby stabilising the carbocation. Due to the higher activation energy for the FC reaction of toluene lower yields were obtained and for reasons as of yet unknown, the reaction was found to selectively produce the *para*-substituted product.

An experiment to assess the affect of changing *t*-BuCl to *t*-BuOH was carried out on the FC reaction of anisole in HFC 32 at 363 K. With the change to the alcohol a vast increase in the yield and the rate was observed. At 250 bar employing *t*-BuCl gave a yield and rate of 17.19 % and $3.87 \times 10^{-4} \, mol^{-1} \, dm^3 \, s^{-1}$ respectively whereas with *t*-BuOH the yield and rate were found to be 52.04 % and $2.07 \times 10^{-3} \, mol^{-1} \, dm^3 \, s^{-1}$ respectively. The increase in reaction rate supports the inclusion of the alkylating species in the previously calculated rate law.

The increased yield and rate using *t*-BuOH is expected because the leaving group formed with the alcohol, H_2O, is a better leaving group than HCl, which is formed with the *t*-BuCl. To justify the observed results using *t*-BuOH a thorough investigation into the effect of this alkylating agent on the yield, selectivity and rate will have to be carried out. This will be the basis of future research.

6.2.4 Effect of Supercritical Solvent on the Friedel-Crafts Reaction Rate

To assess the affect of the sc solvent on the yield, selectivity and rate of FC alkylation, CO_2 was employed and results compared to those presented earlier in HFC 32. The dielectric constant of sc CO_2 is less than 2 and is not greatly affected by changes in pressure, whereas with HFC 32, the dielectric constant is higher and strongly dependant on pressure changes.[39] The differences in the dielectric constants of these two sc solvents at 363 K and a variety of pressures are shown in Figure 6.16. Measurements on the unoptimised FC alkylations of anisole and *t*-BuCl using *p*Tos catalyst were carried out at 363 K in CO_2 at various pressures to assess the effect of the sc solvent on this reaction.

Figure 6.17 and Table 32 of the appendix present the conversion for the reaction of anisole (0.16 M) and *t*-BuCl (0.4 M) after 1 hour in sc CO_2 at 363 K as a
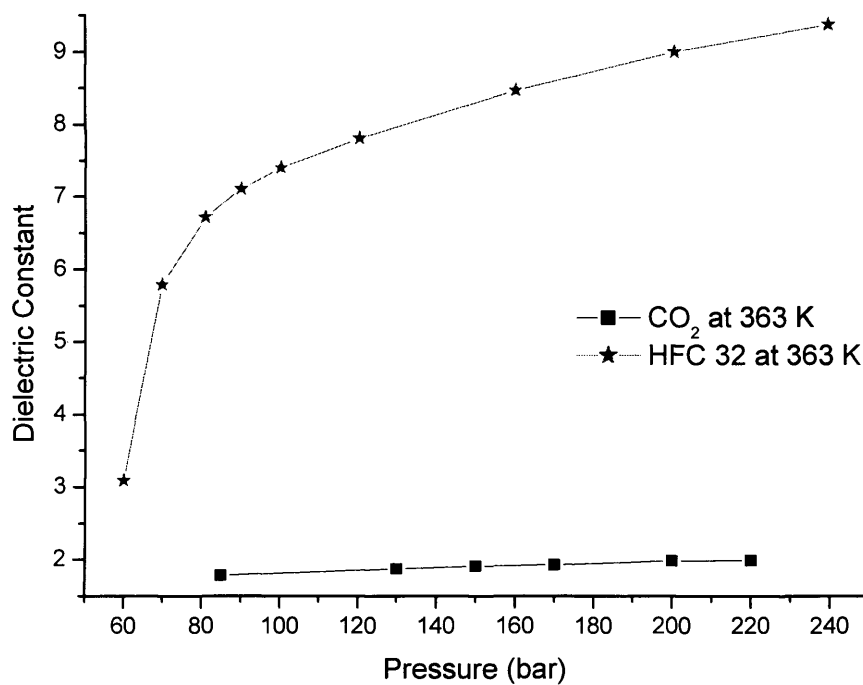
Figure 6.16 Change in dielectric constant for the sc fluids used in this work at 363 K and a function of pressure
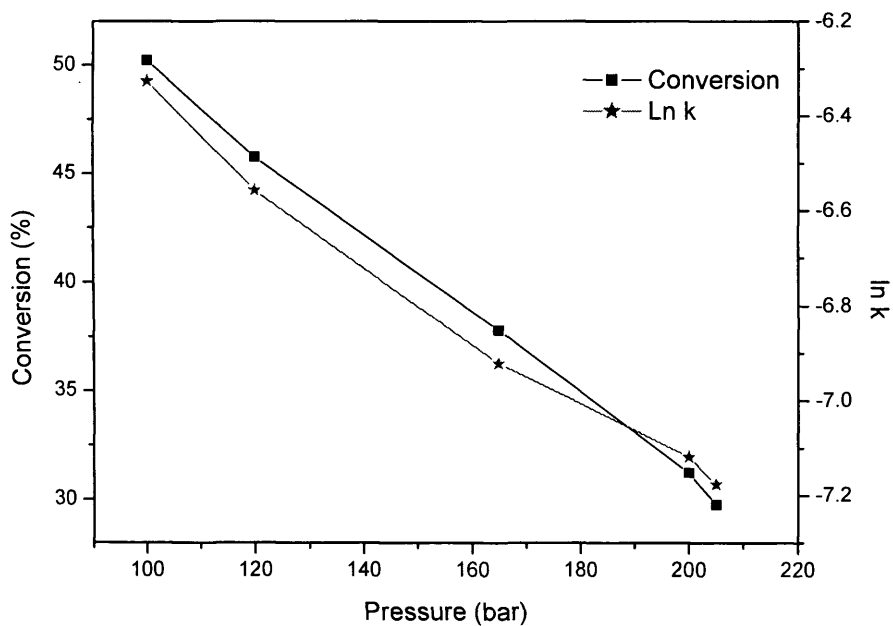
Figure 6.17 Change in conversion and ln k with pressure for the FC reaction in CO_2 at 363 K

function of pressure. It can be seen from Figure 6.17 that the yield of the reaction decreases as the pressure increases. A reaction was also carried out at 50 bar and at a lower t-BuCl concentration (0.16 M) but no product was isolated in either case. It is assumed that the reaction in sc CO_2 will follow the same mechanism proposed earlier so second order rate constants were calculated and are also shown in Figure 6.17 and Table 32 of the appendix. It can be seen that the rate decreases as the pressure increases, which is consistent with the dilution effect proposed earlier for the work in HFC 32.

To eliminate the effect of dilution on the reaction the mole fraction of the reaction should be kept constant. Therefore, the amount of solute put into the reaction system was adjusted in accordance with the increased number of moles of solvent at higher pressures, thus keeping a constant mole fraction. Constant mole fraction experiments were carried in sc CO_2 at various pressures. The second order rate constants and reaction yields are shown in Table 33 and 34 of the appendix respectively. Figure 6.18 shows the total reaction conversion and individual product yields for these constant mole fraction experiments.

The total conversion of the reaction was found to be around 29 %. The conversion and the rate constant were found to be independent of pressure. On analysis of the product yield for each reaction it was found that all three products shown in Scheme 3 were isolated. The yield of each product is also shown in Figure 6.19 where it can be seen that the *para-* product is most abundant followed by the *di-* and *ortho-* substituted products.

The yield of each product was found to be independent of pressure. In the reactions employing HFC 32 as the solvent the product distributions were found to vary with pressure and it was postulated that the hydrogen-bonding character of HFC 32 resulted in this pressure dependence. In CO_2 it is not possible for hydrogen bonding to occur which may account for the constant product distribution with changing pressure.

Another interesting point to note is the moderately high yields obtained for the FC reaction in sc CO_2. It must be noted here that the amount of t-BuCl used in these reactions is higher than that employed in HFC 32 because the reaction did not proceed at lower t-BuCl concentrations. However, even with this in mind the yields
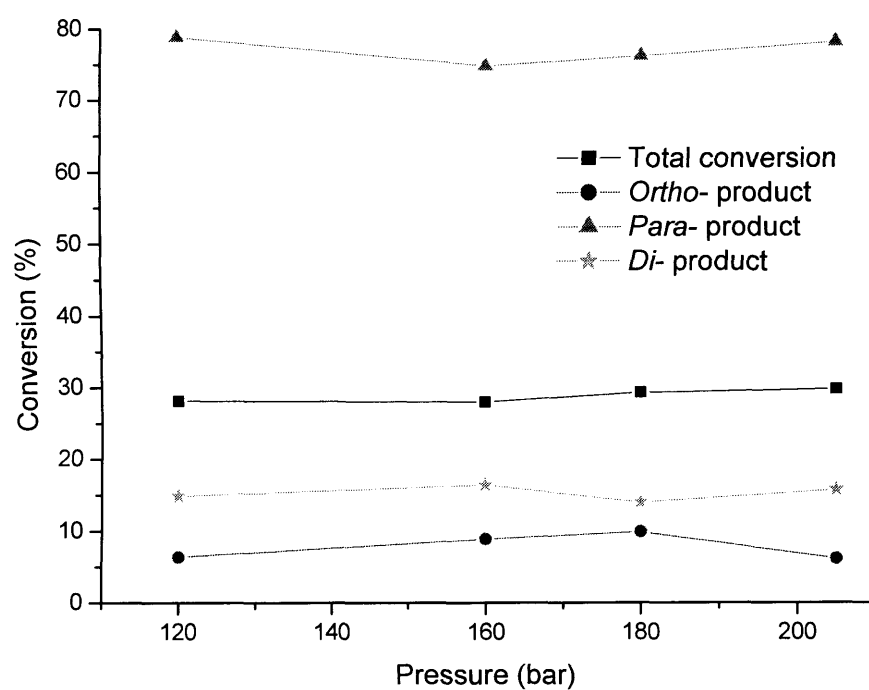
Figure 6.18 Conversion for the FC reaction of anisole with t-BuCl in CO_2 at 363 K

for a variety of pressures at constant mole fraction

are much higher than expected for this FC reaction involving moderate polarity solutes in a non-polar fluid. The solubility of the solutes used in these FC studies would be lower than in HFC 32 and most importantly the dissociation of the acid catalyst should be negligible in low dielectric media.

The reason behind these unexpectedly high yields is thought to be due to the solutes in the FC reaction acting as polar modifiers and therefore causing an increase in dielectric constant of the reaction medium. Figure 6.19 shows the dielectric constant of three different solutions at 363 K; pure CO_2, pTos and anisole in CO_2 and all of the reagents mixed together in CO_2 at the start of the reaction. It is clear that although each reagent is present in $<< 1$ mol % they have a marked effect on the dielectric constant of the solution. It can therefore be assumed that the dissociation of the acid catalyst occurs because it is principally solvated by the reagents. To clarify this point the same reaction was repeated using a lower concentration of t-BuCl (0.16 M) (solution dielectric constant = 3.3). At 363 K and 230 bar the dielectric constant of the solution did not change and no conversion was observed, which suggests that the medium is too non-polar to allow any significant acid dissociation. Nor did the reaction proceed at 50 bar, where the solution is in the near critical state and the dielectric constant ($\varepsilon = 3$) is too low to allow significant acid dissociation.

If these values are compared to those in HFC 32 (solution dielectric constant = 8.5 at 150 bar with all the reagents present), the dielectric constants of the two reaction media are not dissimilar as first thought on the basis of the pure solvent dielectric constant values.

It has been shown in this study that the sc solvent is found to have an effect on the yield, selectivity and rate of FC alkylation. This work has demonstrated that it is in fact the dielectric constant of the solution rather than that of the solvent that affects the yield and rate of reaction. At low solution dielectric constants where acid dissociation is minimal the reaction did not proceed. It has been shown that sc CO_2 can support the FC alkylation of anisole resulting in moderate yields. The main drawback with CO_2 compared to HFC 32 is the inability to control the selectivity of the reaction. With CO_2 it is not possible to form hydrogen bonds at any pressures so the selectivity was found to be independent of pressure.
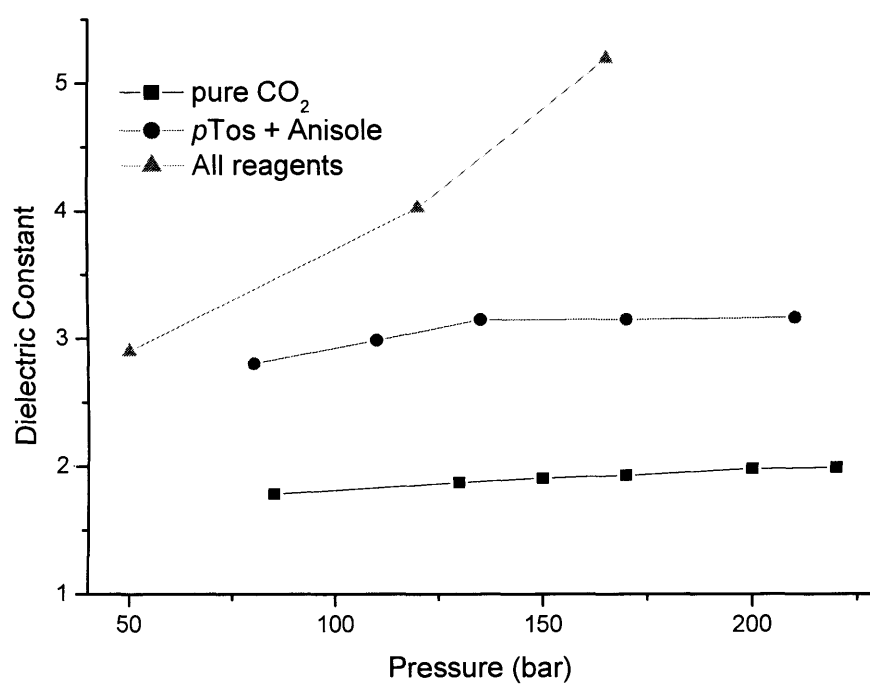
Figure 6.19 The change in solution dielectric constant with pressure in CO_2 at 363 K

6.3 Conclusions

It has been shown that the dielectrometry technique is applicable to following the progress of the FC reaction in sc HFC 32 and sc CO_2. By following the progress of this reaction it was possible to relate the measured capacitance of the solution to the concentration changes of the reactants and products. A rate law for the reaction was proposed, which was found to depend on the concentrations of the aromatic and alkylating species, giving rise to second order reaction kinetics.

It was demonstrated that second order rate constants could be calculated for this reaction and changes in the observed rates with temperature, pressure, reagents and solvent were addressed. If the molar amount of reagents is kept constant as the pressure is increased the ratio of solvent to solute molecules increases resulting in a dilution of the reaction system. The affect of this dilution was observed in the results obtained at various pressures so no meaningful data could be obtained.

The dielectric constant of the reaction solution was discovered to have a high dependency on the reagents present, even when they are present in very small amounts. In the case of CO_2, which has a low dielectric constant, the solutes seemed to behave as polar modifiers causing an increase in the dielectric constant of the whole reaction solution. The yields obtained in CO_2 were also much higher than expected from dielectric constant considerations of the pure solvent. The result emphasises the fact that it is the solution dielectric constant not the solvent dielectric constant that has a controlling influence on the reaction.

6.4 References

(1)   Jessop P, G.; Leitner W. *Chemical Synthesis using Supercritical Fluids*; Wiley-VCH: Weinheim, **1999**.

(2)   Brenneke J, F.; Tomasko D, L.; Pehkin J.; Eckert C, A. *Ind. Eng. Chem. Res.* **1990**, *29*, 1682.

(3)   Heitz M, P.; Bright F, V. *J. Phys. Chem.* **1996**, *100*, 6889.

(4)   Kim S.; Johnston K, P. *Ind. Eng. Chem. Res.* **1987**, *26*, 1206.

(5)   Zhang J.; Lee L, L.; Brennecke J, F. *J. Phys. Chem.* **1995**, *99*, 9269.

(6)   Zhang J.; Roek D, P. *J. Phys. Chem.* **1995**, *49*, 8793.

(7)   Worrall D, R.; Wilkinson F. *J. Chem. Soc., Faraday Trans.* **1996**, *92*, 1467.

(8)   Kajimoto O. *Chem. Rev.* **1999**, *99*, 355.

(9)   Tucker S, C.; Maddox M, W. *J. Phys. Chem. B* **1998**, *102*, 2437.

(10)   Tucker S, C. *Chem. Rev.* **1999**, *99*, 391.

(11)   Atkins P, W. *Physical Chemistry*, 5 ed.; Oxford University Press: Oxford, **1994**.

(12)   Roek D, P.; Kremer M, J.; Roberts C, B.; Chateauneuf J, E.; Brennecke J, F. *Fluid Phase Equilib.* **1999**, *158-160*, 713.

(13)   Dillow A, K.; Brown J, S.; Liotta C, L.; Eckert C, A. *J. Phys. Chem. A* **1998**, *102*, 7609.

(14)   Lineham J, C.; Yonker C, R.; Bays J, T.; Autrey S, T. *J. Am. Chem. Soc* **1998**, *120*, 5826.

(15)   Guan Z.; Combers J, R.; Menceloglu Y, Z.; deSimone J, M. *Macromolecules* **1993**, *26*, 2663.

(16)   Worrall D, R.; Abdel-Shafi A, A.; Wilkinson F. *J. Phys. Chem. A* **2001**, *105*, 1270.

(17)   Rhodes T, A.; O'Shea K.; Bennett G.; Johnston K, P.; Fox M, A. *J. Phys. Chem.* **1995**, *99*, 9903.

(18)   Giese B.; Huise R. *Tetrahedron Lett.* **1967**, *18*, 89.

(19)   Thompson R, L.; Glaser R.; Bush D.; Liotta C, L.; Eckert C, A. *Ind. Eng. Chem. Res.* **1999**, *38*, 4220.

(20)   Reaves J, T.; Roberts C, B. *J. Chem. Soc., Chem. Eng. Comm.* **1999**, *171*, 117.

(21)   Knutson B, L.; Dillow A, K.; Liotta C, L.; Eckert C, A. *Innovations in Supercritical Fluids* **1995**, *608*, 166.

(22)   Weinstein R, D.; Renslo A, R.; Vanheiser R, L.; Harns J, G.; Terter J, W. *J. Phys. Chem.* **1996**, *100*, 12337.

(23)   Paulaitis M, E.; Alexander G, C. *Pure Appl. Chem.* **1987**, *59*, 61.

(24)   Friedel C.; Crafts J, M. *Compt. Rend.* **1877**, *84*, 1450.

(25)   Olah G. *Friedel-Crafts and Related Reactions*; Wiley Interscience: New York and London, **1963-1964**; Vol. I-IV.

(26)   Baiker A. *Chem. Rev.* **1999**, *99*, 453.

(27)   Chandler K.; Deng F.; Dillow A, K.; Liotta C, L.; Eckert C, A. *Ind. Eng. Chem. Rev.* **1997**, *36*, 5175.

(28)   Chateauneuf J.; Nie K. *Adv. Environ. Res.* **2000**, *4*, 307.

(29)   Fan L.; Nakamura I.; Ishida S.; Fujimoto K. *Ind. Eng. Chem. Res.* **1997**, *36*, 1458.

(30)   Hitzler M, G.; Smail F, R.; Ross S, K.; Poliakoff M. *J. Chem. Soc., Chem. Comm.* **1998**, *133*, 359.

(31)   Savage P, E. *Chem. Rev.* **1999**, *99*, 603.

(32)   Clark M, C.; Subramaniam B. *Ind. Eng. Chem. Res.* **1998**, *37*, 1243.

(33)   Mahindaratne M, P, D.; Wimalasena K. *J. Org. Chem.* **1998**, *63*, 2858.

(34)   Lange S. University of Leicester *unpublished results* **2000**.

(35)   Olah G, A.; Olah J, A.; Ohyama T. *J. Am. Chem. Soc.* **1984**, *106*, 5284.

(36)   Simth M, B.; March J *March's Advanced Organic Chemistry*, 5th ed.; Wiley & Son: New York, **2001**.

(37)   DeHaan F, P.; Delker G, L.; Covey W, D.; Ahn J.; Cowan R, L.; Fong C, H.; Kim G, Y.; Kumar A.; Roberts M, P.; Schubert D, M.; Stoler E, M.; Suh Y, J.; Tang M. *J. Org. Chem.* **1986**, *51*, 1587.

(38)   Blandamer M, J.; Burgess J.; Robertson R, E.; Scott J, M., W,. *Chem. Rev.* **1982**, *82*, 259.

(39)   Abbott A, P.; Eardley C, A.; Tooth R, J. *J. Chem. Eng. Data* **1999**, *44*, 112.

CHAPTER 7
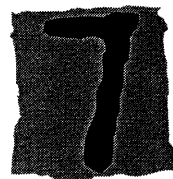
SUMMARY AND FUTURE WORK

7.1 Summary

This study has shown that difluoromethane (HFC 32) and 1,1,1,2-tetrafluoroethane (HFC 134a) are polar fluids with solvent properties that change markedly with temperature and pressure. HFC 32 is known to have accessible critical constants, relatively high dielectric constants and low viscosity; these properties alone make HFC 32 ideal for use in supercritical (sc) fluid applications. It has been shown in this work that sc HFC 32 also displays high solubilities, relatively high polarisability/dipolarity and hydrogen bonding properties making this solvent even more attractive for use in sc fluid applications. The first examples of reactions in HFC 32 were carried out in this work to justify these findings.

7.1.1 Solubility

The first solubility measurements of a number of *p*-benzoic acids and *p*-phenols in HFC 32 at 363 K over a range of pressures have been reported. The identity of the functional group at the *para* position of the benzoic acid and phenol backbones was found to have a large affect on the measured solubilities. The Peng-Robinson equation-of-state (PR EOS) was used to model the solubility data for the solutes where vapour pressure data was available. A good fit was obtained for all solutes over the temperature and pressure range studied showing that the PR EOS can be used to predict solubilities in HFC 32.

It has been shown in this work that the dielectrometry technique is especially suitable for measuring solubilities in sc HFC 32. It is shown to be a quick, simple and precise *in situ* technique that can be applied to measure the solubility of polar ad non-polar liquid and solid solutes.

7.1.2 Solvent Properties

This work has shown that HFCs 32 and 134a have relatively high polarisability/dipolarity and they also exhibit significant hydrogen bond donor characteristics, particularly in the sc state. The hydrogen bond donor properties of the two solvents decrease with increasing pressure and this trend is suggested to be due to a decrease in solvent-solvent interactions and an increase in the preferential solvation around the polar moieties as the local solvent density decreases.

The Log solubility of aromatic solutes in HFC 32 was modelled using the solvent properties obtained in this study and published solute descriptor data. The

159

linear solvation energy relationship (LSER) approach commonly employed was found to be successful for the solutes under investigation and can rival equation of state methods. The accuracy of this LSER model was found to increase with the addition of a number of solute descriptors but the data set was not large enough to draw any accurate conclusions about the applicability of this model to predict other solute solubilities. It is thought however, that it would be successful for the prediction of solubilities with similar aromatic solutes.

7.1.3 Reactions

The first reactions in sc HFC 32 have been carried out. The Esterification, Aldol condensation and Friedel-Crafts reaction were chosen as examples. It was demonstrated that *in situ* dielectrometry could be used to follow the progress of these reactions, and the measured capacitance values are directly related to the concentration of reactants and products in the reaction media at any one time. It was found that by application of dielectrometry that equilibrium and rate constants could be calculated for the reactions as a function of temperature, pressure, solvent and reactants.

For these reactions it was found that the dielectric constant of the reaction medium was considerably higher than the pure sc solvent, especially in the case of CO_2, which is a low dielectric constant medium. Even though the reagents were present in less than 1 mol % they were found to have a marked affect on the dielectric constant and it is thought that they are behaving as polar modifiers, which is the cause of the observed increase in the dielectric constant of the reaction solution. The result emphasises the fact that it is the solution dielectric constant and not the solvent dielectric constant that has a controlling influence on the reaction.

7.2 Future Work

7.2.1 Solubility Measurements in Hydrofluorocarbons

A knowledge of the ability for a sc fluid to act as a solvent for a particular solute is essential in process design. The hydrofuorocarbons used in this work have shown many characteristics that make these solvents attractive for sc fluid applications but in the literature there is a large void in the solubility data needed for these solvents. This data must be extended to cover a wider range of solutes, temperatures and pressures. It is then possible that these solvents will be seen as possible alternatives to CO_2.

7.2.2 Local Composition Enhancement

The reactions rates reported in this work are found to increase dramatically around the critical pressure. The idea of local composition enhancements is proposed to account for the observed increase in rate. The concept of local composition enhancement is that the concentration of a reactant or a product around other reactants or products is higher than that of the bulk. A solvatochromic probe can be used as a representative polar solute and then by addition of a reagent used in the reactions it is possible to measure the local composition of this reagent about the solvatochromic probe from measurement of the wavelength of maximum absorption. The affect of temperature and pressure on local composition enhancement can also be found.

7.2.3 Reactions in Hydrofluorocarbons

The use of these hydrofluorocarbons to support chemical synthesis needs to be extended to cover a wide range or reactions. In this work only a few reactions are briefly mentioned and a whole new hydrofluorocarbon application has been shown to be feasible. The affect of heterogeneous catalysts compared to homogeneous catalysts and concentrated solutions compared to dilute solutions needs to be addressed. In concentrated solution it may be possible to form emulsions and then by application of light scattering techniques it may be possible to gain knowledge of the size and stability of the colloids formed.

To conduct a simple reaction in a sc fluid there are a number of variables that can be altered and each of these will have an effect on the reaction yield, rate and selectivity. To address the possibility of chemical reactions in sc fluids being

commercially viable, and to take full advantage of the tunability of reactions in sc fluids, the reactions must be optimised.

APPENDIX

Solutes	$\alpha \times 10^{39}$ $(J^{-1} C^2 m^2)$	$\mu \times 10^{30}$ (C m)	A_e^s $(dm^3 mol^{-1})$	T_c (K)	P_c (bar)
o-hydroxybenzoic acid	1.37	8.839	0.155474	704.24	50.02
m-hydroxybenzoic acid	1.24	7.972	0.129226	-	-
p-hydroxybenzoic acid	1.43	9.206	0.167295	-	-
p-toluic acid	1.68	6.671	0.108998	772.04	40.01
p-aminobenzoic acid	1.76	1.34	0.209952	-	-
p-chlorobenzoic acid	1.79	6.738	0.112815	-	-
o-chlorobenzoic acid	1.81	8.172	0.147347	-	-
p-chlorophenol	1.45	6.671	0.103579	699.5	49.38
p-aminophenol	1.42	6.071	0.090902	781.78	56.62
Naphthalene	1.83	0	0.041586	748.4	40.5
Anthracene	2.82	0	0.064017	869.3	32.43
Water (343 K)	0.161	6.071	0.065715	647.1	220.64
Water (363 K)	0.161	6.071	0.062296	647.1	220.64
Water (383 K)	0.161	6.071	0.059233	647.1	220.64

Table 1. Molecular polarisability, dipole moment, first dielectric virial coefficients and critical constants for the solutes used in this work

Pressure (bar)	Molarity (mol L^{-1})	Mole Fraction
90	0.10211	0.00838
114	0.14554	0.01111
120	0.24364	0.01749
150	0.31299	0.02106
170	0.32756	0.02138
200	0.36726	0.02313

Table 2. Solubility data for naphthalene in CO_2 at 318 K

Pressure (bar)	Molarity (mol L^{-1})	Mole Fraction
80	0.00756	0.0007
100	0.00883	0.0008
120	0.01120	0.0010
140	0.01362	0.0012
160	0.01749	0.0015
180	0.02083	0.0018
200	0.02340	0.0020
210	0.02474	0.0021

Table 3. Solubility data for water in HFC 134a at 343 K

Pressure (bar)	Molarity (mol L^{-1})	Mole Fraction
110	0.02080	0.0020
140	0.03062	0.0029
160	0.04185	0.0039
187	0.04795	0.0044
210	0.05731	0.0052
221	0.06725	0.0061

Table 4. Solubility data for water in HFC 134a at 363 K

Pressure (bar)	Molarity (mol L^{-1})	Mole Fraction
88	0.03771	0.0043
110	0.05517	0.0060
125	0.06920	0.0073
149	0.09710	0.0100
180	0.11502	0.0115
199	0.12519	0.0123

Table 5. Solubility data for water in HFC 134a at 383 K

Pressure (bar)	Molarity (mol L^{-1})	Mole Fraction
140	0.04663	0.0032
180	0.05286	0.0034
209	0.05740	0.0036
230	0.06399	0.0039
241	0.07252	0.0044

Table 6. Solubility data for *o*-hydroxybenzoic acid in HFC 32 at 363 K

Pressure (bar)	Molarity (mol L^{-1})	Mole Fraction
89	0.00483	0.00040
106	0.00575	0.00043
130	0.00856	0.00061
198	0.01122	0.00071
252	0.01308	0.00078

Table 7. Solubility data for *m*-hydroxybenzoic acid in HFC 32 at 363 K

Pressure (bar)	Molarity (mol L^{-1})	Mole Fraction
89	0.00210	0.00017
100	0.00467	0.00036
159	0.00618	0.00041
170	0.00702	0.00046
200	0.00836	0.00053
240	0.00889	0.00055

Table 8. Solubility data for *p*-hydroxybenzoic acid in HFC 32 at 363 K

Pressure (bar)	Molarity (mol L^{-1})	Mole Fraction
90	0.095731	0.0078
118	0.153864	0.0111
139	0.201735	0.0139
162	0.215366	0.0142
180	0.222893	0.0144

Table 9. Solubility data for *p*-toluic acid in HFC 32 at 363 K

Pressure (bar)	Molarity (mol L⁻¹)	Mole Fraction
135	0.118530	0.0082
170	0.130444	0.0085
200	0.145446	0.0092
221	0.149951	0.0093

Table 10. Solubility data for *p*-chlorobenzoic acid in HFC 32 at 363 K

Pressure (bar)	Molarity (mol L⁻¹)	Mole Fraction
100	0.13555	0.0105
134	0.15147	0.0106
170	0.17751	0.0115
190	0.18162	0.0116
219	0.18915	0.0117
248	0.22332	0.0135

Table 11. Solubility data for *o*-chlorobenzoic acid in HFC 32 at 363 K

Pressure (bar)	Molarity (mol L⁻¹)	Mole Fraction
69	0.00018	0.000029
90	0.00046	0.000039
120	0.00070	0.000051
153	0.00083	0.000056
175	0.00101	0.000066
220	0.00120	0.000074

Table 12. Solubility data for *p*-aminobenzoic acid in HFC 32 at 363 K

Pressure (bar)	Molarity (mol L⁻¹)	Mole Fraction
79	0.00448	0.000422
125	0.00615	0.000436
148	0.00697	0.000471
175	0.00815	0.000528
220	0.00964	0.000596

Table 13. Solubility data for anthracene in HFC 32 at 363 K

Pressure (bar)	Molarity (mol L^{-1})	Mole Fraction
122	0.64861	0.046
150	0.76806	0.051
185	0.80820	0.052
220	0.85666	0.053
258	0.86390	0.054

Table 14. Solubility data for p-chlorophenol in HFC 32 at 363 K

Pressure (bar)	Molarity (mol L^{-1})	Mole Fraction
89	0.013214	0.00109
111	0.016135	0.00119
132	0.029776	0.00207
188	0.032882	0.00209

Table 15. Solubility data for p-aminophenol in HFC 32 at 363 K

Pressure (bar)	Molarity (mol L^{-1})	Mole Fraction
70	0.00481	0.00071
90	0.01504	0.00124
120	0.01886	0.00135
145	0.02465	0.00167
180	0.03585	0.00231
220	0.04034	0.00249
250	0.04504	0.00271
270	0.04799	0.00285

Table 16. Solubility data for p-acetamidophenol in HFC 32 at 363 K

Pressure (bar)	Molarity (mol L^{-1})	Mole Fraction
65	0.01315	0.0027
75	0.03818	0.0041
100	0.09266	0.0071
140	0.15870	0.0109
180	0.21201	0.0136
220	0.22888	0.0141

Table 17. Solubility data for acetyl salicylic acid in HFC 32 at 363 K

Solvent	Pressure (bar)	Time (hrs)	Extracted (g)	Mole Fraction
HFC 32	200	2	0.010	0.00018
HFC 32	220	4	0.015	0.00027
HFC 32	200	7	0.038	0.00070
HFC 32	180	14	0.073	0.00138
HFC 32	200	24	0.080	0.00148
CO_2	220	4	0.002	0.00004

Table 18. Paracetamol extraction results as a function of time at 363 K

Solvent	Pressure (bar)	Time (hrs)	Extracted (g)	Mole Fraction
HFC 32	190	2	0.068	0.00107
HFC 32	200	3	0.073	0.00112
HFC 32	200	4	0.085	0.00131
HFC 32	190	7	0.092	0.00144
HFC 32	180	10	0.103	0.00163
HFC 32	180	22	0.107	0.00169
HFC 32	200	24	0.109	0.00167
CO_2	200	4	0.016	0.00033
CO_2	190	8	0.048	0.00102

Table 19. Aspirin extraction results as a function of time at 363 K

Solvent	Pressure (bar)	Time (hrs)	Extracted (g)	Mole Fraction
HFC 32	75	2	0.001	0.00003
HFC 32	110	2	0.045	0.00082
HFC 32	150	2	0.060	0.00099
HFC 32	190	2	0.068	0.00106
HFC 32	240	2	0.085	0.00127
CO_2	190	4	0.016	0.00033

Table 20. Aspirin extraction results as a function of pressure at 363 K

Solvent	NR Expt (kK)	NR Calc (kK)	4N Expt (kK)	4N Calc (kK)	NN Expt (kK)	NN Calc (kK)
Dichloromethane	18.60	18.39	28.67	28.73	25.32	25.12
Cyclohexane	19.95	19.98	30.73	30.82	28.00	27.96
Toluene	19.14	19.10	-	-	26.27	26.16
Dichloroethane	18.72	18.67	-	-	25.34	25.27
Hexane	19.96	20.11	30.83	31.03	28.30	28.23
Anisole	18.75	18.77	28.17	28.15	25.50	25.51
Diethylether	19.82	19.53	28.54	25.47	27.00	27.05
Acetonitrile	18.75	18.75	-	-	25.35	25.48
THF	18.94	19.04	27.29	27.41	26.06	26.04
DMSO	18.14	18.35	25.61	25.57	24.57	24.63
Methanol	18.02	18.13	26.90	27.10	25.60	25.44
Ethanol	18.46	18.32	26.77	26.73	25.87	25.69
iso-butanol	-	-	30.89	30.82	-	-
Propan-2-ol	18.45	18.48	26.40	26.26	25.97	25.93
Chloroform	18.47	18.62	-	-	25.47	25.78
t-butanol	18.66	16.67	-	-	25.88	26.21

Note: NR = Nile Red, 4N = 4-nitroaniline and NN = N,N-dimethyl-4-nitroaniline

Table 21. Comparison between experimental and calculated ν_{max} values

Solvent	Pressure (bar)	Conversion (%)	K_X
HFC 32	70	42.64	0.74338
HFC 32	75	32.70	0.48588
HFC 32	80	27.32	0.37589
HFC 32	100	25.02	0.33369
HFC 32	125	19.00	0.23457
HFC 32	145	12.01	0.13649
HFC 32	165	9.24	0.10181
HFC 32	170	8.17	0.08897
HFC 32	200	5.28	0.05574
HFC 32	220	4.93	0.05186
DCE	1	16.77	0.20149
CH	1	16.10	0.19190

Table 22. Apparent equilibrium constants for the esterification reaction at 363 K

Solvent	Pressure (bar)	Conversion (%)	K_X
HFC 32	70	19.50	0.12111
HFC 32	90	10.01	0.05561
HFC 32	120	8.80	0.04824
HFC 32	140	7.92	0.04300
HFC 32	200	6.31	0.03367

Table 23. Apparent equilibrium constants for the aldol reaction at 363 K

Temperature (K)	1/Temperature (K^{-1})	Rate ($mol^{-1}\ dm^3\ s^{-1}$)	Ln k
363	0.00275	3.87×10^{-4}	-7.858
373	0.00268	9.12×10^{-4}	-7.000
383	0.00261	1.87×10^{-3}	-6.282

Table 24. Parameters used to form an Arrhenius plot for the FC reaction of anisole with t-BuCl at 260 ± 10 bar

Pressure (bar)	Conversion (%)	Ortho product (%)	Para product (%)	Di product (%)
40	31.11	15.71	63.42	20.87
60	43.94	15.07	65.86	19.07
70	63.08	13.51	52.51	33.98
100	58.54	11.93	61.79	26.28
110	52.45	8.03	62.78	29.19
130	52.09	7.53	62.69	29.78
160	44.62	7.89	66.70	25.41
170	43.23	5.70	69.09	25.21
180	44.12	5.92	69.00	25.08
205	42.19	5.63	73.22	21.15
250	38.17	2.99	74.98	22.03

Table 25. Conversion for the FC reaction of anisole with t-BuCl in HFC 32 at 363 K for a variety of pressures

Pressure (bar)	Rate Constant ($mol^{-1}\ dm^3\ s^{-1}$)	Ln k	R
40	0.00110	-6.812	0.9987
60	0.00148	-6.516	0.9945
70	0.00220	-6.119	0.9738
110	0.00199	-6.220	0.9577
160	0.00154	-6.476	0.9926
205	0.00131	-6.638	0.9851
250	0.00122	-6.709	0.9942

Table 26. Second order rate constants for the FC reaction of anisole with t-BuCl in HFC 32 at 363 K for a variety of pressures

Pressure (bar)	Solvent (mf)	Anisole (mf)	t-BuCl (mf)	Rate	Ln k
55	0.97	0.01	0.02	0.00190	-6.266
72	0.97	0.01	0.02	0.00220	-6.119
110	0.97	0.01	0.02	0.00199	-6.220
120	0.97	0.01	0.02	0.00196	-6.235
180	0.97	0.01	0.02	0.00197	-6.230
210	0.97	0.01	0.02	0.00198	-6.225
DCE (1 bar)	0.97	0.01	0.02	0.00057	-7.468

Table 27. Second order rate constants for the FC reaction of anisole with t-BuCl in HFC 32 at 363 K for a variety of pressures at constant mole fraction

Pressure (bar)	Conversion (%)	Ortho Product (%)	Para Product (%)	Di Product (%)
55	50.14	22.66	40.8	36.55
72	58.00	14.47	53.3	32.25
110	52.45	8.03	62.8	29.19
120	51.80	7.29	64.7	27.97
180	52.10	5.17	72.7	22.20

Table 28. Conversion for the FC reaction of anisole with t-BuCl in HFC 32 at 363 K for a variety of pressures at constant mole fraction

Pressure (bar)	Conversion (%)	Ortho Product (%)	Para Product (%)	Di Product (%)
60	16.13	0	100	0
75	19.91	0	100	0
95	16.19	0	100	0
100	15.69	0	100	0
155	10.62	0	100	0
195	7.32	0	100	0
210	5.12	0	100	0
260	3.80	0	100	0
265	3.09	0	100	0

Table 29. Conversion for the FC reaction of toluene with t-BuCl in HFC 32 at 363 K for a variety of pressures

Pressure (bar)	Rate Constant (mol^{-1} dm^3 s^{-1})	Ln k	R
60	3.88×10^{-4}	-7.851	0.969
75	5.02×10^{-4}	-7.604	0.981
95	3.90×10^{-4}	-7.852	0.971
100	3.76×10^{-4}	-7.890	0.989
155	2.42×10^{-4}	-8.335	0.973
195	1.60×10^{-4}	-8.742	0.982
210	1.09×10^{-4}	-9.122	0.992
260	7.99×10^{-5}	-9.434	0.977
265	6.45×10^{-5}	-9.655	0.975

Table 30. Second order rate constants for the FC reaction of toluene with *t*-BuCl in HFC 32 at 363 K for a variety of pressures

Temperature (K)	1/Temperature (K^{-1})	Rate (mol^{-1} dm^3 s^{-1})	Ln k
363	0.00275	5.92×10^{-5}	-9.734
373	0.00268	2.64×10^{-4}	-8.239
383	0.00261	6.24×10^{-4}	-7.379

Table 31. Parameters used to form an Arrhenius plot for the FC reaction of toluene with *t*-BuCl at 260 ± 20 bar

Pressure (bar)	Conversion (%)	Rate (mol^{-1} dm^3 s^{-1})	Ln k
50	0	0	0
100	50.21	1.79×10^{-3}	-6.326
120	45.74	1.42×10^{-3}	-6.557
165	37.81	9.87×10^{-4}	-6.921
200	31.25	8.10×10^{-4}	-7.118
205	29.77	7.65×10^{-4}	-7.176

Table 32. Conversion for the FC reaction of anisole with *t*-BuCl in CO_2 at 363 K for a variety of pressures

Pressure (bar)	Solvent (mf)	Anisole (mf)	t-BuCl (mf)	Rate	Ln k
120	0.965	0.01	0.025	7.06×10^{-4}	-7.256
160	0.965	0.01	0.025	7.00×10^{-4}	-7.264
180	0.965	0.01	0.025	7.48×10^{-4}	-7.198
205	0.965	0.01	0.025	7.65×10^{-4}	-7.176

Table 33. Second order rate constants for the FC reaction of anisole with t-BuCl in CO_2 at 363 K for a variety of pressures at constant mole fraction

Pressure (bar)	Conversion (%)	Ortho Product (%)	Para Product (%)	Di Product (%)
120	28.12	6.36	78.77	14.87
160	27.95	8.89	74.73	16.38
180	29.31	9.88	76.16	13.96
205	29.77	6.15	78.10	15.75

Table 34. Conversion for the FC reaction of anisole with t-BuCl in CO_2 at 363 K for a variety of pressures at constant mole fraction